



Reliability based Assessment of Quay Walls

T.J. van der Wel

Reliability based Assessment of Quay Walls

By

T.J van der Wel

in partial fulfilment of the requirements for the degree of

Master of Science
in Civil Engineering

at the Delft University of Technology,
to be defended publicly on 17 December 2018 at 1:00 PM

Graduation committee:

Prof. dr. ir. S.N. Jonkman	TU Delft
Ir. P. Quist	TU Delft / Witteveen+Bos
Dr. Ir. T. Schweckendiek	TU Delft / Deltares
Ir. A.A. Roubos	TU Delft / Havenbedrijf Rotterdam

Daily supervisor:

Ir. D.J. Jaspers Focks	Witteveen+Bos
------------------------	---------------

An electronic version of this thesis is available at <http://repository.tudelft.nl/>.

ACKNOWLEDGMENTS

This thesis is the final work for my master program Hydraulic Engineering at Delft University of Technology. The research concerns a reliability analysis of quay walls and was conducted at Witteveen+Bos, in agreement with Port of Rotterdam and TU Delft.

First of all, I would like to thank Witteveen+Bos for providing me with the opportunity and all the facilities to conduct this research. In particular, I am grateful to my two supervisors Peter Quist and Dirk-Jan Jaspers Focks. Peter, thank you for your support and guidance throughout my entire research. I appreciate the positive feedback you gave and your flexibility with regard to planning of meetings. Dirk-Jan, thanks for the fruitful discussions we had and for sharing all your geotechnical knowledge. Additionally, I would like to thank all other colleagues at Witteveen+Bos for their help and for making it a pleasant period.

Furthermore, words of thanks to all members of my graduation committee. I appreciate their advices and their constructive feedback. It let me critically analyse my own work and helped me heading in the right direction. Special thanks to Alfred Roubos, for sharing his experience and knowledge about probabilistic calculations of quay walls. Also, I am grateful to Plaxis, and Dr. Ir. R. Brinkgreve in particular, for providing me with the newest probabilistic module.

Finally, I would like to thank my friends and family for the grammar checking of my work and of course for all their support during my entire study period at TU Delft.

*Thijs van der Wel
Delft, December 2018*

SUMMARY

Uncertainties in the soil parameters play a major role in the design of quay walls. In the current design approach, partial factors are prescribed to account for uncertainties in the soil, as well as for other types of uncertainties. This semi-probabilistic (level I) design approach needs to result in a reliable design for a range of quay structures and for multiple soil stratifications. It is therefore expected that, in general, this method results in overdimensioning of the structure. Whether this assumption holds, is investigated in this thesis by carrying out a reliability analysis for two quay walls in the Port of Rotterdam.

Failure of a quay wall can be caused by plenty of different failure mechanisms. In this research, the failure mechanisms yielding of the combi-wall, yielding of the anchor bar, shear failure of the grout body and soil mechanical failure are assessed. Such failure mechanisms are complex soil-structure interaction problems. Therefore, both the soil and the quay structure have been modelled with the finite element program Plaxis 2D, using the Hardening soil model. For performing the probabilistic calculations on this model, the probabilistic module ProbAna has been used. This is a package developed by Plaxis which couples several types of reliability methods to the finite element software of Plaxis 2D. As the computational effort is relatively large with the hardening soil model, the First Order Reliability Method (FORM) was used over sampling methods like Directional Sampling and Crude Monte Carlo simulation.

The first case study concerned a combi-wall anchored by two grout anchors in the tubular steel piles of the combi-wall. The results of the probabilistic calculations showed that the as-built quay wall has significant overcapacity for all four failure mechanisms considered. This is in line with the expectations, but for the failure mechanism yielding of the wall, it was also partly caused by the fact that the contractor had chosen to use tubular piles with a larger wall thickness than originally required in the design.

Regarding the influence of variables, the calculations revealed that for the reliability of the anchor bar and the combi-wall, the friction angle and the yield strength (both anchor and wall) were the most important parameters. For the reliability of the grout body, it turned out that the pile class factor α_t was most dominant. For the purpose of deriving partial factors, the as-built design of the quay wall has been adjusted by reducing the wall thickness of the tubular piles. In this way the design was more in line with the current design guidelines. When comparing the derived partial factors with the prescribed partial factors of NEN9997, the general finding is that slightly lower partial factors are found. The most important deviations were found for the friction angle (a slightly lower partial factor was found) and the yield strength (a higher partial factor was found).

In the second case study a quay wall with relieving platform was considered. This quay wall is equipped with monitoring sensors right from the construction. The available monitoring data for this quay wall is used for a calibration of the Plaxis-model. Subsequently, the calibrated set of soil parameters was used as a starting point for the probabilistic calculations. Two mechanism were evaluated for this quay wall, being yielding of the wall and soil mechanical failure. For both limit states, the friction angle of the dense Pleistocene sand layer has major influence on the reliability. It turned out that the obtained reliability indices are too low compared to the target reliability. One of the explanations is that in the initial design, optimistic soil conditions were used, especially for the Pleistocene sand layer, which might have resulted in a too optimistic design. Next to that, the reliability is dominated by one single parameter, which can also result in a too low reliability index.

Although each case study concerned a different type of quay wall, the results reveal that choices made in the design, either optimistic or pessimistic, can have large influence on the reliability. Perhaps just as important, are the assumptions made regarding the stochastic description of the soil. It is still under discussion up to what distance soil parameters are correlated in space and how spatial averaging should be applied. Reference calculations showed that choices regarding the amount of independent soil layers and the degree of spatial averaging have a large influence on the reliability. More fundamental research to these topics is therefore recommended.

LIST OF ABBREVIATIONS

AR	Abdo-Rackwitz
CC	Consequence Class
CMCS	Crude Monte Carlo Simulation
COBYLA	Constraint Optimization By Linear Approximation
CPT	Cone Penetration Test
DS	Directional Sampling
COV	Coefficient Of Variation
CUR	Civieltechnisch Centrum Uitvoering Research en Regelgeving
EC	Eurocode
EMO	Europees Massagoed Overslagbedrijf
FEM	Finite Element Method
FORM	First Order Reliability Method
GWL	Ground water level
LLWS	Low Low Water Spring
LSF	Limit state Function
LSFE	Limit State Function Evaluation(s)
MCS	Monte Carlo Simulation
OWL	Outer water level
PDF	Probability Density Function
SLS	Serviceability Limit State
ULS	Ultimate Limit State
UC	Unity check
RC	Reliability Class

LIST OF SYMBOLS

Reliability symbols

α	Sensitivity factor	[-]
β	Reliability index	[-]
μ	Mean	[-]
σ	Standard deviation	[-]
γ	Partial factor	[-]
P_f	Failure probability	[-]
X_k	Characteristic value / Representative value	[-]
X_d	Design value	[-]
X_i	Random variable of vector X	[-]
X^*	Design point in FORM	[-]
Z	Limit state function	[-]

Geotechnical symbols

α_t	Pile class factor	[-]
c	Cohesion	[kPa]
γ_{unsat}	Unsaturated volumetric weight	[kN/m ³]
γ_{sat}	Saturated volumetric weight	[kN/m ³]
τ	Shear stress	[kPa]
φ'	Friction angle	[°]
Ψ	Dilatancy angle	[°]
δ	Wall friction angle	[°]
E_{oed}^{ref}	Oedometer stiffness	[kN/m ²]
E_{50}^{ref}	Secant stiffness	[kN/m ²]
E_{ur}^{ref}	Unloading / Reloading stiffness	[kN/m ²]
K_0^{nc}	Neutral lateral earth pressure coefficient for non-consolidated soil	[-]
K_a	Active lateral earth pressure coefficient	[-]
K_p	Passive lateral earth pressure coefficient	[-]
m	Power in stress-dependent stiffness relation	[-]
Msf	Safety factor from a phi-c reduction in Plaxis	[-]
q_c	Cone resistance	[MPa]
R_{inter}	Interface strength ratio	[-]

Structural properties

A	Area	[m ²]
D_{tube}	Diameter tubular pile	[m]
E	Youngs' modulus	[kN/m ²]
f_y	Yield strength	[N/mm ²]
M	Moment force	[kNm]
N	Normal force	[kN]
O	Circumference	[m]
t_{tube}	Wall thickness tubular pile	[m]
W_{el}	Elastic section modulus	[m ³]

TABLE OF CONTENTS

ACKNOWLEDGMENTS	V
SUMMARY	VII
LIST OF ABBREVIATIONS	VIII
LIST OF SYMBOLS	IX
1 INTRODUCTION	1
1.1 Background	1
1.1 Problem definition	1
1.2 Objective and research questions	2
1.3 Thesis outline	2
2 THEORETICAL BACKGROUND	4
2.1 Quay walls	4
2.1.1 History of quay walls in Rotterdam	4
2.1.2 Functions of a quay wall	5
2.1.3 The Rotterdam quay wall	6
2.2 Soil mechanics related to quay walls	9
2.2.1 Lateral earth pressure	9
2.2.2 Working of a relieving platform	10
2.3 Modelling of soil and structure	12
2.3.1 Soil models	12
2.3.2 Limitations	12
2.5 Uncertainty and reliability	15
2.5.1 Sources of uncertainty in Civil Engineering	15
2.5.2 Safety philosophy	16
2.6 Design methods	17
2.6.1 Level IV	17
2.6.2 Level III	17
2.6.3 Level II	19
2.6.4 Level I	21
2.6.5 Level 0	23
2.7 Design guidelines for quay walls	24
2.7.1 CUR 166 Sheet pile structures	24
2.7.2 CUR 211 Quay walls	24
2.7.3 Probabilistic background of the CUR211	24

2.8	Conclusion	27
3	METHOD DESCRIPTION	28
3.1	Selection of Failure Mechanisms	29
3.2	Limit State Functions	31
3.2.1	Failure of combi-wall profile	31
3.2.2	Anchor rod failure	33
3.2.3	Soil mechanical failure	34
3.3	Coupling of FEM with Reliability Analysis Methods	36
3.3.1	Main findings in previous research on coupling Reliability Analysis Methods with Plaxis	36
3.3.2	Overall conclusion	38
3.3.3	Functionality of ProbAna	38
3.3.4	Selection of FORM algorithm	40
4	STARTING POINTS	41
4.1	Introduction	41
4.2	Soil parameter uncertainties	42
4.3	Structural parameters	45
4.4	Geometrical parameters	47
4.5	Load parameters	48
5	CASE STUDY 1: DOUBLE ANCHORED COMBI-WALL	49
5.1	Introduction	49
5.2	Starting points	50
5.2.1	Soil parameters	50
5.2.2	Structural parameters	52
5.2.3	Construction stages and meshing	53
5.2.4	Loads, water levels and geometry	53
5.3	LS1: Yielding of the combi-wall	54
5.3.1	FORM sensitivity analysis	56
5.3.2	FORM with correlated parameters	57
5.3.3	Run with characteristic yield strength	59
5.3.4	Influence of time-dependent loads	62
5.3.5	Validation of Abdo-Rackwitz algorithm	63
5.3.6	Redesign of the retaining wall	64
5.3.7	First conclusions	65
5.4	LS2: Yielding of the anchor rod	66
5.5	LS3: Soil mechanical failure	68
5.6	Intermediate conclusion	71
5.6.1	Reliability of the structure	71

5.6.2	Plaxis-FORM coupling (ProbAna)	71
5.7	LS4: Shear resistance of anchorage inadequate	73
5.8	Derivation of partial factors	78
5.8.1	Approach	78
5.8.2	LS1: Yielding of the wall	79
5.8.3	LS2: Yielding of the anchor bar	81
5.8.4	LS3: Soil mechanical failure	81
5.8.5	Differentiation between Reliability Classes	82
5.8.6	Overall conclusion partial factors	83
6	CASE STUDY 2: QUAY WALL WITH RELIEVING PLATFORM	85
6.1	General description of the structure	85
6.2	Description of the measurement program	87
6.3	Approach for calibration and reliability analysis	89
6.4	Calibration of the model	91
6.4.1	Measured displacements versus calculated displacements	92
6.5	Probabilistic calculations	94
6.5.1	Starting points	94
6.5.2	LS1: Soil mechanical failure	94
6.5.3	LS2: Yielding of the combi-wall	96
7	DISCUSSION	98
7.1	Influence of soil stratification	98
7.2	Influence of the stochastic description of soil parameters	98
7.3	Extreme values for soil parameters in FORM design points	100
7.4	Influence of the use of monitoring data on the reliability	101
7.5	Wider applicability of the results of both case studies	102
8	CONCLUSIONS AND RECOMMENDATIONS	103
8.1	Conclusions	103
8.2	Recommendations	106
	REFERENCES	108
	APPENDICES	
A	Fault tree for CUR211, first edition	113
B	Performance of algorithms OpenTURNS	115
C	Monte Carlo Simulation for Structural properties combi-wall	120
D	Fault tree simple quay wall	124

E	Plaxis output results simple quay wall	126
F	FORM output simple quay wall	129
G	FORM output for deriving partial factors	131
H	Plaxis soil models	133
I	Soil profile EMO	136
J	FORM output EMO quay wall	140
K	FORM output EMO quay wall for non-calibrated design	142

1

INTRODUCTION

1.1 Background

In the Netherlands thousands of kilometres of quay walls have been built. These quay walls are used for all kinds of purposes. You can think for example of quay walls in city centres and quay walls in port areas. Although we have gained a lot of experience and knowledge over the years regarding the design and construction of these type of structures, still a lot of topics remain not fully understood. One of the main challenges lies in the description and modelling of the soil and its interaction with the structure. Of course, with local soil investigation useful information regarding soil stratification and soil properties is gathered. However it does not provide specific information regarding the soil-structure interaction. Uncertainties in the soil properties arise due to several causes:

- Spatial variability of soil properties
- Sample disturbance in laboratory tests
- Imprecision of in-situ testing methods
- Imprecision and differences in laboratory tests and equipment

For the design of quay walls the engineer has to account for all the uncertainties. Apart from uncertainties in the description of the soil also other aspects are uncertain, think of the uncertainty in the use of the quay walls during their lifetime or the lack of knowledge to describe reality with a model. These uncertainties have to be accounted for to guarantee a reliable design. To quantify reliability, it is coupled to the probability of failure of a structure. In design guidelines, the reliability of a quay wall is expressed in a reliability index (β), which is directly related to the probability of failure. Based on the consequences of failure, a specific value for the reliability index, the target reliability, is prescribed. Structures with high economical and societal risk require a higher degree of safety than structures with minimal consequences in case of failure.

Current design guidelines make use of a semi-probabilistic method (Level I) to reach the prescribed target reliability. This method makes use of partial safety factors to account for the uncertainty in the model, the load and the resistance. The magnitude of these factors is either based on experience gathered in large amount of completed projects or calibration with a probabilistic analysis (Level II or level III). As guidelines should be applicable to a certain range of similar structures, the partial factors should guarantee the safety in all of these cases. This can result in conservative values of the partial factors and respectively 'over-design' of the structure.

1.1 Problem definition

The main reasons why almost all quay walls are designed using a semi-probabilistic method instead of a full probabilistic analysis are the lack of statistical data, the complexity of a full probabilistic method and the time it takes to perform such an analysis.

Calibration studies regarding partial factors for quay walls, mostly in the Port of Rotterdam, have been performed in the past by Huijzer (1996), de Grave (2002), Havinga (2004) and Wolters (2012). However probabilistic calculations with more advanced soil models, like the Plaxis Hardening Soil model, for quay walls with relieving platform has only been performed by Wolters. Therefore it is still a relatively open field of research. Thus, it is uncertain whether the semi-probabilistic design method results in the required level of safety. It is possible that quay walls have more capacity than expected and thus are safer, which would allow heavier loading of the quay wall or alternatively a cheaper design. On the other hand quay walls might turn out less safe than expected.

To get better insight into this question, multiple quay walls within the Port of Rotterdam have been equipped with sensors to measure e.g. water levels, anchor forces and displacements, resulting in monitoring data of many years. This data provides useful information about how well a model predicts the actual behaviour of a quay wall

1.2 Objective and research questions

The main questions described in the problem definition is whether the use of a semi-probabilistic design approach for quay walls results in the required level of safety and the most cost-efficient design. This can be investigated by performing a full probabilistic analysis in which the uncertainties in the load and resistance parameters are taken into account. The objective of this research is threefold:

- 1 Establishing the actual reliability index of a quay wall in operation
- 2 Exploring possibilities for an increase in retaining height making use of probabilistic calculations
- 3 Verifying the partial factors of the current design guidelines

The term actual refers here to the as-built design of the structure and the more or less known loading conditions. The availability of monitoring data for the quay wall with relieving platform considered in this research allows for a calibration of the Plaxis-model, which subsequently will be used as a starting point for the probabilistic calculations.

The following sub questions will help to reach the above described objectives:

- 1 What are the most suitable probabilistic methods to determine the reliability of a quay wall modelled with FEM?
- 2 What are the most sensitive parameters for each failure mode and for the overall system reliability?
- 3 How can monitoring data be used for model calibration and parameter distribution updating ?
- 4 How can this research contribute to an improvement of the current design guidelines?

Answers to these questions will be gathered in this thesis in order to contribute to the main objectives.

1.3 Thesis outline

This subchapter describes the outlines of the report. Starting with Chapter 1, in which the problem is defined and the main objective of the thesis is described.

Chapter 2 covers a summary of the performed literature study. First the history of quay walls in Rotterdam has been described together with the main functions and components of a quay wall. The knowledge about the most relevant soil mechanics is summarized. Thereafter, the different types of uncertainty that play a role in the design or assessment of a structure are defined. Then, the concept of safety and the different design methods to account for uncertainty are described. This knowledge is helpful to understand the background of the relevant codes and guidelines for the design of quay walls, which are elaborated at the end of the chapter.

In Chapter 3 the methodology of the research is given. First, a more thorough analysis in the system reliability of a quay wall will be performed. The fault tree presented in Chapter 2 will be discussed and it will be decided which failure mechanisms will be assessed and which one will be left out of this research. For each failure mechanism the limit state function will be formulated and the appropriate probabilistic method should be chosen to perform the limit state evaluations based on a consideration of computational effort, accuracy and stability. Thereafter the coupling between a FEM and a reliability analysis by using ProbAna is explained.

In chapter 4 the starting points for the two considered case studies are defined. Already many research has been done into the statistical distributions and correlations between parameters. Therefore, to save time, the determination of the parameters will be mainly based on the findings in previous research.

Chapter 5 is devoted to the first case study, in which a simple quay wall is handled. First, the quay structure is described together with all the assumptions made. Thereafter, the reliability index for four mechanisms have

been determined for the as-built structure. In the end of this chapter, a new set of partial factors is derived based on the outcomes of the probabilistic calculations. These partial factors are compared with the current prescribed factors and their validity has been discussed.

Chapter 6 covers the case study about a quay wall with relieving platform. At first, the structure is described together with the monitoring program for this quay wall. Following, the calibration of the model using the monitoring data is treated. Thereafter, for two critical limit states the failure probability is determined.

In chapter 7 the obtained results of the research are discussed. The influence on the reliability of changing the soil stratification and the stochastic description of soil parameters is investigated. Also the influence of the use of monitoring data with respect to the reliability is investigated.

To end, in chapter 8, the conclusions and recommendations will be given.

2

THEORETICAL BACKGROUND

In this chapter the existing knowledge about quay walls, uncertainties and reliability is described. The chapter is predominantly focussed on quay walls in the region of the Port of Rotterdam. In the first subchapter the focus is on the structure itself, while the second subchapter is devoted to the soil behaviour and interaction of the soil with the quay wall structure. Thereafter the different sources of uncertainty are treated together with design methods to account for these uncertainties.

2.1 Quay walls

To get a better understanding of the choices made in the design of quay walls, the development of the quay walls in Rotterdam is analysed by considering its history, functions and structural elements.

2.1.1 History of quay walls in Rotterdam

The easiest method to transport large amounts of heavy goods has always been over water as it requires relatively seen the least amount of energy. The oldest sea trade is dated from already 6000 years ago in the region of Egypt, where they transported cargo like grains and cattle over sea. It was not before the seventeenth century the Port of Rotterdam really started to develop. In the city centre of Rotterdam the first quays were constructed to accommodate fishing boats. In the late 19th century, with the start of the industrial revolution in the Netherlands, the port started to develop rapidly, see Figure 2.1. The introduction of new materials like steel and the introduction of ship engines had a large impact on the vessel size and therefore on the draught of the vessel.

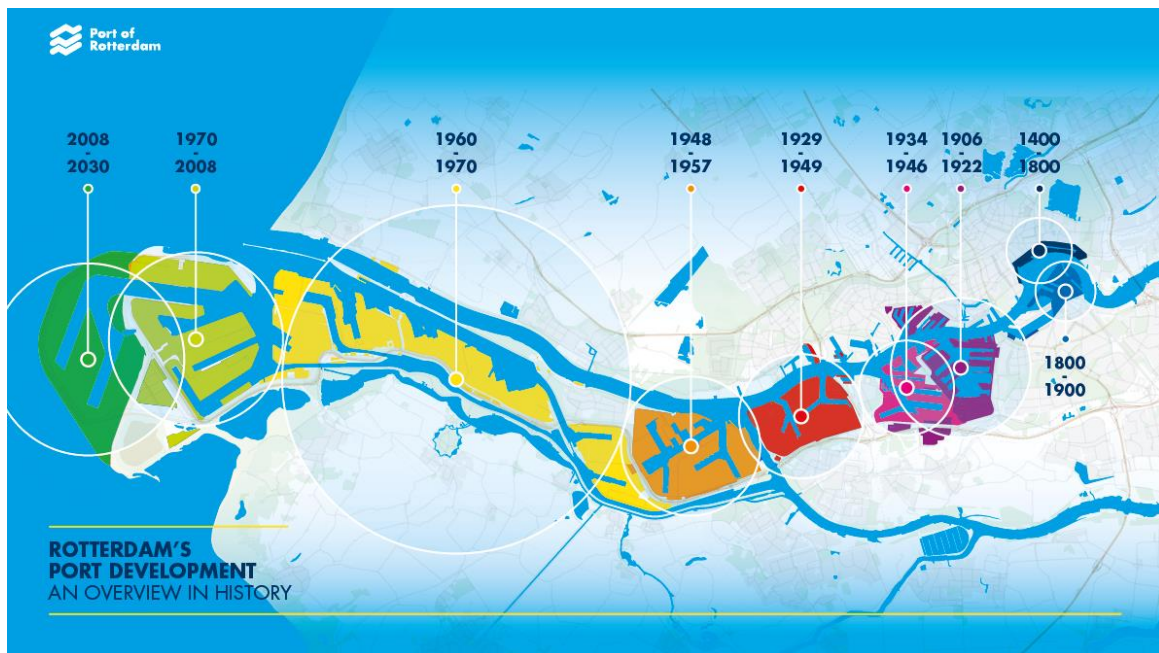


Figure 2.1 Rotterdam's port development. Source: Port of Rotterdam (n.d.)

This required larger water depths and therefore the port started to grow in the direction of the sea, where larger depths were available. The increase in retaining height of quay walls also resulted in changes in the design. Due to the soft clay and peat deposits in Rotterdam, gravity type structures were losing popularity

because of the expensive soil improvements that were required. Therefore quay walls on foundation piles were introduced in the period around 1930 to cope with this problem, see Figure 2.2.

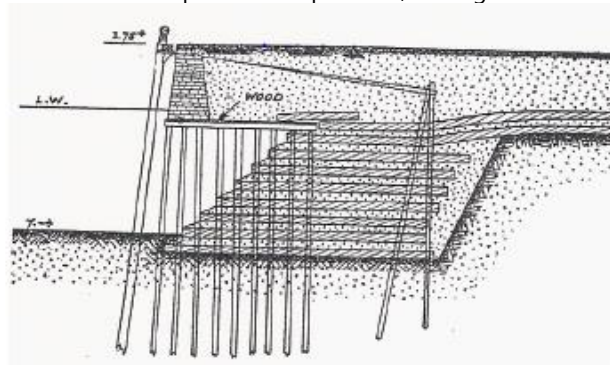


Figure 2.2 Cross section of a quay wall in Rotterdam, 1930, Source: de Gijt (2010)

After the Second World War, in which large parts of the port were destroyed, the Port of Rotterdam was quickly rebuilt and started to grow to a port of world size. Especially the handling of dry bulk, liquid bulk and containerized goods contributed to the growth up to the largest port in the world in 1962. The continuous increase in retaining height, crane size and surcharge load resulted in further adaption of the quay wall structures. A more or less typical quay structure was arising in PoR, shown in Figure 2.3. This typical "Rotterdam quay wall" will be further described in the remainder of this chapter.

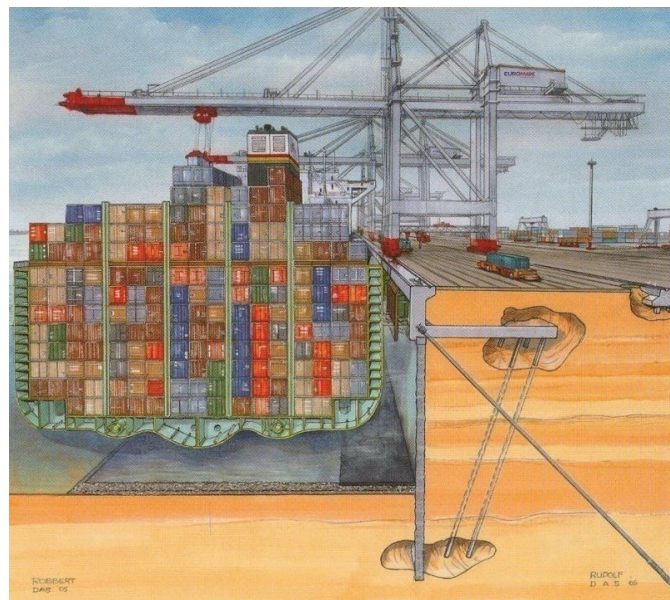


Figure 2.3 Cross-section of the Euromax terminal in Rotterdam, 2007. Source: de Gijt (2010)

2.1.2 Functions of a quay wall

Before going more in depth into the composition of the quay wall, first the main functions will be elaborated for a better understanding of the relevance of the different components. The main functions a quay wall can explained on the hand of Figure 2.3.

- Retaining function
As depicted, the quay wall creates a clear separation between soil and water. Without the quay wall it would not be possible to create a step in surface level of 26,5m. The result of this sharp separation is a large horizontal load of the soil body to be retained by the quay structure. Another important aspect is the water retaining function. As ports are often in coastal zones, the port can be part of a flood protection system. With a sufficient height of the surface level, a flood will not be able to reach the hinterland.
- Mooring function
The container vessel that is depicted is moored nicely along the quay. However, this is not so self-evident as it seems. The vessels position is influenced by hydraulic conditions like currents, waves and

wind, whereas for safe container handling, the vessel is not allowed to move significantly. By mooring of the vessel, the hydraulic loads on the vessel are transferred via the mooring lines and the bollards to the quay structure, making container handling or other ship to shore activities possible.

- Protection function

Before the vessel is moored along the quay, a whole operation of approaching the quay, called berthing, is already behind. With a large vessel and expensive quay structure it should be prevented that one of the two get damaged. This is realised by the installation of fenders and berthing dolphins. Fenders are (often) steel objects attached to the side of the quay wall. When the vessel is approaching the quay, the hull of the vessel is pushing against the fender. The fender is relatively elastic in comparison with the concrete top structure of the quay and deforms during the berthing process. With this deformation, the kinetic energy of the vessel is adopted by the fender, leaving the quay and the vessel undamaged. The force in the fender is transferred to the quay though and have to be further transferred to the soil.

- Bearing function

On the land side of the quay wall, port operations like loading and unloading of the vessel and storage of goods close to quay are ongoing. This results in mainly vertical loads imposed on the quay structure and the adjacent soil body. The quay wall must be able to bear the imposed loads to guarantee safe and secure port operations.

2.1.3 The Rotterdam quay wall

Although several solutions are available for the design of a quay wall, most of the quay walls in Rotterdam show a similar type of design. To be able to explain this, the different type of retaining structures are considered together with their applicability in the Port of Rotterdam:

- Gravity structures (Picture A of Figure 2.4)

The main principle of this type of structure is to use the weight of the structure to create sufficient friction between soil and structure to resist the lateral loads.

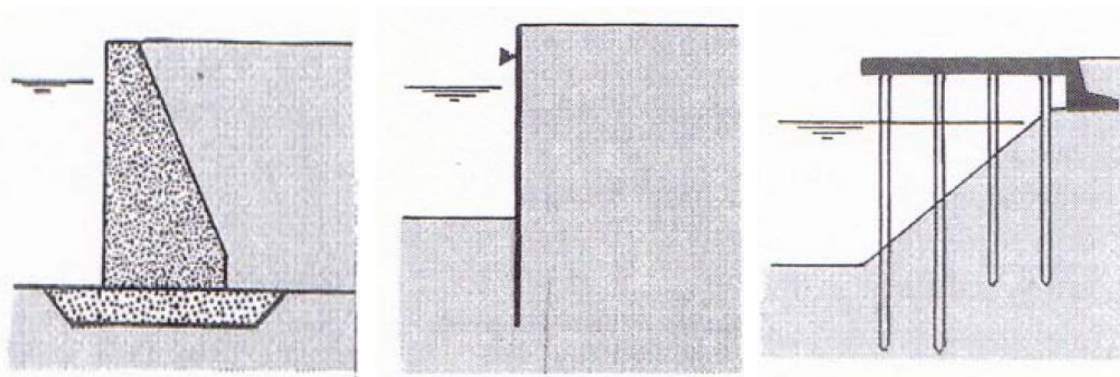
- Sheet pile structures (Picture B)

Sheet pile structures creates a balance between horizontal loads by their extra embedded depth and/or installed anchors

- Piled structures (Picture C)

Piled structures are basically a concrete deck element supported by vertical or raked piles. This type of structure allows for an open structure where the water can flow underneath the top element

- Combinations of the above mentioned types



A) Gravity structure

B) Sheet pile structure

C) Piled structure

Figure 2.4 Different types of quay wall structures. Source: de Gijt (2010)

For the design of a quay wall the designer has to make a decision on which type to use. This decision is influenced by many factors, of which the most important are:

- geological conditions
- retaining height
- loading on the structure
- constructability

Due to the heavy weight of gravity type structures, a significant load on the subsoil is imposed and therefore good subsoil conditions are required. In Rotterdam the subsoil consists of several very weak layers of peat and clay making soil improvements a prerequisite for this type of structures. Besides, all vertical loads and the moment generated by the horizontal loads have to be taken by only compressive stresses in the subsoil, which can cause problems in case of large retaining heights.

Sheet pile structures are a more convenient solution in case of weak soil conditions. Especially with the use of anchors to reduce the horizontal load on the sheet pile, this system is cheap and relatively easy to construct. However, in case of large retaining heights (>15m) and heavy surcharge loads problems start to arise with respect to constructability, bending moment resistance and vertical bearing capacity of sheet piles. The driveability of sheet piles is limited to approximately 30-35m, after which the chance of interlocking failure and damage to sheet piles considerably increases. This problem, together with the other two, can be partly solved by the use of combi-walls. This is a combination of steel tubular piles with sheet pile elements in between. The tubular piles take the main loads in this system, whereas the sheet pile elements function as retention for soil and water. For retaining heights larger than 20m, this system reaches its limits as well.

Piled systems are a suitable solution as well in case of soft soil deposits. Large surcharge loads can be easily transferred to the subsoil with this system. The horizontal resistance of a pile system is limited though and thus a system that combines the benefits of both a piled system and a sheet pile system have arisen in the Port of Rotterdam (Figure 2.5).

The structure consist of a concrete superstructure with a relieving platform placed several meters below ground level. The superstructure is supported by a combi wall at the waterfront, compression piles at the back side and an anchor placed under an angle of approximately 45 degrees. The relieving platform creates many benefits; as the word says, it has a relieving function. Surcharge loads and the weight of the soil above the platform is transferred through the piles to the subsoil and therefore the combi wall is relieved from the resulting horizontal earth pressures and can have smaller dimensions.

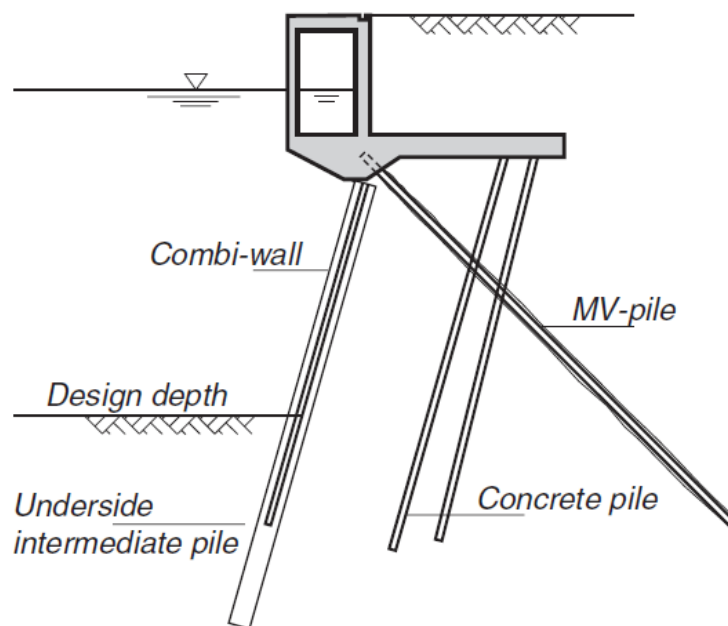


Figure 2.5 Quay wall with relieving platform. Source: CUR211 (2013)

A second advantage is the reduction in required length of the combi wall, reducing the risks with respect to driveability. Another advantage of the low position of the relieving platform is the prevention of corrosion of the steel combi wall. In the splash zone, the zone just above the high tide level, corrosion seems to be the most severe and also the most difficult to prevent. With the combi wall starting at a level below low tide, corrosion can be prevented more easily and a longer lifetime is guaranteed. The downsides of a low lying relieving platform are the costs and the constructability of the superstructure. A deeper construction pit is required and the loads on the concrete structure increase with depth. Therefore a balance should be found between the savings on the piles and the extra costs of a larger superstructure.

Both the combi wall and the compression piles are placed under an angle. In this way, the piles can take up lateral loads on the superstructure in their axial direction as well, reducing the horizontal load on the anchors and the combi wall. The combi wall is often placed directly under the crane rail track of the of the quay, so that crane loads can directly be transferred to the combi wall without inducing large bending moments in the superstructure.

These main design principles can be recognized in most quay walls with a large retaining heights in Rotterdam. Client specific requirements and local boundary conditions make that quay walls still deviate at certain aspects from one to another.

2.2 Soil mechanics related to quay walls

The main load on a quay wall as well as the resistance of the quay wall is provided by the surrounding soil. Therefore the soil mechanics that play a role in the design of a quay wall are discussed in this subchapter.

2.2.1 Lateral earth pressure

Most quay wall structures in the Netherlands consist of a sheet pile wall. The main mechanism of a sheet pile wall is the allowance of displacements and rotations of the sheet pile wall to generate active and passive soil pressures in the adjacent soil body. Depending on the displacement of the retaining wall three stages are defined (Figure 2.6):

- The retaining wall does not displace → Neutral soil pressures
- The retaining wall moves away from the soil → Active soil pressures
- The retaining wall moves into the soil → Passive soil pressures

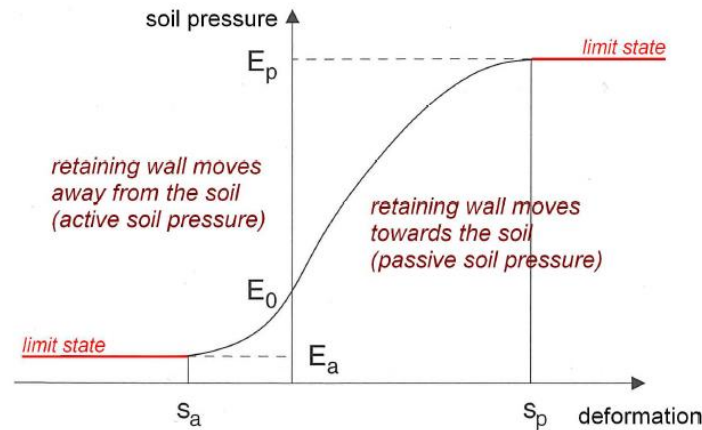


Figure 2.6 Correlation between soil pressure and deformation. Source: Vrijling et al. (2015)

The horizontal effective soil stresses are correlated to the vertical effective soil stresses with the use of soil pressure coefficients:

$$\sigma'_a = \sigma'_v K_a + 2c'\sqrt{K_a} \quad (2.1)$$

$$\sigma'_p = \sigma'_v K_p + 2c'\sqrt{K_p} \quad (2.2)$$

For the derivation of the earth pressure coefficients it is assumed that before failure occurs, large deformations in the wall develop and that the limit states of active and passive soil pressures are reached. The elasticity and yielding capacity of steel sheet piles allows for these displacements and therefore support this assumption. Several analytical expressions are derived for the lateral earth pressure coefficients. Coulomb (1776) was the first one to study the lateral earth pressures on retaining structures. He derived his expressions in an analytical way, assuming failure along predefined straight slip surfaces (Verruijt & van Baars, 2009):

$$K_a = \frac{\sin^2(\alpha + \varphi)}{\sin^2 \alpha \sin(\alpha - \delta) \left[1 + \frac{\sqrt{(\sin(\varphi + \delta) \sin(\varphi - \beta)) / (\sin(\alpha - \delta) \sin(\alpha + \beta))}}{\sin^2(\alpha - \varphi)} \right]^2} \quad (2.2)$$

$$K_p = \frac{\sin^2(\alpha - \varphi)}{\sin^2 \alpha \sin(\alpha - \delta) \left[1 + \frac{\sqrt{(\sin(\varphi - \delta) \sin(\varphi + \beta)) / (\sin(\alpha - \delta) \sin(\alpha + \beta))}}{\sin^2(\alpha - \varphi)} \right]^2} \quad (2.3)$$

where

- α inclination of the wall
- φ friction angle
- δ wall friction angle
- β slope of the ground surface

The sign convention of the parameters is shown in Figure 2.7.

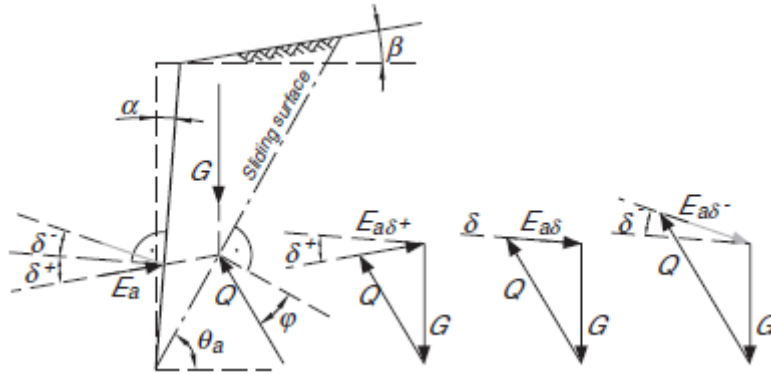


Figure 2.7 Sign convention of β , α and δ . Source: CUR211 (2013)

Especially for the case of passive earth pressure the assumption of straight failure planes is partly incorrect, as it can result in overestimation of the passive resistance. Therefore the answer should be interpreted carefully. Many theories with curved slip planes are developed to better represent the actual behaviour and achieve more reliable results. The theory of Caquot & Kerisel (1948) assumes an elliptical slip surface, which seems to represent the actual slip surface the most precise and is therefore widely used in geotechnical practice. This theory can however not be described with simple expressions (Ou, 2013)

2.2.2 Working of a relieving platform

As the horizontal active soil stresses on the sheet pile wall are depending on the vertical stresses, it is beneficial regarding the costs of the sheet pile wall to reduce the vertical stresses with a relieving platform. The relieving platform transfers the vertical loads, consisting of surcharge and the weight of the upper soil body, through the combi wall and vibro piles to the deeper sand layer. The width and depth of the platform is determinative for amount of reduction of horizontal earth pressures. The principle is shown in Figure 2.8. Just below the relieving platform the horizontal stresses are only generated by the small slice of soil below the relieving platform. The influence of the surcharge next to the relieving platform σ'_{k0} starts where the line of the angle of internal friction intersects the wall. The depth until which the influence of the relieving platform reaches is depending the width of the platform and the angle of the sliding planes in the different soil layers. The expression for θ_a holds:

$$\tan \theta_a = \frac{1 + \frac{1}{\cos \alpha} \sqrt{\frac{\sin(\varphi + \delta) \cos(\alpha + \beta)}{\cos(\delta - \alpha) \sin(\varphi - \beta)}} \sin \varphi}{\tan \alpha + \frac{1}{\cos \alpha} \sqrt{\frac{\sin(\varphi + \delta) \cos(\alpha + \beta)}{\cos(\delta - \alpha) \sin(\varphi - \beta)}} \cos \varphi} \quad (2.4)$$

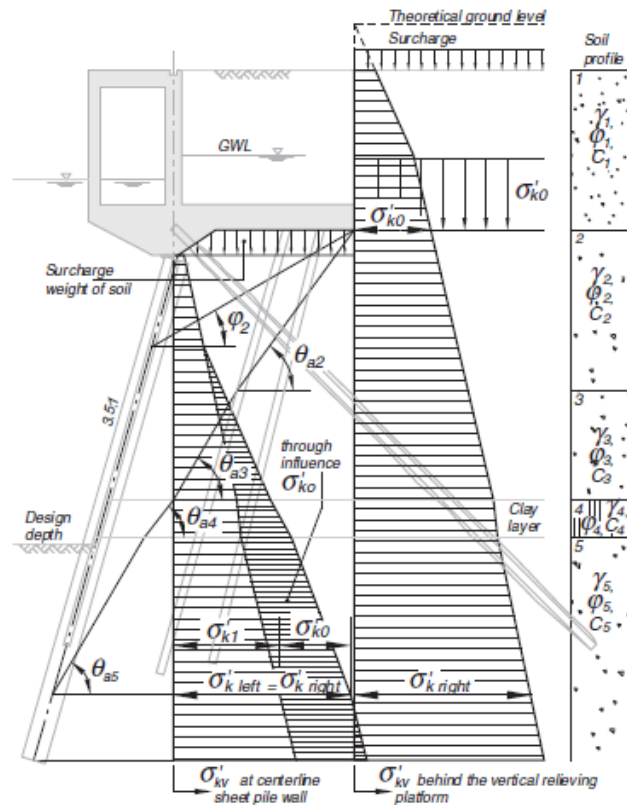


Figure 2.8 The effect of a relieving platform. Source: CUR211 (2013)

As Figure 2.8 shows, the influence of the relieving platform is almost reaching to the entire depth of the sheet pile wall.

When using equation 2.4 the wall friction angle should be chosen carefully. The wall friction angle on the active side of the wall is chosen positive when the adjacent soil settles more than the sheet pile wall. In most cases this situation holds, but in case of a bearing function of the wall the situation can change. Settling of the toe of the wall can result in relatively larger displacement of the wall with respect to the soil, which can imply a change in sign for the wall friction angle, resulting in larger horizontal earth pressures on the wall. This phenomena is illustrated in Figure 2.7 in which E_a represents the reaction force of the wall on the soil body, which is in the opposite direction of the resultant of active soil pressures on the wall.

The magnitude of the wall friction angle is depending on the roughness of the wall compared to the soil. In case of a smooth surface, the soil particles are less able to develop shear stresses than in the case of a soil-soil interface and therefore the wall friction angle is below the angle of internal friction of the soil. Research by Deltares showed that in general the wall friction angle lies between $\delta = \frac{2}{3}\phi'$ and $\delta = 0.8\phi'$. However, in the Netherlands most large quay walls are constructed with a combi wall instead of a flat wall. The assumed failure interface is a straight line in front of the quay wall which only partially interferes with the wall as shown in Figure 2.9. Therefore an interface strength ratio, which is the required input parameter in Plaxis, is assumed to be in the order of 0.8 to 0.9.

$$R_{int} \approx \frac{\tan(\delta)}{\tan(\phi')} \approx 0.8 \text{ to } 0.9 \tag{2.5}$$

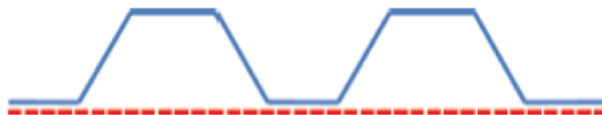


Figure 2.9 Failure interface of a sheet pile wall. Source: CUR211 (2013)

2.3 Modelling of soil and structure

The shape of a quay wall and the behaviour of soil are often too complex to describe with simple analytical equations, whereas advanced equations e.g. partial differential equations become too complex to solve analytically. Besides, the soil-structure interaction can hardly be described with analytical equations. This can result in inaccurate outcomes in (geo)technical calculations of e.g. forces and displacements.

With the development of the Finite Element Method the soil and the structure are described in a more fundamental way. Finite Element refers to the fact a structure is divided in a finite number of small elements. These elements are all interconnected by nodes. The partial differential equations that describe the constitutive relations, are discretized and approximated in the nodes. Together with the boundary conditions in the nodes, the set of equations is solved using matrix computations. This finally results in displacements and stresses for the entire considered structure.

The number of nodes, or the mesh size, determines for a large part the accuracy of the calculations. A finer mesh leads to more accurate results but the downside is the increase in computational time.

The most commonly used FEM-software to model soil-related problems in the Netherlands is Plaxis. This software package is thus used throughout this thesis.

2.3.1 Soil models

Within Plaxis multiple material models are available for the description of the behaviour of the soil. The applicability of a method depends on the soil type and the required accuracy of the calculation. For soils in the Netherlands the constitutive models based on the criterion of Mohr-Coulomb are most relevant.

The three models that obey this criterium are:

- Mohr-Coulomb model
- Hardening Soil model
- Hardening Soil model with small strain stiffness

A detailed description of the three models is given in Appendix H. When comparing the three models, it can be stated that the Hardening Soil model is the most accurate method for modelling the soil as it accounts for stress-dependant stiffness and the cap yield surface in a more comprehensive way than the Mohr-Coulomb model. The Hardening Soil model with small strain stiffness accounts for stiffer behaviour of soils for small strains. For performing probabilistic calculations in Plaxis, the regular Hardening Soil model is assumed to be accurate enough, as the addition of small strain stiffness also increases the computational effort.

2.3.2 Limitations

As previously stated, a model cannot perfectly describe reality. Therefore the user of a model should always be aware of the limitations of the model. It is important to know for what type of problem or situation a model was intended for. When a model will be used for other purposes, it might result in unreliable outcomes. Related to this is the input of model parameter. An often used sentence for the use FEM-models is "Rubbish in = Rubbish out" as the accuracy of a calculation mainly depends on the user. An experienced engineer knows the physical background of parameters and the shortcomings of a model and is therefore able to critically judge the outcomes.

2.4 Failure mechanisms and Fault Tree

The main objective of designing is to prevent failure of the structure for its entire design lifetime. Failure is defined as the condition in which the structure is not able to fulfil one or more of its functions anymore. It is therefore relevant to know all the possible ways the structure can fail so that no failure mechanism is overseen in the reliability analysis. For the check on failure, two types of limit states are distinguished:

- Ultimate Limit State (ULS)
- Serviceability Limit State (SLS)

The ULS refers to a state in which in case of exceedance, the structure or part of the structure fails or collapses. This state resembles an extreme situation that will only occur seldomly.

The SLS is referred to the performance of a structure during normal daily conditions. It is more related to the non-usability of the structure than to failure. For example in case of too large deformations of a quay wall, the

internal distance of a crane track can become too large, resulting in non-usability of the crane. No failure has occurred but still the functionality has decreased.

2.4.1 Fault tree

A fault tree gives a good overview of the different ways a structure can fail. The fault tree presented in Figure 2.10 is an example of a fault tree for a quay wall. The top event in the tree is the collapse of the quay wall which is caused by either excessive deformations or quay wall failure. The term excessive deformation is more related to SLS. Deformations do not directly result in collapse of the quay wall, but it can possibly hinder the quay wall from fulfilling its functions. The term 'collapse of the quay wall' as top event is therefore maybe not the right description. The other event, failure of the quay wall, is related to the ULS. Failure in ULS can be caused by either the failure of one of the primary components or other failure mechanisms:

- Failure of the combi wall
- Superstructure fails
- Bearing piles fails
- Tension member fails
- Lack of equilibrium
- Groundwater flow too high
- Other causes

Failure occurs if one on the above mentioned mechanisms is activated, which implies that the system can be considered as a serial system, symbolised by an OR-gate in Figure 2.10. The seven failure mechanisms are consisting of underlying secondary failure mechanisms. In general two main types of failure mechanisms are distinguished: soil mechanical failure and structural mechanical failure. All the soil mechanical failure mechanisms are depending for a large part on the same soil characteristics and therefore dependency between different soil mechanical failure mechanism exists. Besides, the load in both soil mechanical and structural mechanical failure mechanisms is also mainly determined by the soil. This makes that the system for failure of the quay wall can be considered as a serial system with a certain dependency between the different failure mechanisms.

In general the failure probability of the top event of the tree is calculated using a bottom-up approach. First the failure probabilities of all the base events are calculated, whereafter all higher order events can be calculated to finally arrive at the top event. The degree of the dependency between failure modes is important for the calculation of the overall failure probability. However, it is difficult to exactly quantify this dependence. There are three standard cases for which analytical solutions hold (Table 2.1):

Table 2.1 Standard cases of a series system

	Mutually exclusive	Independent	Fully dependant
Correlation coefficient ρ	-1	0	1
System failure probability	$\sum_{i=1}^n P_i$	$1 - \prod_{i=1}^n (1 - P_i)$	$\max(P_i)$
Boundary	Upper bound (safe)		Lower bound (less safe)

These are extreme boundaries, the reality is often somewhere between independent and dependent. The consequence of the choice for the type of dependency on the system reliability is determined for the fault tree of CUR211 (Appendix A) and is given in Table 2.2. This table shows that the failure probability decreases roughly by a factor 3 when assuming full dependency. Although these are extreme boundaries, it shows that taking no correlation into account is a conservative/safe assumption. This research focusses only on a limited amount of failure mechanisms.. Hence, it will not be possible to calculate the failure probability of the system. The selection of the failure mechanisms is treated in Chapter 3

Table 2.2 Failure probability for quay wall failure for different limit cases of dependency

	Mutually exclusive	Independent	Fully dependant
Correlation coefficient ρ	-1	0	1
β_{system}	3.4	3.4	3.7
Failure probability	$3.37 \cdot 10^{-4}$	$3.37 \cdot 10^{-4}$	$1.05 \cdot 10^{-4}$

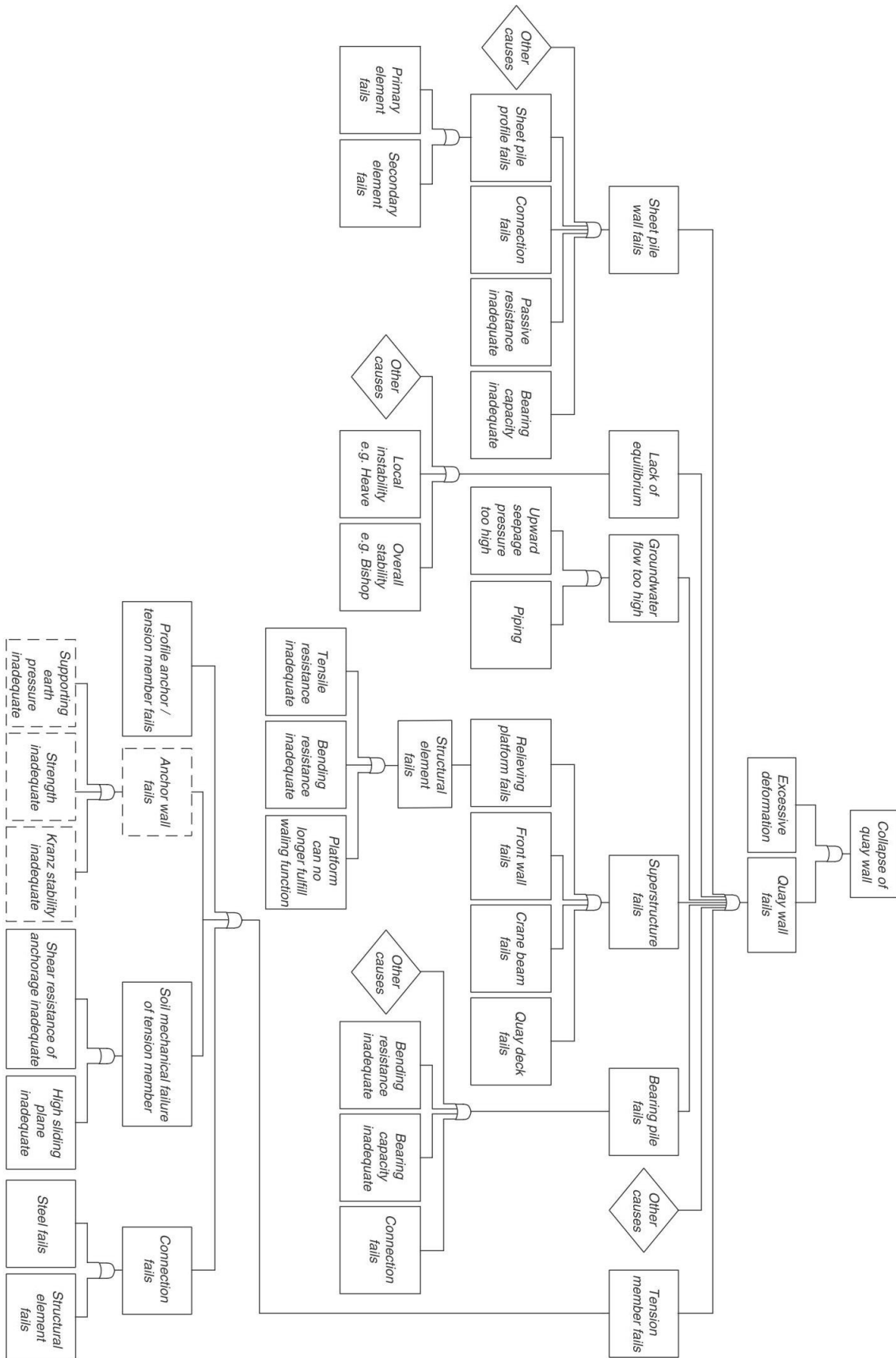


Figure 2.10 Fault tree of a quay wall. Source: CUR211 (2013)

2.5 Uncertainty and reliability

2.5.1 Sources of uncertainty in Civil Engineering

When designing a structure, uncertainty plays a key role. Uncertainty is present in all kind of different ways. Usually the availability of statistical data is limited and therefore the exact value of a parameter is uncertain. But not only the parameters are uncertain, some phenomena in the engineering world are not fully understood or too complex to describe in a model. To be able to design for those uncertainties, it is helpful to know what type of uncertainties are present and how they can be reduced:

The uncertainties can be divided into two categories (van Gelder, 2000):

- inherent uncertainties
- epistemic uncertainties

These two main categories are divided in five subcategories (Figure 2.11):

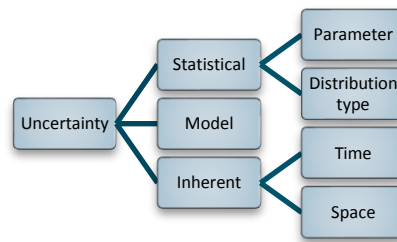


Figure 2.11 Types of uncertainties. Source: van Gelder (2000)

Inherent uncertainties are related to the randomness that exist in nature. Mankind is not able to exactly predict what will happen in the future, for example what the highest water level will be during the working design life time of a structure, even when a large historical dataset is available. The inherent uncertainty, also called aleatory variability, is divided into uncertainty in time and in space. The uncertainty in time is already mentioned above with the example of the prediction of the water level. This type of uncertainty cannot be reduced. Uncertainty in space is related to the fact that for example the soil properties vary in space. In theory it is possible to know all the soil properties in a considered area by doing an infinite amount of tests, but in practice this is not possible and hence you have to take the variability in the soil into account

Epistemic uncertainties consists of model and statistical uncertainties. Model uncertainties arise from the fact that processes in reality are too complex and not fully understood to describe exactly in a model. Assumptions and simplification are therefore made to be able to model a process or structure, resulting in model outcomes that have a certain degree of uncertainty. Model uncertainties can be reduced by using a more elaborated model or doing more research, but it will never fully eliminate all uncertainties.

Statistical uncertainties occurs due a limited availability of data and can be divided into parameter uncertainty and distribution type uncertainty. Parameter uncertainty relates to the size of the dataset. For a larger dataset the distribution parameters of a variable can be estimated more accurate than for a small dataset. Also the decision on the distribution type is an uncertainty. Extreme water levels for example can be described by different distribution types. With limited data available it can be uncertain which distribution type fits the real extreme water level distribution the best.

For the design of a quay wall, especially the soil parameters are an important source of uncertainty. The uncertainty in these parameters mainly arise from: (Baecher & Christian, 2003)

- Spatial variability of soil properties
- Sample disturbance for laboratory tests
- Imprecision of in-situ testing methods
- Imprecision and differences in laboratory tests and equipment

The soil parameters are used in models to describe the soil behaviour, which are subsequently used in numerical models (e.g. FEM) of the complete structure. In this way the uncertainty in the soil parameters is

further entrained in the calculations due to multiple model uncertainties. This shows that uncertainty is accumulated in the design process.

2.5.2 Safety philosophy

By taking the uncertainty into account in the design a certain level of safety is reached. In a simple way a structure is considered to be safe when the resistance (R) is larger than the load or solicitation (S):

$$R > S \tag{2.6}$$

This criterion is the underlying background for every design approach. In the past a single value for load and resistance was determined by taking conservative values. The structure was considered safe when the requirement of equation 3.1 was met. This is a deterministic way of designing. The issue with this approach is that the values for the resistance and the load are stochastic variables and therefore the exact level of safety was uncertain, or in other words the probability of failure was unknown.

The probability of failure P_f is often formulated with the use of a limit state function (LSF). The LSF describes the boundary between failure and non-failure and is denoted here as Z:

$$Z = R - S \tag{2.7}$$

Failure occurs when $S > R$ so when $Z < 0$, so for the failure probability holds:

$$P_f = P_f[Z < 0] \tag{2.8}$$

As the resistance and the load are often depending on multiple stochastic random variables like material properties, actions and geometrical properties, the LSF is implicitly also a function of these variables and can be expressed as function of it in which \underline{x} is the vector consisting of n random variables:

$$g(\underline{x}) = Z \tag{2.9}$$

The probability of failure can be calculated if the Probability Density Function (PDF) of each variable is determined. When $f_{\underline{x}}(\underline{x})$ is the joint PDF of all n random variables together, the failure probability becomes:

$$P_f = \int_{g(\underline{x}) < 0} f_{\underline{x}}(\underline{x}) d\underline{x} \tag{2.10}$$

In case of only two dimensions, the joint PDF can be plotted in a graph as shown in Figure 2.12. The probability of failure in this case is equal to the volume under the graph of the joint PDF that is in the unsafe domain.

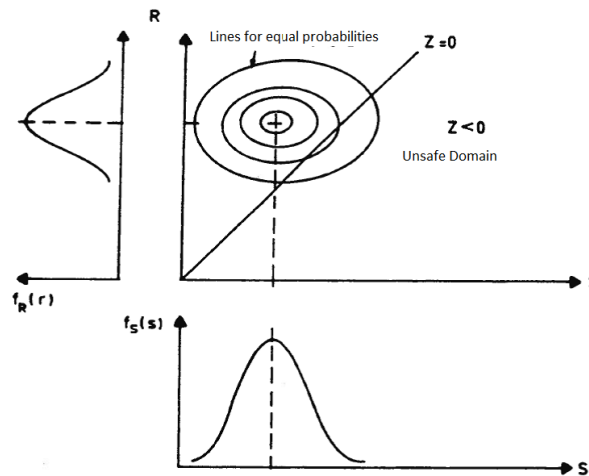


Figure 2.12 Joint probability density function in case of 2 dimensions. Source: Jonkman et al. (2016)

In design guidelines the target reliability for the design of a structure is often prescribed in the form of a reliability index (β). The target reliability is determined based on the consequences of failure and the working design lifetime. The probability of failure is directly related to the reliability index by:

$$P_f = \Phi(-\beta) \tag{2.11}$$

In which Φ represents the cumulative normal distribution. The reliability index describes the distance between the mean value of $g(\underline{X}) = Z$ and the limit state of Z ($Z=0$) in units of the standard deviation σ_Z as shown in Figure 2.13.

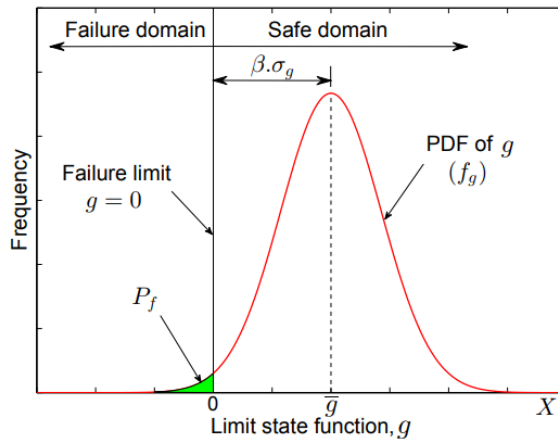


Figure 2.13 Limit state function and probability of failure. Source: Bach (2014)

2.6 Design methods

To design a structure that meets the requirements regarding reliability, several options are available ranging from basic methods to quite advanced probabilistic calculations.

The methods are divided into five levels:

- Level IV (risk-based)
- Level III (probabilistic)
- Level II (probabilistic with approximations)
- Level I (semi-probabilistic)
- Level 0 (deterministic)

2.6.1 Level IV

With a level IV approach the design of a structure is based on an optimisation between the risks (costs in case of failure) and the costs of the design. In this way the economic most beneficial solution can be determined. This approach is used in the design of dikes in the Netherlands. For every dike section the required reliability is determined based on the risks. This way of designing is generally quite time-consuming and expensive and is therefore mainly used for structures with large economical and societal risks.

2.6.2 Level III

A level III analysis is a full probabilistic method that calculates the failure probability exactly. It could be performed in an analytical way or with numerical integration but the most common way of performing a level III analysis is by using a Monte Carlo Simulation (MCS). A MCS is a sampling method that simulates a given situation numerous times and counts how many times failure occurs. This results are subsequently used to determine the failure probability of the structure. There are several techniques to perform a MCS, of which the most relevant ones for this research are described below:

Crude Monte Carlo simulation (CMCS)

The most simple and robust technique is the Crude Monte Carlo Simulation. In a CMCS, N samples are generated from the distribution function of every random variable in the system. For every set of sampled variables it is checked with the LSF whether failure occurs. The number of times this occurs is counted and

when all realisation are performed, the probability of failure is calculated by dividing the number of failures N_f by the total number of samples N :

$$P_f = \frac{N_f}{N} \quad (2.12)$$

The number of required simulations depends on the probability of failure and the desired accuracy of the answer. In case $P_f \ll 0$, the chance of sampling failure is very low and therefore the amount of required simulations increase rapidly. The minimal number of samples can be determined based on the probability of failure and the target accuracy, defined by the coefficient of variation $V(P_f)$ (Waarts, 2000):

$$N > \frac{1}{V(P_f)^2} \left(\frac{1}{P_f} - 1 \right) \quad (2.13)$$

For structural systems the reliability index is often desired to be around $\beta=4$ ($\rightarrow P_f = 3.2 * 10^{-5}$). When a target $V(\beta)$ of 0.05 is assumed acceptable, the minimum number of samples can be approximated by translating $V(\beta) = 0.05$ to $V(P_f) = 0.57$ and filling this into the equation above:

$$N > \frac{1}{0.57^2} \left(\frac{1}{P_f} - 1 \right) \approx \frac{3}{P_f} \rightarrow N > \frac{3}{3.2 * 10^{-5}} > 100,000$$

The minimal required number of calculations in this case is around 100,000. When performing this amount of computations in a reliability analysis on a FEM-Model, the computational time is in the order of weeks, depending on the size of the Finite Element Model and the computational power. Therefore several other types of sampling methods have been developed that require less computations. Schweckendiek (2006) evaluated the most common types of sampling methods on the applicability in structural reliability computations. Aside from the calculation effort also other aspects were considered:

- the accuracy of the method
- the applicability in a system analysis
- the need for prior knowledge (which is often not available)

The most suitable sampling methods, available for use, are Directional Sampling and Directional Adaptive Response Sampling.

Directional Sampling (DS)

Directional Sampling is quite different from a standard CMCS, but it is still based on sampling of random variables. The method is an iterative process in which multiple vectors are sampled and scaled up to a length for which holds $Z = 0$. The method is carried out in the u -space. This means that the random variables are transformed to independent standard normal variables. The method can be explained by the steps described by Schweckendiek (2006):

- 1 The origin of the u -vector is determined with a mean (or median) value calculation in $u = 0$.
- 2 A point in the parameter space is generated from the random joint probability function. The vector u is defined as the vector with its starting in the origin and the randomly generated point as end point.
- 3 The vector is scaled to a predefined length $|u| = u_0$ (often u_0 is chosen as 1=unit vector). In this way only the direction of the vector is kept as information of the random realization. Thereafter a Limit State Function Evaluation (LSFE) is carried out in this point.

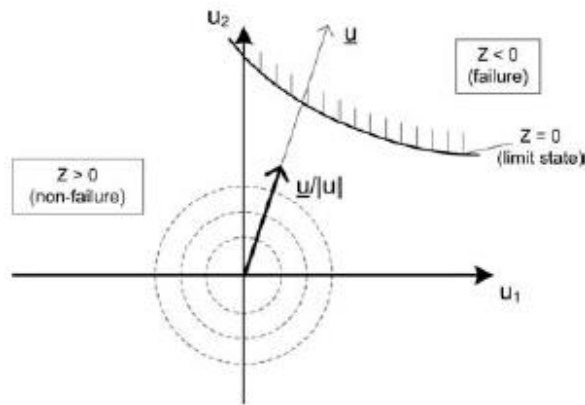


Figure 2.14 Directional Sampling carried out in a 2-dimensional u-space (steps 1 to 3). Source: Schweckendiek (2006)

- The vector is scaled with a factor λ ($\lambda \geq 0$) in an iterative procedure until the LSF is equal to zero ($Z = 0$). This requires a LSFE for every time the vector is scaled, which is of importance for the computational time.

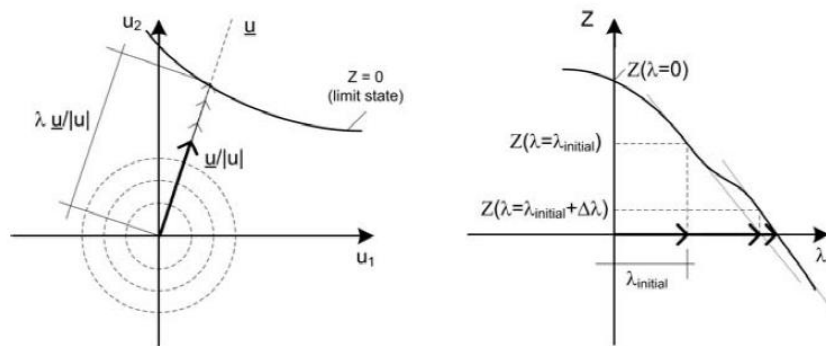


Figure 2.15 Scaling of the vector with λ until the limit state function is found. Source: Schweckendiek (2006)

- $\sum_{i=1}^n \lambda_i^2$ is χ^2 -distributed with n degrees of freedom. If λ was constant for all directions, the probability of failure could be written as:

$$P_f = 1 - \chi^2(\lambda^2, n) \tag{2.14}$$

If we have N random realisations of u with different results for λ , the failure probability is estimated as:

$$P_f = \frac{1}{N} \sum_{j=1}^N (1 - \chi^2(\lambda_j^2, n)) \tag{2.15}$$

The corresponding variance for N realisations is:

$$\sigma_{P_f}^2 = \frac{1}{N(N-1)} \sum_{j=1}^N (P_j - P_f)^2 \text{ with } P_j = 1 - \chi^2(\lambda_j^2, n)$$

- The steps 1 till 5 are repeated until the accuracy in terms of variance is below a desired value. Other stop criteria are also possible, for instance a maximum number of calculations.

2.6.3 Level II

With a level II analyses the failure probability is still explicitly calculated, but the problem is simplified by using approximations of the random variables and the limit state function. It effects in considerable less computational effort while the degree of accuracy is almost the same as for level III methods in many cases. For complicated (highly non-linear) limit state functions and non-normally distributed random variables the method becomes less accurate. Another important aspect is that a level II analysis cannot be used for a complete system with multiple failure modes. For every failure mode the failure probability has to be calculated

separately and therefore system effects are not taken into account when determining the system reliability. Despite these limitations it is a very useful method.

First Order Reliability Method (FORM)

The most commonly applied level II analysis is the First Order Reliability Method introduced by Hasofer and Lind (1974). The term First Order refers to the linearization of the limit state function, which is a first order Taylor approximation. The theory can be explained using two uncorrelated normally distributed variables. These variables are transformed into normalized variables (variables with $\mu = 0$ and $\sigma = 1$) by:

$$U_i = \frac{X_i - \mu_i}{\sigma_i} \tag{2.16}$$

With resistance and load described by respectively μ_R and σ_R and μ_S and σ_S , the limit state function $g(X) = R - S = 0$ can be rewritten as function of the normalized variables:

$$g(\underline{U}) = \sigma_R U_R - \sigma_S U_S + (\mu_R - \mu_S) = 0 \tag{2.17}$$

The function plotted in the U-space is shown in Figure 2.16. The reliability index β is defined as the shortest distance from the origin to the failure surface described by the limit state function and can be derived with goniometrical relations to:

$$\beta = \frac{(\mu_R - \mu_S)}{\sqrt{\sigma_R^2 + \sigma_S^2}} \tag{2.18}$$

The reliability can be decomposed in two vectors for this case. The length of each vector is given by $\alpha_i \beta$. These α -values are a measure for the relative importance of a variable with respect to the reliability index and are therefore called importance factors or sensitivity factors. Analysing these factors helps to give insight into the most relevant parameters in the design.

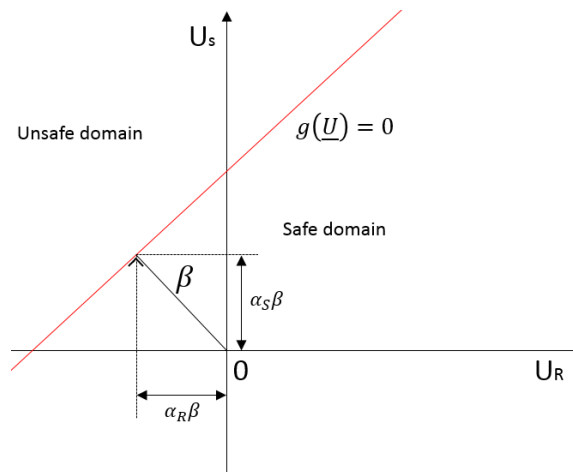


Figure 2.16 Reliability index for a linear limit state function

Also for non-linear limit state functions the definition for the reliability index still holds. However it is more difficult to calculate the shortest distance. For this reason the LSF is approximated by a linear approximation in a certain point. It should be determined which point on the LSF is the closest to the origin and therefore has the highest probability density. When failure occurs it will most likely occur in this point and thus it is called the design point, indicated by d^* in Figure 2.17.

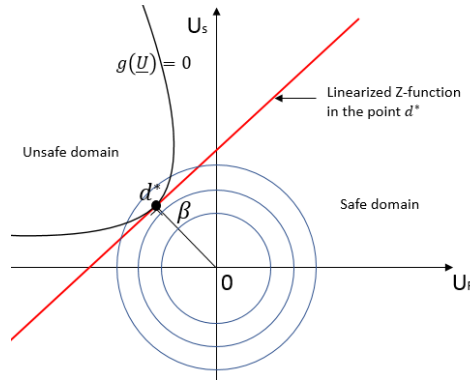


Figure 2.17 Design point for a non-linear limit state function

The location of the design point is found in an iterative way, which is described below:
 Let's assume a limit state function $g(\underline{X})$ in which \underline{X} is a vector consisting of N random variables:

$$g(\underline{X}) = Z = g(X_1, X_2, \dots, X_N) \quad (2.19)$$

The design point for each random variable X_i can be determined with:

$$X_i^* = \mu_i - \alpha_i \beta \sigma_{X_i} \quad (2.20)$$

In the first iteration the importance factors and the reliability index are still unknown so the mean values are used a first guess for the design point. Subsequently the following steps are performed:

- 1 Linearization in the design point with a Taylor series approximation and calculation of the mean value of Z:

$$\mu_Z = g(X_1^*, X_2^* \dots X_N^*) + (\mu_{X_1} - X_1^*) \frac{\partial g}{\partial X_1}(X_1^*, X_2^* \dots X_N^*) + (\mu_{X_2} - X_2^*) \frac{\partial g}{\partial X_2}(X_1^*, X_2^* \dots X_N^*) \quad (2.21)$$

- 2 Determination of the standard deviation of Z:

$$\sigma_Z = \sqrt{\sum_{i=1}^n \left(\frac{\partial Z}{\partial X_i} \right)^2 \sigma_{X_i}^2} \quad (2.22)$$

- 3 Determination of the reliability index and the sensitivity factors:

$$\beta = \frac{\mu_Z}{\sigma_Z} \quad (2.23)$$

$$\alpha_i = \frac{\left\{ \frac{\partial}{\partial X_i} g(\underline{X}^*) \right\} \sigma_{X_i}}{\sigma_Z} \quad (2.24)$$

- 4 Finally the new design point can be calculated:

$$X_i^* = \mu_i - \alpha_i \beta \sigma_{X_i} \quad (2.25)$$

- 5 The reliability index, the sensitivity factors and the design point should be compared with the values obtained from the previous iteration to check whether convergence has reached.

The convergence rate of this method depends on the non-linearity of the function around the design point. The validity of a level II method can be checked by performing a level III method and comparing the results of both methods.

2.6.4 Level I

When a level I method is applied, the reliability is not calculated explicitly but it is incorporated in the design with the use of partial factors. That is why it is called a semi-probabilistic approach. The main concept is that strength parameters are reduced while load parameters are increased. The magnitude of the partial factors is depending on the uncertainty in the parameter and the target reliability of the structure. The current design guidelines (e.g. EC and CUR) are generally based on this approach.

The magnitude of parameters can be divided into three types:

- Mean values
- Characteristic values
- Design values

The definition of mean values speaks for itself. Characteristic values are values with a prescribed probability of not being exceeded. Generally, values with a low exceedance probability (5%) are used in case of load parameters and values with a high exceedance probability (95%) in case of strength parameters. Depending on the parameter type also the mean value is sometimes used as characteristic value. The design values are calculated by dividing or multiplying the characteristic values by partial factors. For the calculation of a design resistance parameter holds:

$$X_{R,d} = \frac{X_{R,k}}{\gamma_{R,d}} \tag{2.26}$$

Where

- $X_{R,d}$ design value of a resistance parameter
- $X_{R,k}$ characteristic value of a resistance parameter
- $\gamma_{R,d}$ partial safety factor for the corresponding resistance parameter

For a load parameter holds:

$$X_{S,d} = X_{S,k} * \gamma_{S,d} \tag{2.27}$$

The design load and the design strength of a structure can be expressed as function of the design parameters:

$$R_d = R(X_{R,d1}, X_{R,d2}, \dots, X_{R,dn})$$

$$S_d = S(X_{S,d1}, X_{S,d2}, \dots, X_{S,dn})$$

The design is assumed to be safe when for the limit state holds:

$$R_d \geq S_d$$

For the simple case of a single load and resistance parameter, this principle is shown in Figure 2.18.

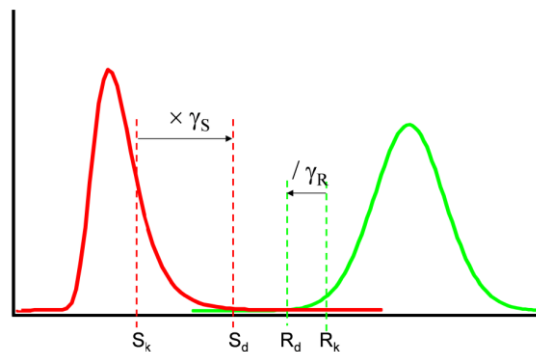


Figure 2.18 Principle of design load and design resistance. Source: Jonkman et al. (2016)

The partial safety factors are either determined in an empirical way or a probabilistic way (Figure 2.19). The empirical method is based on the calibration of a long experience in building history and has no or few probabilistic background.

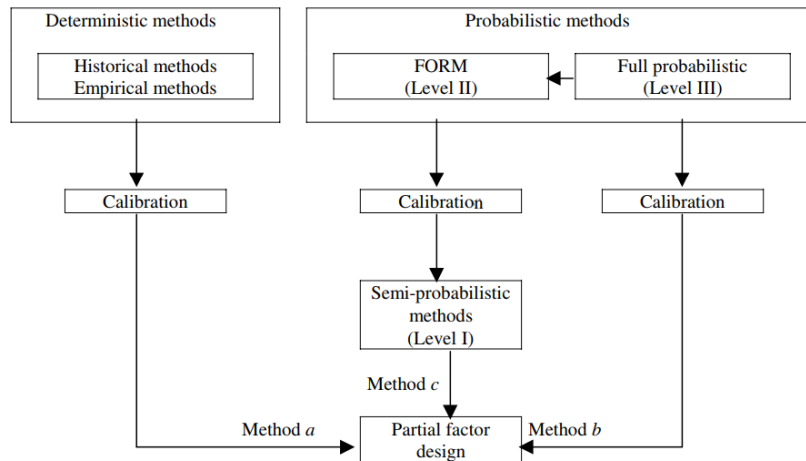


Figure 2.19 Methods to arrive at partial factors. Source: NEN-EN 1990 (2002)

A more mathematical approach is the calibration of the partial factors with a probabilistic calculation using a level II method. In this way the reliability index obtained from the level II analysis is incorporated in the partial factors of the level I method. With a FORM calculation the design point of every random parameter is determined, together with the sensitivity factors and the reliability index. This output can be used to determine the partial factor. For a partial factor on a resistance parameter holds:

$$\gamma_{R,d} = \frac{X_{R,k}}{X_{R,d}} = \frac{\mu_R - k_R \sigma_R}{\mu_R + \alpha_R \beta \sigma_R} = \frac{\mu_R (1 - k V_R)}{\mu_R (1 + \alpha_R \beta V_R)} = \frac{1 - k_R V_R}{1 + \alpha_R \beta V_R} \quad (2.28)$$

Where

- k characteristic factor (for a normally distributed parameter and an exceedance probability of 5 or 95%, a value of 1.645 is used)
- V_R coefficient of variation: $V_R = \frac{\sigma_R}{\mu_R}$
- α_R importance parameter obtained from the FORM analysis (in case of a favourable influence on the reliability index, the α -value is returned as a negative value in FORM)
- β target reliability index
- μ_R mean value of the concerned parameter
- σ_R standard deviation of the concerned parameter

In the same way the partial factor on a load parameter can be determined:

$$\gamma_{S,d} = \frac{X_{S,d}}{X_{S,k}} = \frac{\mu_S + \alpha_S \beta \sigma_S}{\mu_S + k \sigma_S} = \frac{1 + \alpha_S \beta V_S}{1 + k V_S} \quad (2.29)$$

The partial factors in design guidelines are often calibrated on a few specific structures. This makes the applicability of these factors doubtful in case of structures that deviate considerably from the calibrated structures. This is partly taken into account by prescribing slightly conservative partial factors. The use of partial factors can therefore result in a deviation of the actual reliability compared to the target reliability. With a full probabilistic analysis this problem is avoided. Especially for one-of-a-kind structures the use of a full probabilistic method can result in considerable cost savings due allowance for a more economical design.

2.6.5 Level 0

A very basic approach is the level 0 approach. With this method nominal values are taken for all the variables after which one single global safety factor is applied. The structure is considered safe when the following equation holds:

$$R_{nom} \geq \gamma S_{nom} \quad (2.30)$$

The problem with this type of analysis is that it doesn't take the degree of uncertainty into account. This is illustrated with Figure 2.20. In all the three figures the mean load and resistance is the same and therefore the global safety factor γ is also for all three cases identical. However, the failure probability in figure a (the green surface) is much smaller than in figure b and c due to the differences in uncertainty, Hence, this method is not applicable to design a structure for a target reliability.

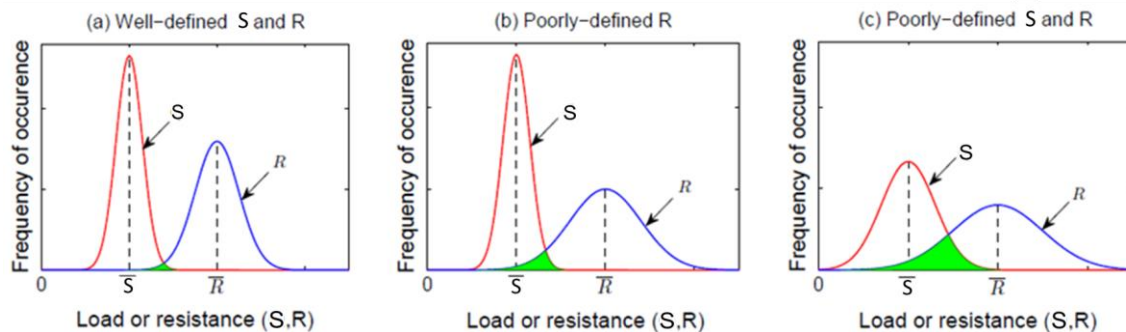


Figure 2.20 Failure probability (in green) for different distributions of load and resistance, all with the same mean load and resistance. Source; Bach (2014)

2.7 Design guidelines for quay walls

Design codes are published to implement a framework for a systematic approach to safety in the design process of structures. Several national and international standards and guidelines have been developed concerning design in general and the design of quay walls. The European guideline, the Eurocode (EC), is the governing standards since 2012. It consist of ten parts of which each considers a certain aspect in the design of (geo)technical structures. Each country is allowed to add a national annex to the Eurocode to prescribe additional specific parameters relevant for their country. Especially EC 7 is relevant for the design of quay walls as this one treats soil retaining structures. The guidelines are developed to be applicable to a wide range of structures. For this reason the guidelines can be on a too general level in case of complex structures. That is why in the Netherlands structure-specific guidelines are developed by the CUR (Civieltechnisch Centrum Uitvoering Research en Regelgeving). Relevant for the design of quay walls are especially the CUR 211 and the CUR166.

2.7.1 CUR 166 Sheet pile structures

CUR166 is the Dutch guideline for the design of simple sheet pile structures. In this guideline a step by step approach for the design of sheet piles structures is described. The design approach used in this guideline is semi-probabilistic (level II) and prescribes partial factors on both the load and the resistance parameters. Besides the design of sheet pile walls, also planning, construction and maintenance aspects are treated in this guideline.

2.7.2 CUR 211 Quay walls

As quay wall structures are more complex than a single sheet pile wall, the need for a specific guideline for quay wall structures arose. In 2005 the CUR211 was published to provide the designer with a semi-probabilistic design approach for quay walls together with technical knowledge and information about the planning, construction and maintenance. The experience of users of the handbook, new technical knowledge and the increasing popularity of FEM-models resulted in a second version published in 2013. Some of the main additions to the original version were the recommendations on the use of the FEM. When this type of analysis is used to model the structure, it is recommended to use characteristic values for the strength parameters and design values for the load parameters In this way the model represents the behaviour of the structure more realistically.

2.7.3 Probabilistic background of the CUR211

The design method and the partial factors of the CUR211 are mostly based upon previous research into the probabilistic validation of the partial factors. Before going into depth about these researches, the important aspects with respect to reliability incorporation in the design method are described.

Important aspect of the approach of the CUR211

Before starting with the actual design of a quay wall, the starting points (e.g. bottom level, quay level and the consequence class) should be agreed upon with the client. The consequence class (CC), or in the Netherlands described as reliability class (RC), is selected from Table 2.3. For most quay walls in the Port of Rotterdam CC2 is applicable which corresponds to a reliability index of 3.8 and a failure probability of $7.2 \cdot 10^{-5}$.

Table 2.3 Reliability/Consequence Classes for quay walls. Source: NEN-EN 1990 (2002)

Description of reliability classes	Reliability index β	Design life in years	Example
RC 1/CC 1 Consequences of failure – Risk of danger to life negligible – Risk of economic damage low	$\beta = 3.3$	50	Simple sheet pile structure/quay wall for small barges. Retaining height till 5 m
RC 2/CC 2 Consequences of failure – Risk of danger to life negligible – Risk of economic damage high	$\beta = 3.8$	50	Conventional quay wall for barges and seagoing vessels. Retaining height > 5 m
RC 3/CC 3 Consequences of failure – Risk of danger to life high – Risk of economic damage high	$\beta = 4.3$	50	Quay wall in flood defence/ LNG-plant or nuclear plant (hazardous goods)

The choice of the consequence class is determining the magnitude of the prescribed partial factors. The EC describes three design approaches for the use of partial factors, whereas in the National Annex design approach 3 is prescribed in the Netherlands. This implies partial factors on the material characteristics and partial factors on the loads. The partial factors of the EC7 are based on calculations on simple quay walls. Therefore probabilistic calculations are carried out for quay walls with a relieving platform to attain more accurate partial factors. This has resulted in a set of partial factors for the load and resistant parameters. The factors for the soil parameters are given as example in Table 2.4. For the partial factors of all the other variables reference is made to the CUR 211.

Table 2.4 Partial safety factors on the soil parameters for quay walls with relieving platform. Source: NEN 9997 (2017)

Soil parameter	Symbol	Combination			
		M1	M2		
			Overall Stability* & Quay wall with relieving floor on piles		
			Reliability/Consequence Class		
		RC1/CC1	RC2/CC2	RC3/CC3	
Angle of internal friction ^a	γ_{ϕ}	NA	1.2	1.25	1.3
Effective cohesion	γ_c	NA	1.3	1.45	1.6
Undrained shear strength	γ_{cu}	NA	1.5	1.75	2.0
Unconfined compression strength	γ_{qu}	NA	1.5	1.75	2.0
Density	γ_{γ}	NA	1.0	1.00	1.0

^aThis factor is applied to $\tan \phi'$
NA = not applicable

Chapter 6 describes a step-wise approach to determine the safety with respect to all kinds of failure modes. Only the ULS-check on the embedded depth, the bending moments, normal forces and shear forces in the retaining structure and the anchor are highlighted here because of the slightly different approach that is used compared to the NEN 9997. In the FEM-model representative values for the soil strength parameters should be used instead of design values to better represent the actual failure behaviour. Thereafter the strength parameters (ϕ and c) are reduced by a prescribed factor with the 'φ-c reduction' method. Subsequently the design values for the sectional forces are obtained.

Previous research on the partial factors for quay walls

The design approach and the partial factors of the CUR 211 are based on several probabilistic calculations, which go back to the development of the first CUR 166 in 1993. For this guideline (Calle & Spierenburg, 1991) performed one of the first probabilistic analyses for an anchored sheet pile wall. It concerns a level II analysis performed on the a spring model in the software program DAMWAND. In the research a fault tree was created and the total failure space was divided into pieces. Mechanisms which are easy and cheap to improve were given an low acceptable failure probability of '0.2p' whereas the main failure mechanisms (passive resistance failure, failure of the sheet pile profile, total instability, groundwater flow and anchor failure) were given a failure space of 'p'. The system was considered as a serial system with strong dependency between the different failure mechanisms. The failure probability of a top event was calculated by fully counting the largest failure probability and multiplying the other failure probabilities that are at the same level of the tree by $\frac{1}{2}$ before adding to the largest failure probability. The obtained importance factors and reliability index of the level II analysis were used to calculate the partial safety factors for the first CUR166. These values were later validated by Havinga (2004) who concluded that the partial factors are resulting in more or less the correct reliability.

However, a quay wall differs quite much from a sheet pile wall and therefore Gemeentewerken Rotterdam (Huijzer, 1996) conducted a research into the adaption of the partial factors of CUR166 to be applicable for quay walls. This led to an adaption of the fault tree due to the addition of extra components (e.g. the concrete superstructure and bearing piles). Also the division of the failure space has been changed as it appeared that yielding of the sheet pile profile was the main failure mode. Subsequently a new set of partial factors was determined.

de Grave (2002) was the first one to validate this new set of partial factors on four different existing quay walls of which two of them were quay walls of EMO. He performed a level II analysis with the software package PC-Dam (elasto-plastic spring model) and compared the results with the original design that was calculated in a deterministic way. His main conclusions were:

- The partial factors on the soil parameters can remain the same
- The partial factor on the bending moment also result in the right reliability
- The outside water levels and ground water levels should not be considered as independent as it is a too conservative assumption

It should be mentioned that the calculations were performed on a highly simplified model based on conservative assumptions.

Wolters (2012) validated the partial factors based on a coupling of a PLAXIS-FORM and was therefore able to model the structure and the soil-structure interaction much more accurate. One of the two case studies he performed was on the EMO quay wall that is considered in this thesis. However, he adjusted the final design of the structure in accordance with CUR166 to enable a comparison between the design code and the calculation results. The combi-wall is placed vertical instead of under an angle. Due to this adjustment it was necessary to add a second anchor row because otherwise the horizontal deformations at the top were larger than the maximum of 50mm (requirement for the crane track).

Wolters stated that the soil mechanical failure is the most critical failure mechanism. With respect to economic optimisation it should therefore not get a higher target reliability than bending wall failure or anchor failure. As this results in a higher partial factor on the angle of internal friction. The failure space should be taken from 'anchor failure in tension' as this mechanism turned out to have a higher reliability than expected. Furthermore he found out that there is a strong correlation between soil mechanical failure and bending wall failure, whereas anchor failure shows little correlation with respect to those two mechanisms. Also the spatial variability of the soil turned out to have a large influence on the magnitude of the partial factors

Other recommendations were:

- Use different safety factors per failure mechanism to prevent overdimensioning of elements
- Use higher partial safety factors on the internal angle of friction and soil stiffness parameters
- Use lower partial safety factors on the geometrical parameters
- Use mean values for cohesion, sheet-pile parameters and anchor diameter.

With respect to full probabilistic design of quay walls he recommended to perform probabilistic calculations for every new quay wall to accomplish a more optimal design. However the use of FORM is doubtful. The plastic behaviour of soil is non-linear and therefore the linear approximation with FORM is not always accurate.

2.8 Conclusion

The topics described in this chapter has given a general overview of the most relevant existing knowledge regarding the design of quay structures, the main types of uncertainties and available probabilistic methods. This theory helped with composing the research methodology that is extensively described in the next chapter.

3

METHOD DESCRIPTION

As described in the first chapter, the objective of this thesis is to validate the current design approach and to explore possibilities for case-specific load increase by performing probabilistic calculations.

The literature overview in the previous chapter showed that failure of the quay wall can be triggered by numerous mechanisms and that there are multiple options regarding the modelling of the problem and the type of probabilistic methods. Relevant questions that are answered in this chapter are:

- Which failure mechanisms are most relevant regarding the design of quay wall structures ?
- What is an appropriate limit state function for these failure mechanisms?
- Which probabilistic method is most suitable for assessing these LSFs and which software should be used for this?

The answers to these questions have resulted in the research methodology that is applied on two case studies. Both case studies are quay walls located in the Port of Rotterdam. The first case study considers a simple double anchored combi-wall, whereas the second case study considers a quay wall with relieving platform. An general overview of the applied approach is given shown in Figure 3.1.

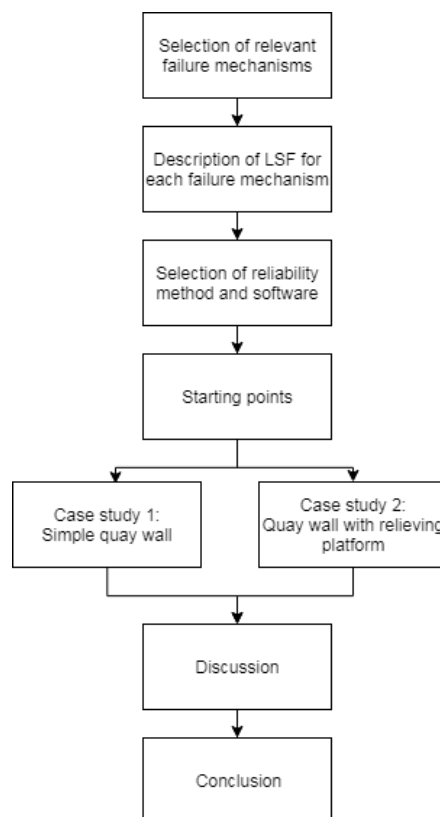


Figure 3.1 Flowchart of research methodology

3.1 Selection of Failure Mechanisms

In this subchapter a selection is made of the failure modes which will be assessed for the two case studies. In chapter 2.4 an introduction on the fault tree of a quay wall is already given.

This fault tree of the CUR211 consists of 23 base events. It is for several reasons not possible and not desired to calculate all their failure probabilities. This thesis is limited to the determination of the failure probability of:

- Events with a significant influence on the overall failure probability of a quay wall
- Events that can be assessed by using a coupling between Plaxis and an appropriate probabilistic method

To determine the contribution of each failure mode to the overall failure probability, the fault tree of CUR211 (2005) (Appendix A) was checked. In this fault tree most of the failure modes are assigned with a target reliability index. The importance of a failure mode can therefore be interpreted from its assigned target reliability. The division of the failure space within this tree is for a large part based on economical choices. Failure modes that are expensive to prevent are assigned with a low target reliability and failure modes that can be prevented with small investments were given a high target reliability. In this way, the most economically beneficial solution is created. When looking at the distribution of the construction costs for combi-walls with a concrete relieving platform as shown in Figure 3.2, it is obvious that the steel of the combi-wall has the largest contribution to the total cost. Thereafter follows the concrete superstructure, which falls mainly under the category concrete, reinforcing steel and labour.

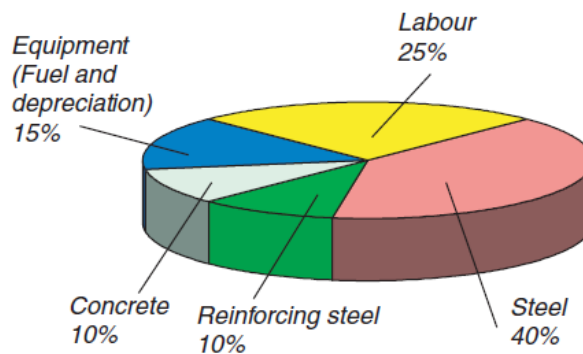


Figure 3.2 Distribution of costs as a percentage of the construction cost for combi-wall structures with a concrete superstructure. Source: CUR211 (2013)

It is therefore not surprising that failure of the sheet pile wall is provided with the most failure space. Thereafter follows the failure of the superstructure and subsequently the bearing piles and the tension members. Soil mechanical failure is included within multiple subcomponents of the previously mentioned failure modes. It covers amongst others the following events:

- Passive resistance in front of the retaining wall inadequate
- Lack of equilibrium (Bishop slip circle)
- Heave
- Piping
- Krantz stability inadequate
- Shear resistance of anchorage inadequate

Not all of the soil mechanical failure modes can be assessed using Plaxis coupled with reliability methods. Piping is an example of this. Besides, it is hardly possible to assess the reliability of soil mechanical failure modes individually as the most dominant failure mode is triggered first.

Previous experience with coupling FORM to Plaxis (see chapter 3.3) has shown that the reliability of steel structural elements can be assessed relatively well, if soil mechanical failure is non-dominant. The determination of the reliability regarding soil mechanical failure caused significantly more problems with convergence in previous research. However new developments in the robustness of FORM calculations enables for this failure mechanism to be assessed more easily.

Conclusion

Yielding of the combi-wall profile and soil mechanical failure are dominant failure modes of which the reliability can be assessed with FORM and are therefore included. Yielding of the anchor profile is often non-dominant but can be assessed with relatively little effort and is therefore included as well. The selected failure mechanisms are marked in the fault tree in Figure 3.3. Each failure mechanism will be treated separately, in which simultaneous failure of other mechanisms is neglected (except when it concerns soil mechanical failure).

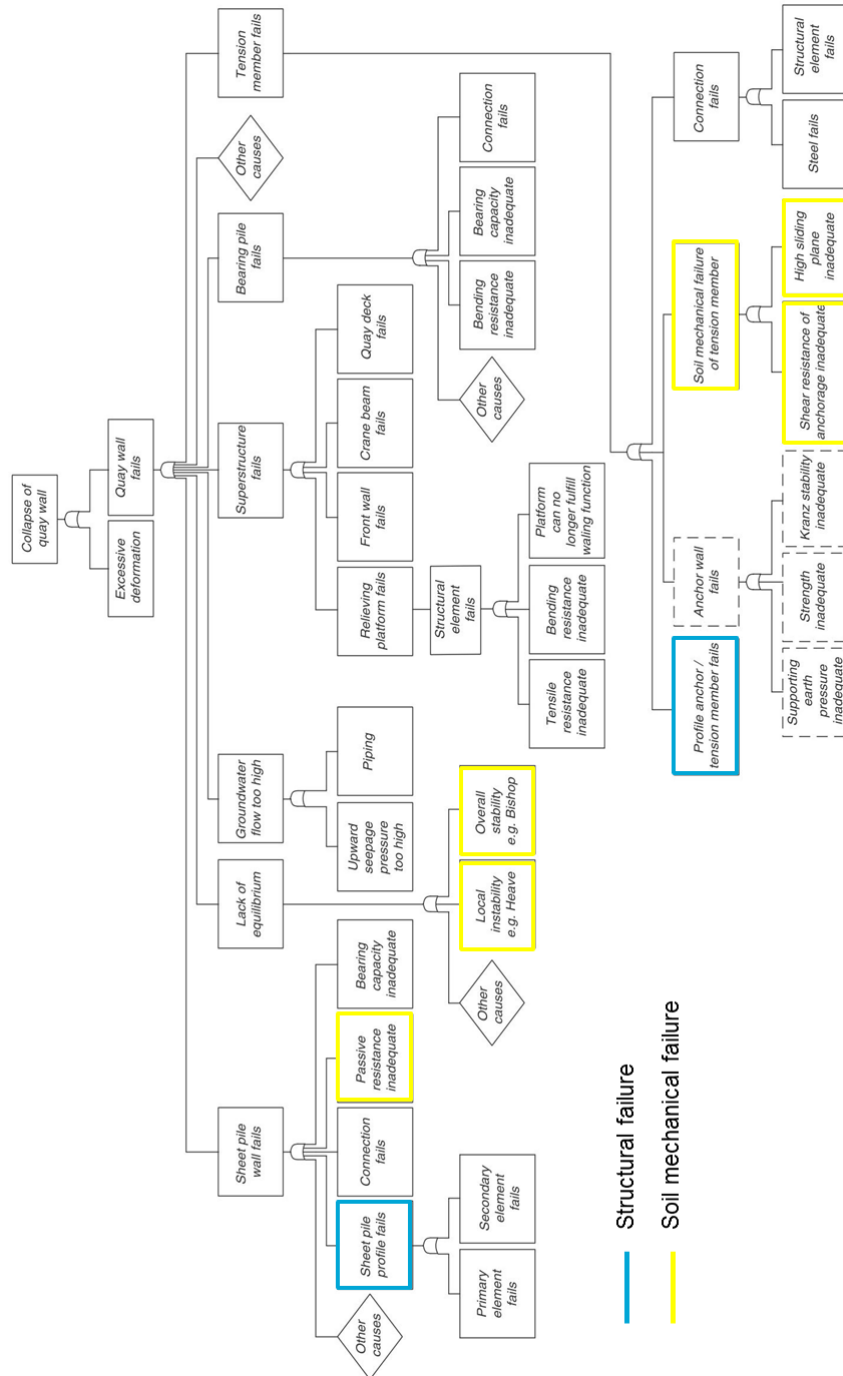


Figure 3.3 Selected failure mechanisms. Adapted from: CUR211 (2013)

3.2 Limit State Functions

The limit state function defines the boundary between failure and non-failure. In this section the limit state functions for the three considered failure modes are described and formulated.

3.2.1 Failure of combi-wall profile

Failure of the combi-wall can have multiple causes as shown in the fault tree of Figure 2.10. For now, only failure due to yielding of the profile is considered, as it is assumed to be the most dominant failure mechanism. An indication of the failure mechanism is shown in Figure 3.4.

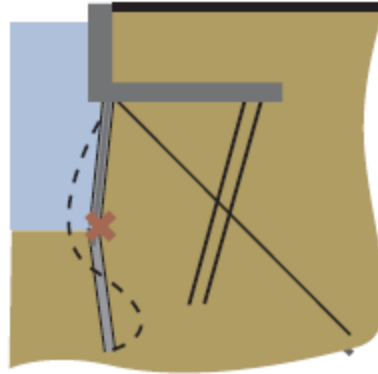


Figure 3.4 Failure of the retaining wall. Source: Roubos et al. (2018)

Most part of the load on the combi-wall is taken by the primary tubular piles. For the determination of the resistance of steel piles, it is necessary to check for the occurrence of local buckling. The susceptibility to buckling of tubular piles depends on the slenderness of the piles, expressed with the ratio below:

$$\frac{D}{t\epsilon^2} \tag{3.1}$$

With

- D Diameter [mm]
- t Wall thickness [mm]
- ϵ Relative yielding stress, determined by $\sqrt{235/f_y}$

Based on this ratio, a distinction in four classes is made in Eurocode 3, as shown in Table 3.1. It must be noted that this division is valid for empty piles. Based on this division, the tubular piles in combi-walls belong to the fourth category, which implies buckling can occur before the yield limit.

Table 3.1 Classification of tubular piles. Source: CUR211 (2013)

Class	Limits	Remarks
1 – plastic	$D/t\epsilon^2 < 50$	<ul style="list-style-type: none"> • Full plastic moment allowed • Section is able to develop a plastic hinge • Plastic redistribution allowed
2 – compact	$50 < D/t\epsilon^2 < 70$	<ul style="list-style-type: none"> • Full plastic moment allowed
3 – semi-compact	$70 < D/t\epsilon^2 < 90$	<ul style="list-style-type: none"> • Full elastic moment allowed (yield limit in outer fibre)
4 – slender	$D/t\epsilon^2 > 90$	<ul style="list-style-type: none"> • Limited effectiveness, buckling stress (below yield limit) allowed in outer fibre • Refer to EN 1993-1-6

Eurocode 3 does not prescribe rules for tubular piles filled with sand. In general, when a pile is loaded in bending, its shape tends to ovalize, reducing the critical strain. However, within a sand-filled pile, the sand is confined and therefore excessive ovalization is prevented.

For the release of the second version of CUR211, tests on sand-filled tubular piles have been executed to investigate the influence of the sand-fill on the bending moment capacity in comparison with empty piles. In total 24 tests were carried on four different pile types, ranging from class 3 to 4. For each pile type, 3 tests were carried out on empty piles and 3 on sand-filled piles. The piles were loaded by pure bending. The results of the tests, depicted in Figure 3.5, clearly shows that that the approach of empty piles of EN-1993 is too conservative.

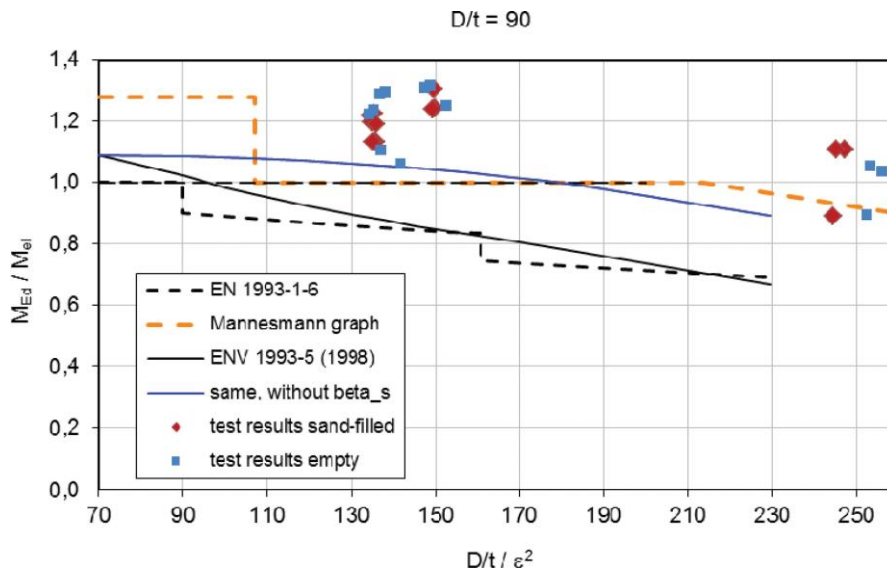


Figure 3.5 Results of design methods of class 3 and class 4 tubular piles for $D/t=90$, with plotted test results (D/t range of tests: 70 to 120). Source: CUR211 (2013)

Especially for tubes with a high slenderness, the sand-fill has a large positive impact on the reduction of ovalization and therefore on the bending moment capacity of the piles. The bending moment capacity of most piles is even higher than the elastic moment capacity. The results of the research confirmed that the method of Gresnigt (1986) to calculate the critical strain provides a good fit. This method is quite elaborated though and therefore difficult to implement into the limit state function. So for the sake of simplicity it seems reasonable considering Figure 3.5 to assume yielding of the outer fibre of the combi-wall as the criterion for failure of the profile.

The maximum stress in the combi-wall is considered as a combination of the contribution of axial force N [kN] and bending moment M [kNm], with both loads being depth-dependant. For the formulation of the stress in the outer fibre holds:

$$\sigma_{max} = \left| \frac{N(z)}{A_{wall}} + \frac{M(z)}{W_{el}} \right| \quad (3.2)$$

With A_{wall} [m^2] being the cross-sectional area and W_{el} [m^3] the elastic section modulus of the combi-wall.

A major limitation of ProbAna, the software package used in the first place, is that only the maximum value of one output variable can be considered in the limit state function, plus the threshold can only be given as a constant value. So a combination of the normal force and the bending moment to compute the stress in the outer fibre is not possible. In theory, also the structural resistance parameters A_{wall} and W_{el} are random variables and depth dependant because corrosion rates differ with depth. Following the assumption that cathodic protection is effective during the entire lifetime of the structure, the depth-dependency can be neglected.

One of the two sectional forces should be assumed constant during the calculation, whereas also the structural properties including f_y cannot be considered as stochastic in the limit state function. It is expected that the normal force is less sensitive to soil parameter variations than the bending moment. When the contribution of the normal force is subtracted from the yield stress, the limit state function is as follows:

$$Z = \left(f_y - \frac{N(z)}{A} \right) * W_{el} - M(z) \tag{3.3}$$

With only the bending moment as variable, the equation simplifies to:

$$Z = M_{res} - M_{max} \tag{3.4}$$

In which M_{res} is the maximum bending moment the wall can resist, and M_{max} the maximum bending moment that occurs in the wall.

3.2.2 Anchor rod failure

An anchor can fail in multiple ways. However not all the failure mechanisms have the same contribution to the overall failure probability of the anchor. For example, the connection of the anchor with the wall or the relieving platform is assumed to have a small contribution as this can be made extra reliable with little extra costs. Soil mechanical failure can occur in the form of a pull-out (shear resistance inadequate) or due to Kranz instability. The shear stress development around a grout body is a complicated 3-dimensional process of which, due to the lack of physical understanding, in current practice mainly empirical relations are used. Also in Plaxis the modelling of this process is not fully representative for the actual behaviour (Plaxis, 2017).

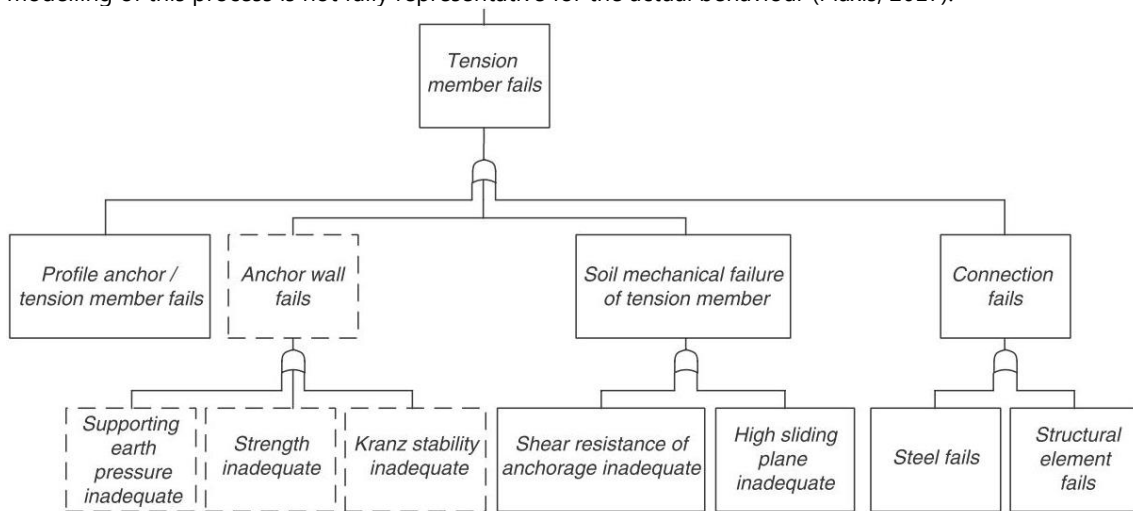


Figure 3.6 fault tree of the anchor. Source: CUR211 (2013)

The failure probability of Kranz instability is implicitly calculated in the soil mechanical failure which is treated in chapter 3.2.3. For failure of the steel rod (Figure 3.7), yielding is assumed as the boundary of failure.

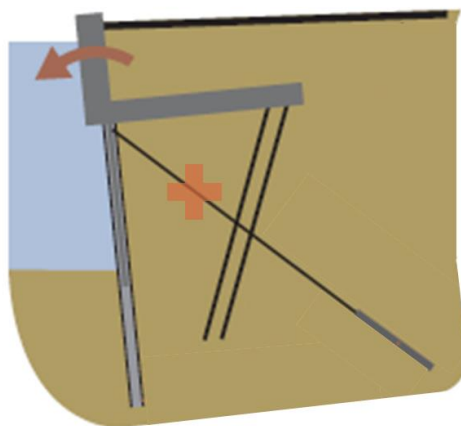


Figure 3.7 Failure of the anchor rod Adapted from: Roubos et al. (2018)

The most important load on the anchor is the axial tension force. Due to uneven settlements along the rod, it is also possible that it is subjected to bending moments. Here it is assumed that the anchor rod will only be subjected to axial forces and that skin friction along the rod can be neglected. This simplifies the limit state function to:

$$Z = f_y A_{anchor} - N_S \quad (3.5)$$

With the resistance consisting of the yield stress f_y [kN/m²] and the cross-sectional area of the rod A_{anchor} [m²]. Considering them as constants yields the following simplified equation:

$$Z = N_R - N_S \quad (3.6)$$

With N_R [kN] representing the strength of the anchor and N_S [kN] the occurring force in the anchor. Again, the yield limit and the cross-sectional area cannot be considered as random variables in the LSF using ProbAna. It should be verified whether assuming them as deterministic is a valid assumption.

3.2.3 Soil mechanical failure

As already mentioned in chapter 3.1, soil mechanical failure can be triggered in multiple ways. An impression of the failure modes is shown in Figure 3.8.

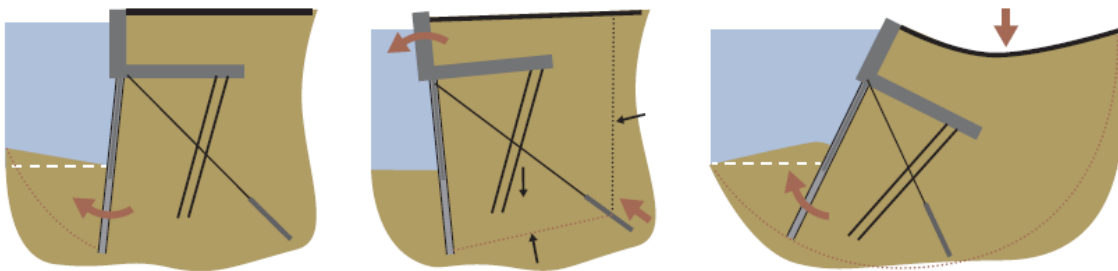


Figure 3.8 Impression of geotechnical failure modes. Left: Failure of the passive wedge, Middle: Failure of anchor system, Right: Macro instability. Source: Roubos et al. (2018)

The most common way to express the stability of a soil body in Plaxis is with the use of the built in 'φ-c reduction' method. With this method, the strength parameters of the soil are reduced with small steps until the soil has just enough strength to maintain equilibrium. The required reduction on the strength parameters is presented as the Multiplier safety factor ($\sum Msf$), which can be considered as the Factor of Safety for the soil:

$$Msf = \frac{\text{available strength}}{\text{minimal required strenght}} = \frac{c}{c_r} = \frac{\tan(\varphi)}{\tan(\varphi_r)} \quad (3.7)$$

In which c_r and φ_r are the reduced strength parameters. It must be noted that not φ_r is reduced but $\tan(\varphi_r)$ to keep the reduction of the shear strength linear. The boundary between failure and non-failure is reached when the safety factor reaches a value of 1.0. Thus in theory the limit state function for a probabilistic analysis should be:

$$Z = Msf - 1.0 \quad (3.8)$$

Experience in combining this limit state formulation with a FORM analysis is gathered by Wolters (2012) and Manoj (2017). Wolters faced problems with soil body collapse in earlier phases than the considered phase because the iterations are performed on the edge of failure. As soil body collapse is not allowed during FORM analysis in his case, he raised the threshold to 1.1 and assumed the impact of this measure on the importance

factors to be small. Manoj actually used the optimization algorithm COBYLA of ProbAna for the assessment of soil mechanical failure. Due to the extra measures added in ProbAna to handle soil body collapse during a FORM calculation, the use of a threshold of 1.0 was possible.

Other points of attention for this method are:

- Performing a Safety analysis in Plaxis is an additional calculation step which increases the computational time of each LSFE with 60-120 seconds. Besides, close to soil mechanical failure a calculation takes considerably more time as it is more difficult for Plaxis to find equilibrium. Due to the aforementioned reasons it can take up to several extra minutes of calculation time per LSFE.

Other possible methods to assess soil mechanical failure are investigated and described by Schweckendiek (2006) and are briefly given below:

1 Relative shear stress

Soil mechanical failure is triggered when the shear stresses along a potential failure become equal to the maximum shear resistance. The ratio between mobilized shear strength τ_{mob} and maximum shear strength τ_{max} is called the relative shear stress τ_{rel} :

$$\tau_{rel} = \frac{\tau_{mob}}{\tau_{max}} \quad (3.9)$$

The mobilized shear strength is equal to the radius of the Mohr's stress circle in a certain point. The maximum shear stress is defined as the value for the shear stress at which the Mohr's stress circle touches Coulomb's failure plane.

If in all points along the failure plane a relative shear stress of 1.0 is reached, the soil body will most likely collapse. In principle this is a clear failure boundary, but the question here is which points should be selected for the LSF and which value should be chosen as threshold for failure. On beforehand the failure mechanism and the exact location of the failure plane is unknown what complicates the selection of points that are on the failure plane. Also for the case of FORM, only one limit state can be evaluated. This implies that the output results of multiple points should be averaged to obtain a single value. When a wide range of points is selected failure can occur even when not all point reached the plastic state. This should be taken into account in determining the threshold value for the LSF.

It can be concluded that this method is not straightforward as it requires prior knowledge on the dominant failure mode, whereas also the definition of failure is not a clear definable boundary.

2 Deformations

Failure of the soil is accompanied by large deformations of both the soil and the structure. As deformations are output of Plaxis, they can be used for the assessment of soil mechanical failure. However, for this method almost the same difficulties as for the relative shear stress method arise. These are:

- Which points should be included in the LSF?
- What value should be used as threshold for the maximum displacement in a certain point or group of points?

Regarding the second bullet, the occurrence of soil mechanical failure often occurs suddenly. This makes the application of FORM more difficult as FORM is especially applicable for problems that are relatively linear, which is not the case for this method. This makes it that this method is not preferred.

3 Plaxis definition of soil failure

When soil mechanical failure occurs during a Plaxis calculation, it basically means that the imposed load cannot be withstand by the soil. The program stops and returns the error message: "soil body collapses". This error message can be used for the definition of soil mechanical failure. This results in a binary (two-sided) LSF: The structure fails or the structure does not fail:

$$Z = \begin{cases} -1, & \text{if computation is not successful} \\ 1, & \text{if computation is successful} \end{cases} \quad (3.10)$$

As the LSF is not continuous, the application of FORM is not possible as no gradients can be computed. Only with higher order (level III) methods like DS or MCS this LSF can be successfully evaluated. Due to the long computational time of these methods it is not used in this thesis.

3.3 Coupling of FEM with Reliability Analysis Methods

For the evaluation of the LSF described in the previous paragraph a coupling between Plaxis and a reliability method is required. For the selection of the reliability method, a decision is taken based on the criteria given below together with the experience in previous research regarding the coupling of Plaxis with reliability methods.

The criteria are:

- **The computational effort**
Performing a LSFE using Plaxis takes considerable computational effort and therefore the aim is to minimise the amount of LSFE.
- **The accuracy of the method**
Minimising the computational effort generally affects the accuracy of the outcome. Therefore the method should still give outcomes with sufficient accuracy.
- **The need for prior knowledge**
Prior knowledge about the problem can be required for certain reliability methods. This is for example information about the location of the failure plane in the parameter space. This information is mostly not available and therefore extra effort is needed to acquire this.

In chapter 2.6 the methods Monte Carlo Simulation, Directional Sampling and FORM are already described in detail. Therefore only a comparison between the three methods is given in Table 3.2.

Table 3.2 Comparison of reliability methods in their applicability with Plaxis, based on (Waarts, 2000)

Method	Computational effort (for $\beta=4$ and 20 random variables in terms of LSFE)	Accuracy	Prior knowledge required
CMCS	+/- 100,000 LSFE, independent of number of variables	Exact, no approximations and therefore fully dependant on the convergence criteria set by the user	No
DS	+/- 12,000 LSFE	Exact, To be steered by convergence criteria	No
FORM	For 25 iterations: +/-600 LSFE	Exact in case of normal distributions and linear LSF. An approximation in case of non-normal variables and non-linear LSF	No

Based on this comparison, it can already be concluded that CMCS is not suitable due to its large computational effort. To get a better overview of the applicability of DS and FORM, previous research on coupling both methods with Plaxis is reviewed and summarized below before a decision is made.

3.3.1 Main findings in previous research on coupling Reliability Analysis Methods with Plaxis

Schweckendiek (2006) studied the applicability of several probabilistic methods on the coupling with FEM-models of retaining structures. The main methods that were tested were FORM/SORM (level II), DS and DARS (level III). He concluded that level II methods results in accurate results for limit states concerning structural elements (retaining wall and anchor rod). For soil mechanical failure, level II methods can cause convergence problems due to the non-linearity of the limit state and the fact that FORM cannot handle instability in Plaxis, whereas level III methods perform considerably better.

Wolters (2012) applied a FORM analysis on two benchmark quay walls in his MSc-thesis to calibrate the partial factors of the CUR211. He confirmed the conclusions of Schweckendiek about the applicability of FORM. Besides convergence problems with FORM also other issues were experienced such as the generation of two design points whereas only one of the two is correct. In case of non-linearities in the limit state the validity of the obtained influence parameters was also doubtful as FORM assumes linearity. He advised to use level III methods to obtain more accurate results.

Rippi (2015) used the library of OpenTURNS for the structural reliability analysis of a dike with a sheet pile wall. She developed a python script for the interface between OpenTURNS and Plaxis and used and tested the reliability methods FORM and DS. The system was checked on the most relevant failure mechanisms: anchor failure, sheet pile wall failure and soil mechanical failure. The applied soil model in Plaxis was Mohr-Coulomb and only the soil parameters were assumed to be stochastic. The coupling with OpenTURNS was achieved successfully and the application of probabilistic methods showed that it is useful for optimizing the design. Again this study showed the difficulty in determining the failure probability of soil mechanical failure. Rippi used a binary limit state for the determination of soil mechanical failure. This means that it is only checked whether failure occurs or not based on the success of computation in Plaxis:

$$Z = \begin{cases} -1, & \text{if computation is not successful} \\ 1, & \text{if computation is successful} \end{cases}$$

This method is only executable with level III methods and therefore DS was used for the LSFE. Also DS was used for the validation of the results acquired with FORM for the LSF of anchor failure. It turned out that the differences in design point and importance factors were small. Furthermore the choice for the optimization algorithm is very important for the convergence and the efficiency of FORM.

Teixeira et al. (2015) (including Rippi) continued with the research into the coupling of Plaxis with the uncertainty library of OpenTURNS for the research project 'Natte Kunstwerken van de Toekomst'. The objective of this research was to enable probabilistic analyses with the FEM using probabilistic libraries of OpenTURNS and Prob2B and to explore the possibilities for a more easy-to-use approach for general soil-structure interaction problems. The aim was also in particular to go further than the studies mentioned above. This was done by studying different probabilistic technics and the incorporation of corrosion. The case study used here was an anchored retaining wall of a lock chamber. The system was considered as a series system with three failure modes: anchor failure, sheet pile wall failure and soil mechanical failure. First the failure modes were checked separately. However the occurrence of soil failure in the determination of the reliability of the anchor and the wall leads to error messages in Plaxis which complicates the process. Therefore they decided to compute the system reliability with DS. With this method all three failure modes can be checked simultaneously. In this system analysis also the time aspect was taken account by considering the load and the water level as random variables. For this simple case it turned out that calculated failure probability was lower or at least equal to the failure probabilities of the CUR166.

A comparison was made between calculating the annual failure probability and transform it to 50 year lifetime reliability and calculating the lifetime failure probability directly. For the transformation from the annual to the design lifetime reliability, complete independency between subsequent years was assumed by using the equation:

$$P_{f,50year} \approx 50 * P_{f,annual} \quad (3.11)$$

For the direct calculations the Gumbel distribution of the time-dependent variables (water level, load and bottom level) were changed by shifting the mean value. The writers concluded that it is beneficial to calculate the reliability index directly for a reference period of 50 years as it result in a higher reliability index (3.8 vs 3.3). Recent research by Roubos et al. (2018) showed that the reliability of quay walls is mainly depending on time-independent variables and is therefore largely a time-invariant problem. Hence, the application of equation 3.11 is not entirely correct for the case of quay walls/sheet pile walls, which explains the discrepancy in the β 's found by Texeira et al.

Besides the conclusions already mentioned in previous research about FORM and DS, Texeira et al recommended to carry out studies closer to the design practice and increase the robustness of the coupling.

With respect to corrosion, which turned out to be a dominant parameter, a systematic data gathering process should be started to acquire more reliable estimates for corrosion rates.

Manoj (2017) validated ProbAna on multiple simple benchmarks and on a case study of a retaining wall on piles. Besides, she focused on the compliance of FORM with EC7 by comparing the design points of FORM (COBYLA) with the design points of EC7. For the simple benchmarks FORM and MCS resulted in accurate answers when it was validated by an analytical calculation. With respect to compliance with EC7, it was concluded that the design points of FORM and EC7 differ considerably as the design point with FORM depends on the problem. The influence of a parameter on the reliability differs for each problem and therefore also its design point is not constant.

3.3.2 Overall conclusion

When considering all the previous studies, the following can be concluded:

- FORM can be useful and accurate in the analysis of structural components. However, for soil failure limit states, the use of FORM can lead to several convergence problems in combination with Plaxis, whereas also the validity of the results are questionable. The type of algorithm and the converge settings are very important for the success of the analysis.
- DS is a more robust and accurate method. It can deal with soil failure in Plaxis and it is also able to evaluate multiple limit states at the same time.
- Computational time is still in the order of days for DS and less or around a day for FORM, depending on the required accuracy, the number of random variables and FE-model size.
- The reliability calculated with a probabilistic analysis is generally higher than the target reliability of a structure.

Given these findings, it was decided to use FORM as the main reliability method. The module used in this thesis for the coupling between FORM and Plaxis is called ProbAna and is developed by Plaxis b.v (2017). The functionality of ProbAna is shortly explained below.

3.3.3 Functionality of ProbAna

The name ProbAna is derived from the words Probabilistic Analysis, which perfectly describes the aim of the application: performing a probabilistic analysis on a geotechnical structure. The application has only recently been released (2017) and uses the open source uncertainty treatment library OpenTURNS (2007) to perform probabilistic analyses on FEM-models in Plaxis. ProbAna provides the connection between user, Plaxis and the reliability analysis methods of OpenTURNS as shown in Figure 3.9. Two types of reliability methods are available in this version:

- 1 Crude Monte Carlo Simulation
- 2 FORM

The user chooses a reliability method and defines the stochastic parameters, the correlations and the LSF. Subsequently ProbAna processes this input and provides it to both Plaxis and OpenTURNS. OpenTURNS runs the reliability analysis and samples (in case of a level III method) or calculates the input parameters, whereas the FEM-model in Plaxis is used for the evaluation of the LSF. The output results of Plaxis are afterwards processed to input for OpenTURNS.

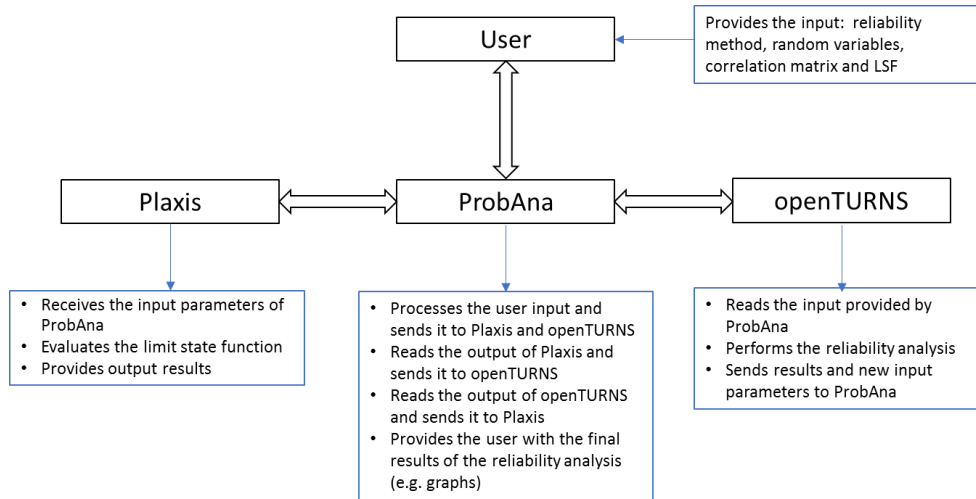


Figure 3.9 Overview of the coupling of FEM with Reliability Analysis

The reliability analysis stops when the maximum number of iterations are performed or when the error tolerance(s) is(are) below a pre-set maximum value. Finally ProbAna presents the output to the user with the reliability index and graphs of the development of the errors and of the calculated iteration points.

Options and features

ProbAna is able to read the input parameters of a Plaxis project and displays them in its own interface. Within this interface it is possible to select the parameters which should be considered as random variables. The following parameters can be selected:

- soil properties
- material properties (parameters of anchors, plates, embedded beam rows, etc.)
- water levels
- loads

After selecting the stochastic parameters, the distribution type can be selected. There are four types of distributions that can be chosen:

- Normal
- Truncated normal (A normal distribution with upper and lower bounds)
- Lognormal
- Uniform

The correlation between the parameters can be given in the correlation matrix of the parameters.

In the next step the criterion for the LSF should be defined together with the phase in which the criterion should be evaluated. After choosing the criterion type, the threshold value can be given. For example, the maximum value for the axial force in the anchor or a maximum displacement in the soil at a certain point in the model. This threshold can only be a deterministic value. This implies that it is not possible to use random variables in the LSF, which is a major limitation of this program. The limit state formulation is limited to the following form:

$$Z = threshold - x$$

In which x is output of Plaxis in the form of displacements or forces.

An overview of the required input for a FORM calculation is shown in Figure 3.10.

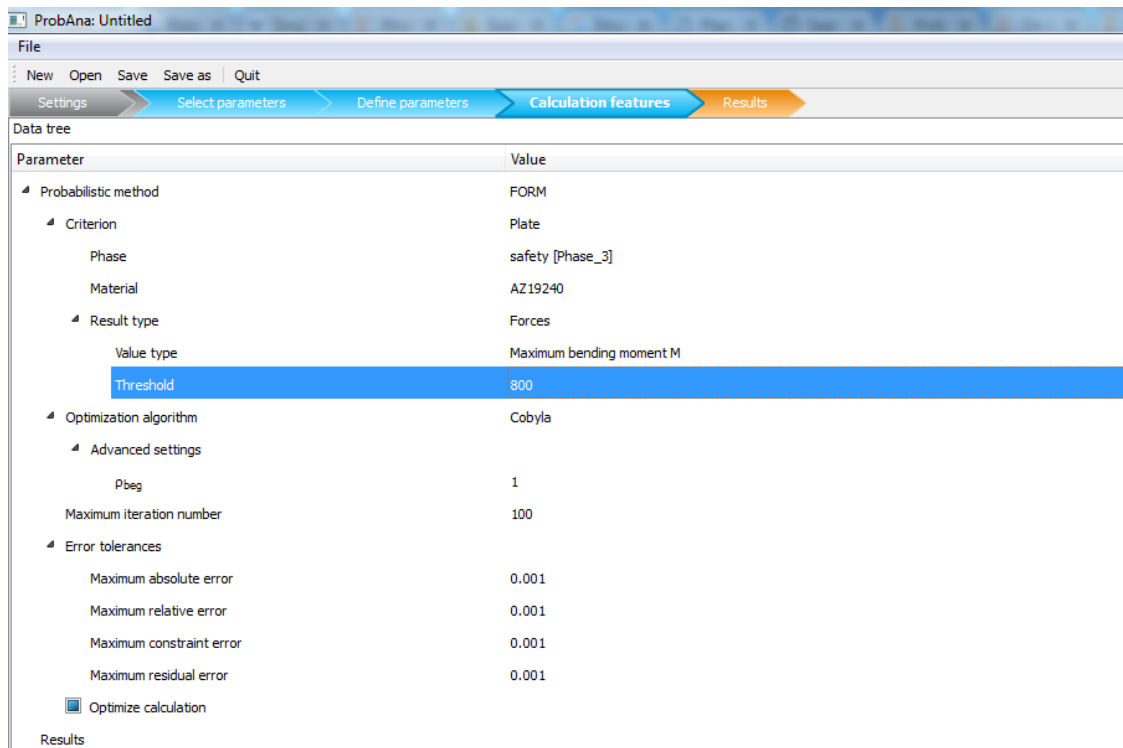


Figure 3.10 Overview of the input required in ProbAna. Source: Brinkgreve and Laera (2017)

3.3.4 Selection of FORM algorithm

ProbAna is equipped with two FORM algorithms from the library of OpenTURNS being COBYLA and Abdo-Rackwitz (AR). The main difference between COBYLA and AR lies in the way the gradient is determined. This is of importance because in structural reliability problems, the LSF is often implicit. In other words, the stochastic variables (e.g. φ' and c') of the problem do not appear in the limit state function. This makes it more complicated to determine the derivative of the LSF with respect to a certain input parameter.

The exact working of both algorithms is extensively described in Appendix B. Here only a brief summary is given. For a comparison between both algorithms, their performance of is judged on the following criteria (Lemaire, 2009):

- Efficiency: the required number of LSFE's (Plaxis runs) to reach convergence to the predefined level of accuracy.
- Robustness: The ability to find the design point under all kinds of different conditions without leading to non-convergence or others errors.
- Capacity: Some algorithms are more capable of handling a high number of random variables or in dealing with complex limit state functions than others.

The performance of both algorithms regarding these criteria is researched by Rippi (2015) and also to some extend for this report, see Appendix B.

In short, it can be concluded that the Cobyla algorithm can show difficulties in finding the design point even for relatively simple problems (few random variables and relatively linear LSF). In cases with more than 8 random variables, the algorithm cannot function properly anymore. An advantage of this algorithm is its relatively short computational time.

The AR algorithm performed significantly better, it is able to find the design point in almost all cases and is able to handle a large amount of random variables. A slight downside of this algorithm is the increase in computational effort, depending on the error tolerances and the amount of random variables.

Based on these findings the AR algorithms is selected as the main reliability method for this thesis.

4

STARTING POINTS

4.1 Introduction

This chapter describes the assumptions made regarding the uncertainties in the input parameters for both case studies. The accuracy and validity of a probabilistic calculation is for the largest part depending on the correctness of the input parameters. The random variables that influence the reliability of a quay wall are divided into five groups:

- Soil parameters
- Structural parameters
- Water levels
- Geometrical parameters
- Loads

Each group will be treated in a separate subchapter, but first the aspect of time and human error is discussed.

Time dependency

The time aspect should be considered when determining the magnitude of input variables and the reliability of the structure. The probability density functions of loads and water levels depends on the considered time span. When a longer time period is considered, also the probability of the occurrence of a specific extreme water level increases. There are basically two options to take this aspect into account:

- 1 Calculate a yearly failure probability and subsequently use this value to calculate the failure probability for the design lifetime (50 years).
- 2 Directly calculate the failure probability for the design lifetime using extreme value distributions with a 50-year return period.

When choosing option 1, the dependency in failure probabilities between successive years should be considered. Dependency between subsequent years implies that when a structure does not fail in year x , it is to a certain degree likely that it will also not fail in the year $x+1$. The degree of dependency depends on the importance of time-dependent stochastic variables to a specific limit state. For quay walls located at the Maasvlakte in Rotterdam, the limit states for geotechnical and retaining wall failure are mainly dominated by time-independent variables (Roubos et al., 2018). Both soil and structural properties can be considered as time-independent. This implies that the failure probability shows a high degree of correlation between successive years and therefore failure of the quay wall is largely a time-invariant problem, at least for geotechnical and retaining wall failure. An example of the development of the lifetime reliability of a quay wall over time is shown in Figure 4.1.

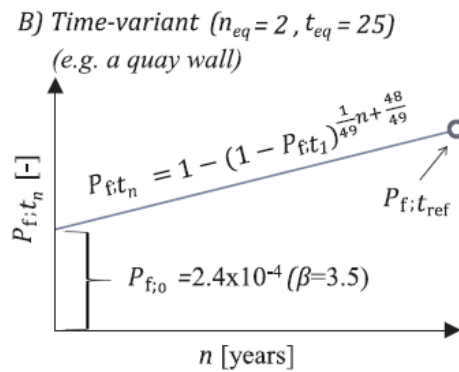


Figure 4.1 Development of the lifetime reliability of a quay wall. Source: Roubos et al. (2018)

In this thesis is chosen to directly calculate the 50-year failure probability by applying lifetime extreme value distributions. In case it turns out that a load variable has negligible importance, an appropriate deterministic value will be used. Multiple loads on the quay wall are time-dependent and therefore the frequency of occurrence of each load should be considered. For example, the occurrence of an extreme low water simultaneously with the maximum lifetime surcharge load seems very unlikely as both events are uncorrelated. By applying an extreme value distribution for both parameters a very conservative load combination would be created.

Human errors

Failure can also be caused by human errors either in the design and construction or by improper use due to for example overloading. Because the magnitude as well as the probability of occurrence of the load or error is unknown it is not possible to incorporate this into probabilistic design calculations. These kind of events are classified as unidentified accidental loads in NEN-EN 1991-1-7. The code prescribes that by making a robust design, failure caused by this type of loads is prevented sufficiently.

4.2 Soil parameter uncertainties

The uncertainty in a parameter is described by its Coefficient Of Variation (COV). The main sources of uncertainty in a soil parameter are (Baecher & Christian, 2003):

- Measurement uncertainty
- The quality of measurements depends on the precision of the measurement devices, the type of test and the skills and experience of the people performing the test.
- Spatial variation
- This type of uncertainty is related to the randomness that exist in nature and cannot be reduced.
- Transformation uncertainty
- Soil properties are often not directly measured but derived using empirical correlations or transformation models. These models contain also uncertainty.
- Statistical uncertainty
- Soil parameters are often derived from limited soil investigation resulting in a certain degree of statistical uncertainty

Ideally, the uncertainty in a local soil parameter is determined from a statistical analysis on a large set of in-situ measurements and lab tests. However, this is very time consuming and requires a sufficient amount of in-situ tests. For this reasons the COV-values will be taken from literature. Table 4.1 gives an overview of values described by several sources: NEN-9997, JCSS (2006), Wolters (2012), Griffiths and Fenton (2007) and Schneider and Schneider (2013). As Table 4.1 indicates, there does not exist one single value that is applicable in every case. The COV-values differs per soil type, per soil parameter -and per location. In principle, all soil properties are normally distributed. However, applying this in a reliability analysis can result in negative values for certain parameters, which is physically impossible. Therefore the log-normal distribution is used for cohesion and stiffness. If needed, for all other parameters a truncated normal distribution is applied to increase the robustness of the FORM analysis. The boundaries are then chosen wide enough not influence on the shape of the distribution.

Table 4.1 Overview on COV-values in literature

Parameter	Symbol	Distribution	NEN 9997	JCSS	Griffiths & Fenton	Wolters	Schneider & Schneider
Density	γ	Normal	0.05	0.05 - 0.1	0 - 0.1	0.05	0.01 - 0.1
Friction angle	φ	Normal	0.10	0.1 - 0.2	0.02 - 0.05 (sand)	0.2	0.05 - 0.15
Cohesion	c	Lognormal	0.20	0.1 - 0.5	0.1 - 0.35	0.8	0.3 - 0.5
Stiffness	E	Lognormal	0.10	0.2 - 1.0		0.30	0.2 - 0.7
Stiffness parameter	m	Normal				0.2	
Interface strength	R_{inter}	Normal				0.2	
Dilatancy angle	Ψ	Normal				0.2	

As one can notice, in the study of Wolters also m , R_{inter} and Ψ at first were chosen as random variables. However, after the sensitivity analysis they appeared to have negligible influence in the limit state function of soil mechanical failure. For this reason they are considered deterministic throughout this thesis.

Spatial averaging and spatial variability

It is important to know whether a given COV value of a certain soil property represents the variation in a certain point in space or the variation in the local average of a layer. For the reliability of quay walls, two aspect are of importance for choosing the COV:

- Spatial averaging (depending on the considered failure mode)
- Inherent spatial variability

Spatial averaging

For several failure modes not the variation in a certain point is of interest, but instead the variation of the mean value of a whole layer. Whether mean values or local point values are of importance for a limit state depends on the ratio between the scale of fluctuation θ and the domain of influence D (Hicks, 2013). The scale of fluctuation is a measure of the distance over which property values are significantly correlated. Due to the geological process of layer deposition, the scale of fluctuation in the horizontal direction is often much larger than in the vertical direction. The scale of fluctuation in vertical direction θ_y is in the order of 2 meter. The scale of fluctuation in the horizontal direction is in the order of 50m. Although this is definitely not a constant value. It depends on the way in which a deposition is formed and it also varies for every parameter (Schneider & Schneider, 2013).

The domain of influence differs for each limit state. When the ratio θ/D is very small, as for a large slip circle, the failure plane cuts through entire soil layers and the mean averaged property values of soil are of importance and therefore also the variation of the mean averaged properties. Mean averaged values have a much narrower distribution (lower COV) than local point values as illustrated in Figure 4.2.

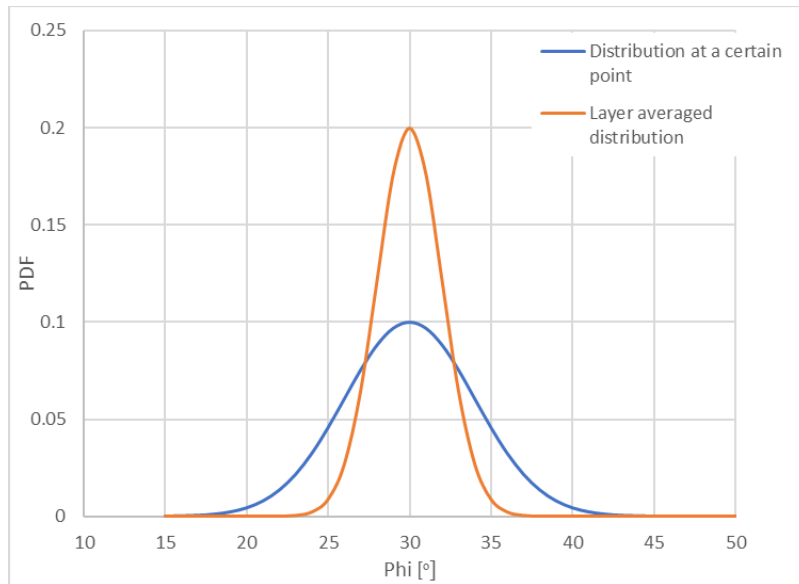


Figure 4.2 Probability density function of local point value vs layer averaged value

On the other hand, a sliding plane has the tendency to follow the path of the least resistance, which partly cancels out the argument just mentioned.

When the domain of influence is small with respect to the scale of fluctuation, the use of point variations is more appropriate. For instance for the bearing capacity of a soil under a pile. For the failure of the wall in bending, the domain of influence is large as the load on the wall is caused by multiple soil layers, whereas the vertical scale of fluctuation is small. Also the concrete superstructure and the combi-wall have a large distribution capacity which causes load spreading in the horizontal direction. For this reason, the variation in mean average values is applicable.

Interpretation of COV-values of NEN9997 and conclusion

The background and interpretation of the values for the COV given in the NEN9997 are not described in the code itself and therefore some debate on this values has been going on. It is known that these values are based on results from soil investigations in The Netherlands combined with expert judgement. The CUR committee C135 has elaborated this values and stated that the values given in NEN9997 can be interpreted as locally layer averaged values (CUR-C135, 2008) which can be used when there is insufficient data from site investigation.

Therefore these values will be used in this thesis. Only the COV for the stiffness is slightly raised to 0.30 as a value of 0.10 is rather low compared to other values given in literature (see Table 4.1). The importance and uncertainty of the stress dependency factor *m*, the interface strength and the dilatancy angle is unknown. In this thesis they are considered deterministic for the sake of simplicity.

An overview on the used values is given in Table 4.2.

Table 4.2 Statistical properties

Parameter	Symbol	Distribution	COV
Density	γ	Normal	0.05
Friction angle	φ	Normal	0.10
Cohesion	<i>c</i>	Lognormal	0.20
Stiffness	<i>E</i>	Lognormal	0.30
Stress-level dependency of stiffness	<i>m</i>	Deterministic	-
Interface strength	R_{inter}	Deterministic	-
Dilatancy angle	Ψ	Deterministic	-

Soil stratification

The schematization of the soil profile is of importance in the determination of the reliability. A higher reliability index will be found when the soil profile is divided into a large amount of thin uncorrelated layers, whereas merging of multiple soil layers into one results in the opposite. This comes from the fact that vertical spatial independency is created when more layers are created. Huijzer (1996) studied this effect by dividing the Pleistocene sand layer into 1, 2 or 4 layers and by merging several sand layers. The results are shown in Table 4.3. It can be concluded that subdivision/merging of layers mainly affects the soil mechanical failure and to a lesser extent wall failure and anchor failure. To prevent overestimation of the reliability, the total number of soil layers should therefore be limited to a reasonable amount.

Table 4.3 Effect of layer division and merging. Source: Huijzer (1996)

Failure mechanism	Splitting Pleistocene sand			Merging sand layers		
	1 layer	2 layers	4 layers	1 layer	2 layers	4 layers
Soil failure	4.32	5.16	7.16	4.78	4.95	4.42
Yielding of the sheet pile	3.65	3.71	3.84	3.95	3.78	3.85
Yielding of the anchor bar	3.65	3.66	3.76	3.97	4.12	4.23

Dependency between soil parameters

Soil properties such as unit weight and friction angle are correlated. Usually a higher unit weight also implies a higher friction angle. This degree of linear dependence between two parameters can be described with the Pearson product-moment correlation coefficient.

Wolters (2012) and Schrijver (2016) both derived correlation coefficients on a database of over 1000 triaxial tests performed in the Port of Rotterdam. Only minor differences can be found when comparing both studies. The correlation coefficient derived by Wolters are shown in Table 4.4 and will be used throughout this study.

Table 4.4 Soil correlation coefficients. Source: Wolters (2012)

	γ_{unsat}	γ_{sat}	φ'	c'	E_{50}^{ref}	E_{oed}^{ref}	E_{ur}^{ref}
γ_{unsat}	-	1.0	0.5	-0.09	0.5	0.5	0.5
γ_{sat}	1.0	-	0.5	-0.09	0.5	0.5	0.5
φ'	0.5	0.5	-	-0.65	0.25	0.25	0.25
c'	-0.09	-0.09	-0.65	-	0.12	0.12	0.12
E_{50}^{ref}	0.5	0.5	0.25	0.12	-	1.0	1.0
E_{oed}^{ref}	0.5	0.5	0.25	0.12	1.0	-	1.0
E_{ur}^{ref}	0.5	0.5	0.25	0.12	1.0	1.0	-

The unsaturated and saturated soil weight are automatically correlated within ProbAna. Only one of the two can be selected as stochastic random variable. The other one is determined by keeping the initial difference between γ_{sat} and γ_{unsat} constant.

4.3 Structural parameters

Combi-wall

In both case studies the quay wall consists of a combi-wall. The uncertainty in the properties of the combi-wall mainly arise from the uncertainty in the properties of the tubular pile as the piles have the largest contribution to the sectional properties (EA, EI) of the combi-wall. The maximum tolerances for the outer diameter and the wall thickness of the piles are prescribed in the NEN-EN 10219-2 and given in Table 4.5.

Table 4.5 Tolerances on tubular steel piles. Source: NEN-EN 10219-2 (2006)

Property	Tolerance
Outer diameter D	$\pm 1\%$ with a minimum of $\pm 0.5\text{mm}$ and a maximum of $\pm 10\text{mm}$
Thickness t	For $D > 406.4\text{mm}$: $\pm 10\%$ with a maximum of $\pm 2\text{mm}$

The tubular piles in both case studies have a diameter of 1420mm. This means that the diameter has a maximum deviation of 10mm. It is assumed that the diameter is uniformly distributed. The wall thickness deviates with a maximum of 10%, and is assumed to be normally distributed with a COV of 0.03, With this value the PDF is for 99.9% within the boundaries of the thickness tolerances of NEN-EN 10219-2 (Figure 4.3).

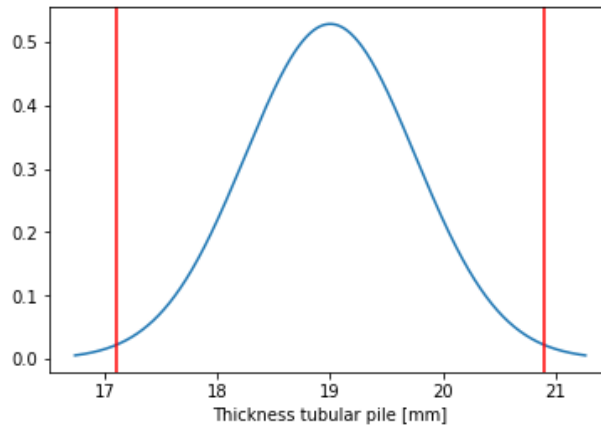


Figure 4.3 PDF of wall thickness with COV of 0.03 (the red lines are the limits for the thickness tolerances given in NEN-EN10219-6)

Uncertainties in the Young’s modulus and the yield strength are taken from the Joint Committee on Structural Safety (2006).The test results of Peters et al. (2017) on the yield strength confirm the COV of 0.07. It also shows that values lower than 0.8 times the nominal value do not appear.

The thickness of the intermediate sheet piles can also deviate by a maximum of 6% but the contribution of the intermediate sheet piles to the sectional properties of the combi-wall can in practice be neglected. Due to the large stiffness difference between the tubular piles and the sheet pile, horizontal soil arches develop and all the load is transferred to the tubular piles. Therefore, the sheet pile properties are not taken into account here.

Table 4.6 COV of the material properties of steel tubular piles

Parameter	Symbol	Distribution	COV
Yield stress	f_y	Normal	0.07
Young’s modulus	E	Normal	0.03
Wall thickness	t	Normal	0.03
Pile diameter	D	Uniform	+/-10mm

With this information the coefficient of variation of the sectional properties of the combi-wall can be determined with a Monte Carlo simulation in Python (Appendix C). The input required in Plaxis is:

- The axial stiffness: EA [kN/m}
- The bending stiffness: EI [kNm²/m]
- Weight per meter length: w [kN/m/m]

Whereas in the LSF for failure of the wall the following properties are required:

- Elastic section modulus W_{el}
- Cross-sectional area A
- Yield strength f_y

The coefficients of variation obtained with the Monte Carlo simulation are given in Table 4.7.

Table 4.7 Distributions of the properties of the combi-wall

Parameter	Distribution	COV
EA	Normal	0.04
EI	Normal	0.04
w	Normal	0.03
W_{el}	Normal	0.03
A	Normal	0.03
f_y	Normal	0.07

The uncertainty in the wall thickness of the tubular pile is the most important uncertainty. The correlation between the structural parameters is also determined in Appendix C. The outcomes are shown in Table 4.8.

Table 4.8 Correlation coefficient of structural parameters combi-wall

	EA	EI	w	W_{el}	A	f_y
EA	-	0.96	0.70	0.68	0.71	0
EI	0.96	-	0.70	0.72	0.70	0
w	0.70	0.70	-	0.96	1.00	0
W_{el}	0.68	0.72	0.96	-	0.96	0
A	0.71	0.70	1.00	0.96	-	0
f_y	0	0	0	0	0	-

Anchor

The properties of the anchor steel bar are also mainly determined by the thickness. It is assumed that the steel thickness can deviate according to the tolerances described in NEN-EN 10219-2 (2006). This code prescribes a maximum deviation in thickness of 0.5mm. A normal thickness for an anchor bar is around 22.0mm. A deviation of 0.5mm corresponds therefore with a change of $0.5/22.0 \cdot 100\% = 2.2\%$

The thickness is assumed to be normally distributed with a COV of 0.02, which implies that 98,8% of the time the thickness is within the tolerance limits. The (composed) random variables of the anchor are given in Table 4.9.

Table 4.9 Probability distribution of the anchor parameters

Parameter	Unit	Distribution	COV
E	N/mm ²	Normal	0.03
t	mm	Normal	0.02
D	mm	Deterministic	-
f_y	N/mm ²	Normal	0.07
EA	N	Normal	0.03

Within Plaxis only the axial strength (EA) and the spacing distance ($L_{spacing}$) are required as input. Therefore no correlation coefficients have to be determined.

4.4 Geometrical parameters

The geometrical parameters are the water levels, the surface levels and the length of the retaining wall. Another important geometrical parameter is the soil layer thickness. In a deterministic analysis, the soil stratification is based on a (conservative) interpretation of a limited number of CPT's, wherein all soil layers are assumed horizontal and for which layer-averaged properties are used. Of course, in reality soil layers are not strictly horizontal as the layer thickness varies in space. The use of perfectly horizontal soil layers with a fixed layer thickness can therefore be a significant simplification of reality. Advanced methods to account for soil variability are for example the application of Random Fields (Vanmarcke et al., 1986) in which soil properties are randomly distributed in space given a certain spatial correlation length. However, this is outside the scope of this thesis. Besides, both case studies are located on the Maasvlakte which means that a large part of the soil profile consists of reclaimed land. Large spatial variations in the soil profile due to natural variability are therefore less likely.

Water levels

The Port of Rotterdam is in direct connection with the open sea. Therefore the tide is influencing the water levels within the port. The normative load case for a quay wall is generally a low outer water level and a high ground water level. Especially the difference between these two water levels is of importance. The degree of correlation between both water levels depends on the presence and functioning of a drainage system, the permeability of the wall and the permeability of the soil.

Surface levels

The surface level on the landside is normally known with high accuracy and does not deviate much because very often the surface is paved up till the edge of the wall.

The bottom level on the water side of the wall is much more uncertain due the inaccuracies of the dredging equipment and the placement of the bed protection. In case no bed protection is applied scour holes are a large threat.

Length retaining wall

The length of the sheet pile or the tubular piles can deviate from its design specifications due to for example installation problems after which the piles are not installed to the predefined depth. This kind of uncertainty will not be taken into account here.

4.5 Load parameters

Next to the load imposed by the soil and the water level difference also other loads are active on the structure. Loads that are of importance for a quay wall in the Rotterdam region are:

- Mooring loads
- Berthing loads
- Surcharge loads (Coal piles, container stacks etc.)
- Crane loads
- Temperature loads
- Wind loads
- Vessel collision

The magnitude and distribution of variables describing the load on a quay wall are largely site-specific, whereas each type of load also has different characteristics. Therefore, they are described separately in each case study.

5

CASE STUDY 1: DOUBLE ANCHORED COMBI-WALL

5.1 Introduction

The first case study considers a quay wall constructed in the Port of Rotterdam near a storage location for LNG. This quay wall is constructed in 2016 and is designed in accordance to RC3. The structure consists of a combi-wall with concrete cap. The combi-wall is anchored by two grout anchors in the tubular steel piles of the combi-wall and has a retaining height of approximately 20m. An overview of original design model is shown in Figure 5.1.

The goal of the first part of this case study is to get familiar with the use of ProbAna and Plaxis. The problem is therefore partly simplified by reducing the amount of soil layers and the amount of construction stages. Also only the load case that was normative for both the anchor and the wall is considered.

The following aspects are considered in this case study:

- The difference in results between calculations using correlated or uncorrelated variables
- The influence of the uncertainty in structural properties on the reliability for the considered limit state. (structural properties cannot be inserted as stochastic in ProbAna)
- The applicability of FORM for the three considered failure mechanisms
- Where possible a comparison with the maximum allowed reliability index prescribed by guidelines
- The influence of time-dependant variables

The second part of the case study is focussed on the derivation of partial factors and the evaluation of an critical limit state.

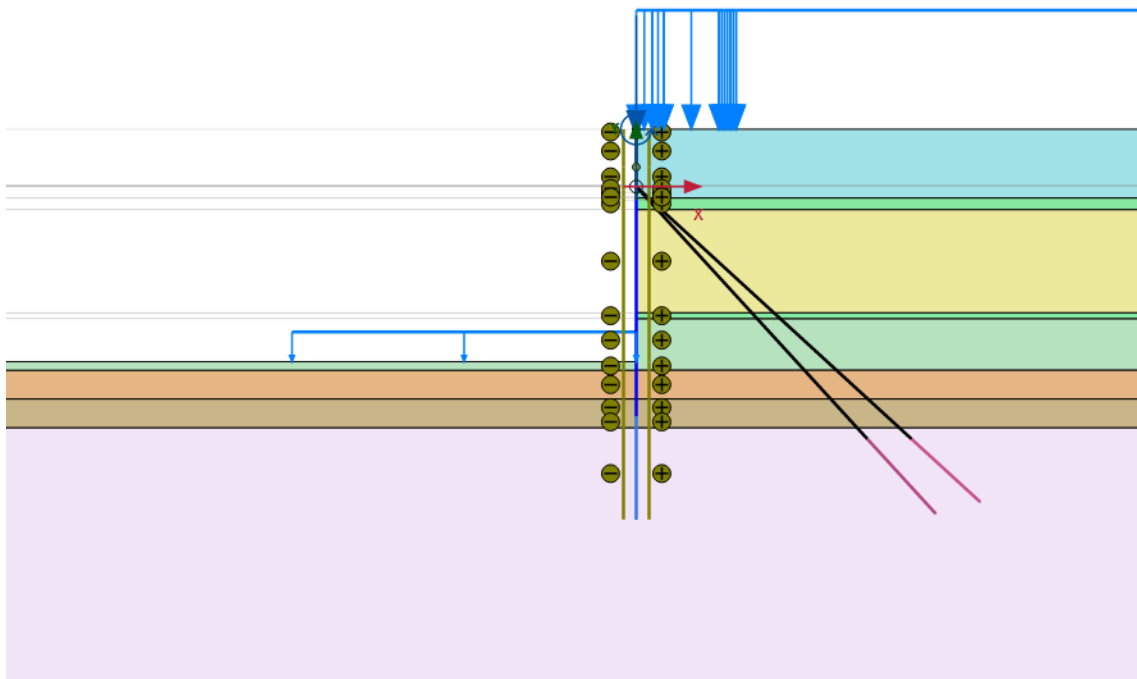


Figure 5.1 Original design model of the quay wall

5.2 Starting points

5.2.1 Soil parameters

The characteristic values of the soil parameters used in the original design are given in Table 5.1.

Table 5.1 Characteristic soil parameters used in the original design

Top layer [m w.r.t. NAP]	Description [-]	γ_{unsat} [kN/m ³]	γ_{sat} [kN/m ³]	c [kPa]	φ [°]
+5.0	Sand, moderate	18.0	20.0	0.0	32.5
-1.0	Clay, sandy, moderate	18.0	18.0	5.0	22.5
-2.0	Sand, loose	17.0	19.0	0.0	30.0
-11.0	Clay, sandy, moderate	18.0	18.0	5.0	22.5
-11.5	Sand, w. clay	18.0	20.0	0.0	25.0
-16.0	Clay, sandy	18.0	18.0	0.0	27.5
-18.5	Clay, sandy, moderate	17.6	17.6	19.0	21.4
-21.0	Sand, dense	19.0	21.0	0.0	35.0

To reduce the computational time of the Plaxis model, the soil profile is simplified. From a depth of NAP -1 m up till NAP -16.0m, the soil consists mostly of loose sand and sandy clay layers with two very thin clay layers. All these layers are replaced by one single slight clayey sand layer. The effect of this simplification on the anchor force and the bending moment in the wall is verified and the parameters of the replacing sand layer are adjusted so that the consequences of the output results are minimal. The impact of this simplification in terms of reliability is evaluated in Chapter 7. The simplified soil profile is given in Table 5.2 whereas the Hardening Soil parameters are given in Table 5.3.

Table 5.2 Characteristic values of the simplified soil profile

Top layer [m w.r.t. NAP]	Description [-]	γ_{unsat} [kN/m ³]	γ_{sat} [kN/m ³]	c [kPa]	φ [°]
+5.0	Sand, moderate	18.0	20.0	0.0	32.5
-1.0	Sand, loose, clayey	17.0	19.0	0.0	27.5
-15.25	Clay, very sandy	18.0	18.0	0.0	27.5
-18.5	Clay, little sandy	17.6	17.6	19.0	21.4
-21.0	Sand, dense	19.0	21.0	0.0	35.0

Table 5.3 Characteristic Hardening Soil parameters

Top layer [m w.r.t. NAP]	Description [-]	E_{50}^{ref} [MN/m ²]	$E_{\text{oed}}^{\text{ref}}$ [MN/m ²]	$E_{\text{ur}}^{\text{ref}}$ [MN/m ²]	m [-]	Ψ [°]	R_{inter} [-]
+5.0	Sand, moderate	45.0	45.0	180.0	0.5	2.5	0.8
-1.0	Sand, loose, clayey	15.0	15.0	60.0	0.5	0.0	0.8
-15.25	Clay, very sandy	8.0	5.3	24.0	0.8	0.0	0.8
-18.5	Clay, little sandy	5.0	3.3	15.0	0.9	0.0	0.8
-21.0	Sand, dense	75.0	75.0	225.0	0.5	5	0.8

The characteristic values are transformed into mean values by the application of the COV-values of Table 4.2. The deterministic values for the stress level dependency factor, the dilatancy angle and the interface strength are determined based on engineering practice.

Depending on whether it is a load parameter or a strength parameter the mean value is determined in the following way:

$$\mu_i = \frac{X_{i,k}}{1 \pm 1.64COV_i} \tag{5.1}$$

In the case of log-normally distributed variables the mean value can be determined by:

$$\mu_{xi} = \frac{X_{k,i} \sqrt{1 + COV_i^2}}{\exp(-1.645 \sqrt{\ln(1 + COV_i^2)})} \tag{5.2}$$

The values for volumetric weight are already mean values and are therefore not changed. For some other parameters the outcomes are slightly adjusted to avoid physically unrealistic values. The expected soil parameters are given in Table 5.4 and Table 5.5

Table 5.4 Mean values of the soil parameters

Top layer [m w.r.t. NAP]	Description [-]	γ_{unsat} [kN/m ³]	γ_{sat} [kN/m ³]	c' [kPa]	ϕ' [°]
+5.0	Sand, moderate	18.0	20.0	0.0	38.9
-1.0	Sand, loose, clayey	17.0	19.0	0.0	32.9
-15.25	Clay, very sandy	18.0	18.0	0.0	32.9
-18.5	Clay, little sandy	17.6	17.6	28.3	25.6
-21.0	Sand, dense	19.0	21.0	0.0	40.0

Table 5.5 Mean values of the HS parameters

Top layer [m w.r.t. NAP]	Description [-]	E_{50}^{ref} [MN/m ²]	E_{oed}^{ref} [MN/m ²]	E_{ur}^{ref} [MN/m ²]	m [-]	Ψ [°]	R_{inter} [-]
+5.0	Sand, moderate	45	45	135	0.5	2.5	0.8
-1.0	Sand, loose, clayey	30	30	90	0.5	0.0	0.8
-15.25	Clay, very sandy	16	10	48	0.8	0.0	0.8
-18.5	Clay, little sandy	10	6	30	0.9	0.0	0.8
-21.0	Sand, dense	70	70	210	0.5	5	0.8

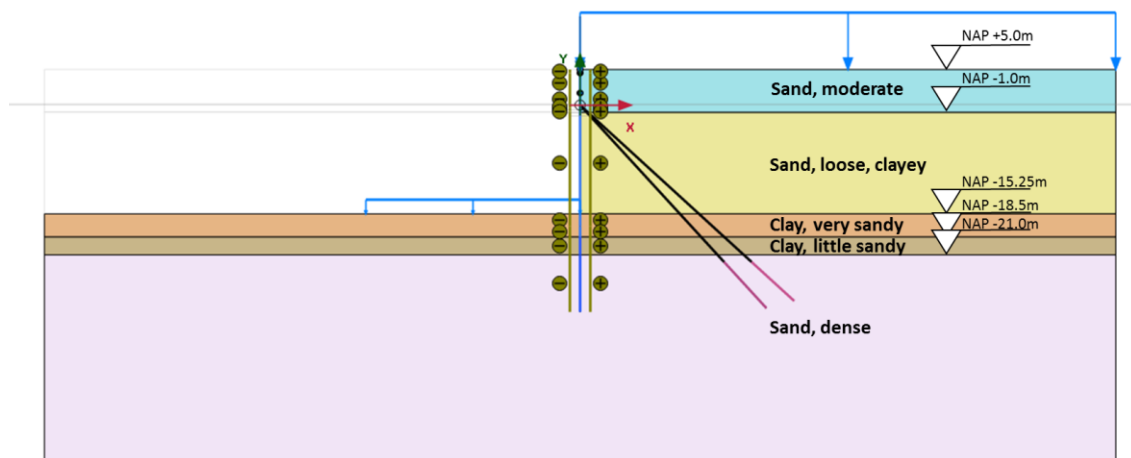


Figure 5.2 Schematization of the quay wall

5.2.2 Structural parameters

The combi-wall consists of tubular piles with a diameter of 1420mm and triple intermediate sheet piles of type PU22. The combi-wall has a system length of 3.294m, whereas in Plaxis only a section of 1 m width is considered. Therefore, the properties of the wall are averaged to acquire input values for a 1 m' wall. It is assumed that the intermediate sheet piles do not contribute to the bearing- and bending moment capacity of the wall. A detailed overview of the structural properties is given in Table 5.6. As cathodic protection is applied, no corrosion is taken into account.

Table 5.6 Properties of the combi-wall

	Description	Symbol	Value	Unit
Sheet piles	type		PU22	-
	Amount		3	-
	Steel grade	f_y	S355GP	N/mm ²
	Tip level		-20.0	m NAP
Tubular piles	Outer diameter	D	1420	mm
	Thickness	t	19	mm
	Steel grade	f_y	X70 (485 MPa)	-
	Pile tip level		-29.0	m NAP
	c.t.c. distance		3.294	m
Properties per m'	Bending stiffness	EI	$1.308 \cdot 10^6$	kNm ² /m
	Axial stiffness	EA	$5.33 \cdot 10^6$	kN/m
	Weight	w	2.77	kN/m/m
	Cross-sectional area	A	$2.539 \cdot 10^{-2}$	m ² /m
	Section modulus	W_{el}	$8.77 \cdot 10^{-3}$	m ³ /m

The combi-wall is anchored by two anchors. Both anchors only differ with respect to the angle with the horizontal and the cross-sectional area of the steel bar. The properties are given in Table 5.7.

Table 5.7 Anchor properties

	Symbol	Anchor 1	Anchor 2	Unit
Angle w.r.t. horizontal		47.5	42.5	°
Anchor type		101.6 x 25.0 mm	101.6 x 22.2 mm	-
Cross-sectional area	A	5,986	5,510	mm ²
Yield stress (characteristic)	f_y	500	500	N/mm ²
Connection with wall		0.0	0.0	m NAP
Top level grout body		-22.0	-22.0	m NAP
Length grout body		8.80	8.10	m
Diameter grout body		380	380	mm
c.t.c. distance		3.294	3.294	m

Except for the yield stress of both the wall and the anchors, all properties of Table 5.6 and Table 5.7 are assumed to be deterministic mean values. The mean values for the yield stress are given in Table 5.8.

Table 5.8 Mean values yield stress

	Parameter	Unit	Distribution	X_k	COV	X_m
Tubular piles	f_y	N/mm ²	Normal	485	0.07	548
Anchor	f_y	N/mm ²	Normal	500	0.07	565

5.2.3 Construction stages and meshing

The computation time for each LSFE depends largely on the amount of construction stages and the coarseness of the mesh. A balance should be found between accuracy and computational time.

The construction stages for this project are:

- 1 Gravity loading
- 2 Installation of the combi-wall
- 3 Excavating to NAP +0.0m
- 4 Installation and prestressing of the grout anchors
- 5 Excavation until construction depth of NAP-15.25m
- 6 Load case
- 7 (safety phase)

The applied mesh size in this model is medium, resulting in the mesh plot shown in Figure 5.3.

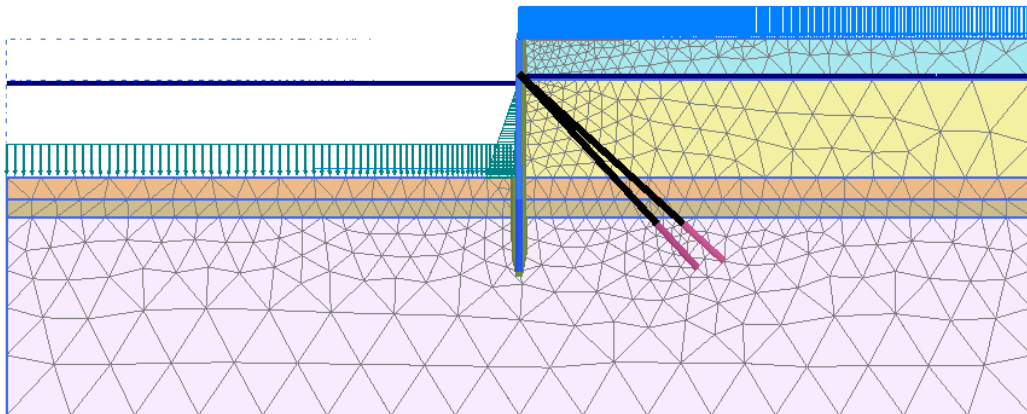


Figure 5.3 Connectivity plot

5.2.4 Loads, water levels and geometry

Due to the time limitations, the reliability of the quay wall is only determined for one load case, which is the normative load case in the original design. This concerns the load combination with a surcharge load of 40 kPa and a bollard load of 28kN/m'.

For the time-dependant variables, the applied values are representative for the design lifetime.

Permanent loads

The considered permanent loads are the weight of the concrete cap beam (400 kN/m) and the weight of the bottom protection (10kPa).

Variable loads

The considered variable loads are the surcharge load of 40 kPa next to the quay wall and the bollard load of 28 kN at a level of NAP +1.7m.

Geometry

The ground surface level is at NAP +5.0m, which can be determined with high accuracy and is therefore considered deterministic. The bottom level is assumed at the design depth of NAP-15.25m. The occurrence of scour holes is prevented by a bed protection. Within the calculation of the design depth, the dredging and placement tolerances are already taken into account. Also, the bottom level is taken as deterministic in this case study.

Water levels

For the first calculations, only the soil parameters are considered as random variables. Therefore, deterministic values for the outer water level and ground water level are determined here.

The difference between the outer water level (OWL) and the ground water level (GWL) is the most important water load on the quay wall. In the final calculation phase in Plaxis the OWL is chosen in accordance to CUR211.

Table 5.9 Fundamental water pressure difference Δh with drainage. Source: CUR211 (2013)

Water level fluctuations	Soil conditions	OWL	GWL	Δh_{min}
Minor	-	MLW	$h_{drainage} + 0.3m$	$> 0.5m$
Major (rivers)	-	OLW/OLR	$h_{drainage} + 0.3m$	$> 0.5m$
Tidal conditions	-	LLWS	$h_{drainage} + 0.3m$	$> 0.5m$

In case of a load combination where the water level difference is not the dominant load, which is the case here, the OWL is taken as Low Low water Spring (LLWS), which is the mean of the lowest spring tide level of every month over 5 years. For this case holds: LLWS = NAP -0.84m.

The quay wall is equipped with a drainage system at LLWS. In case of a working drainage system, the GWL should be the maximum value of ($h_{drainage} + 0.3m$; OWL + 0.5m). The second value is normative, resulting in a ground water level of NAP-0.34m.

It should be noted that the occurrence of extreme low water levels should be considered in a separate accidental load case, which turned out not to be the normative load case for the bending moment of the wall. Considering both extreme loads and extreme water levels in one load case would be very unrealistic, the two loads are uncorrelated and therefore the probability that they occur simultaneously is very small.

During the construction stages, the ground water potential in all layers is taken at NAP +0.07m. In the final calculation phase, the ground water potential in the loose sand layer on the land side is set to NAP-0.34m, whereas the potential in the (deep) dense sand layer is set equal to the outer water level (=LLWS). The two thin clay layers are set on interpolation. The modelling of the groundwater pressures is depicted in Figure 5.4.

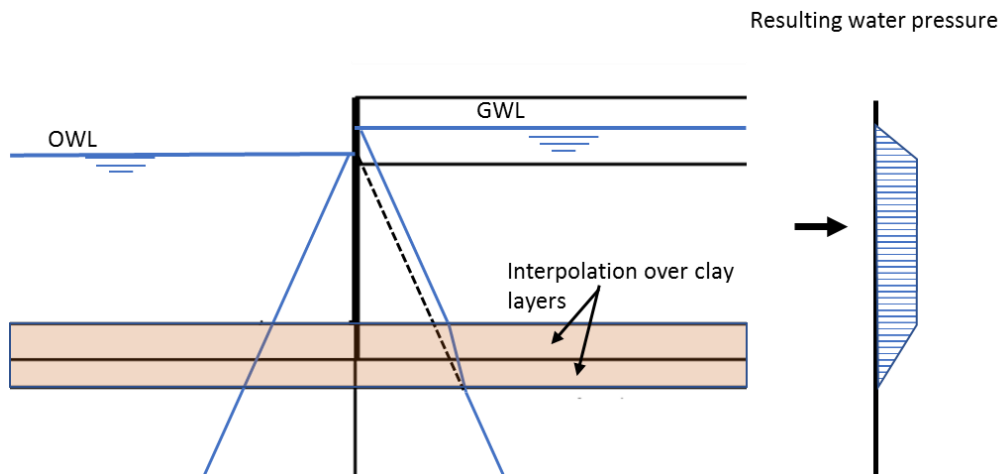


Figure 5.4 Modelling of the ground water pressures

As almost the complete soil profile consists of sand layers and sandy clay layers, all calculations in this case study are performed assuming drained conditions. The present clay layers are thin, which also means they can drain relatively quickly. Therefore, it is expected that this simplification has negligible influence on the outcomes.

5.3 LS1: Yielding of the combi-wall

Firstly, the yielding of the sheet pile wall is considered. The general equation for the limit state of the yielding of the combi-wall was already discussed in chapter 5.2.1.

$$Z = M_R - M_S \tag{5.3}$$

The threshold value for the bending moment can be determined with the following equation:

$$M_R = \left(f_y - \left| \frac{N(z)}{A} \right| \right) * W_{el} \tag{5.4}$$

The magnitude of the normal force is for a large part influenced by the vertical component of the anchor forces. This is shown in Figure 5.5, where at the location of the anchor connection a jump in the normal force can be noticed. Below the anchor connection point, the normal force only slightly increases with depth due to the wall friction. The increase in the maximum normal force from a mean value calculation (A), all the way up to the design point calculation (B), is relatively small (600 kN). For small variations in the soil parameters around the design point, the normal force is almost constant. This supports the assumption that the use of a deterministic value for the normal force does not influence the outcomes significantly.

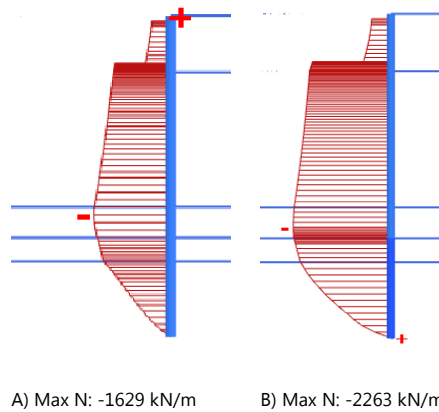


Figure 5.5 Normal force in the combi-wall for: A) mean value calculation B) design point

Using equation 5.4 together with the values for the structural properties given in Table 6.5 holds:

$$M_R = 4046 \text{ kNm/m}$$

The LSF then becomes:

$$Z = 4046 - M_S \tag{5.5}$$

The maximum bending moment using mean values for the soil parameters is 1719 kNm/m (Figure 5.6). This already indicates that there is a lot of extra capacity left in the combi-wall.

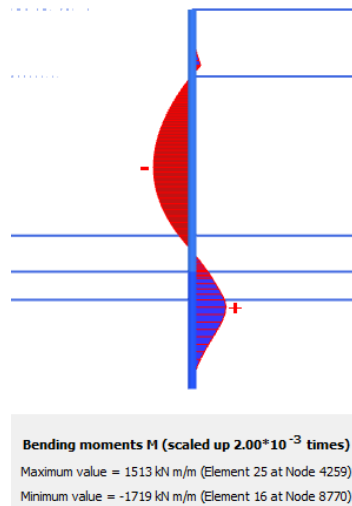


Figure 5.6 Bending moment distribution with a mean value calculation

5.3.1 FORM sensitivity analysis

To determine the most relevant parameters, a sensitivity analysis is carried out with uncorrelated parameters. In this way, a better insight is gathered into the most important parameters, without the effect that a parameter is increased only due to its correlation with another parameter and not due to its own influence.

Only the soil parameters are taken as variables in this first case study. For every layer the volumetric weight, the friction angle and the stiffness are considered as stochastic, except for the clay layers, in which the volumetric weight is not considered due to the small size of these layers and the relatively small uncertainty of this property.

When considering the results of Figure 5.7, it can be clearly concluded that the friction angle is the most dominant soil parameter in this case. This can be explained by the fact that the active lateral soil pressures increase when the friction angle decreases, resulting in a larger load on the wall. Besides, the passive resistance of the soil decreases when the friction angle decreases. The friction angle of the loose sand layer is the most dominant parameter. This was also expected given the vertical extent of this layer and its position covering the entire free span length of the wall between the anchor and fixation in the soil. The soil stiffness seems to have only little influence in this case.

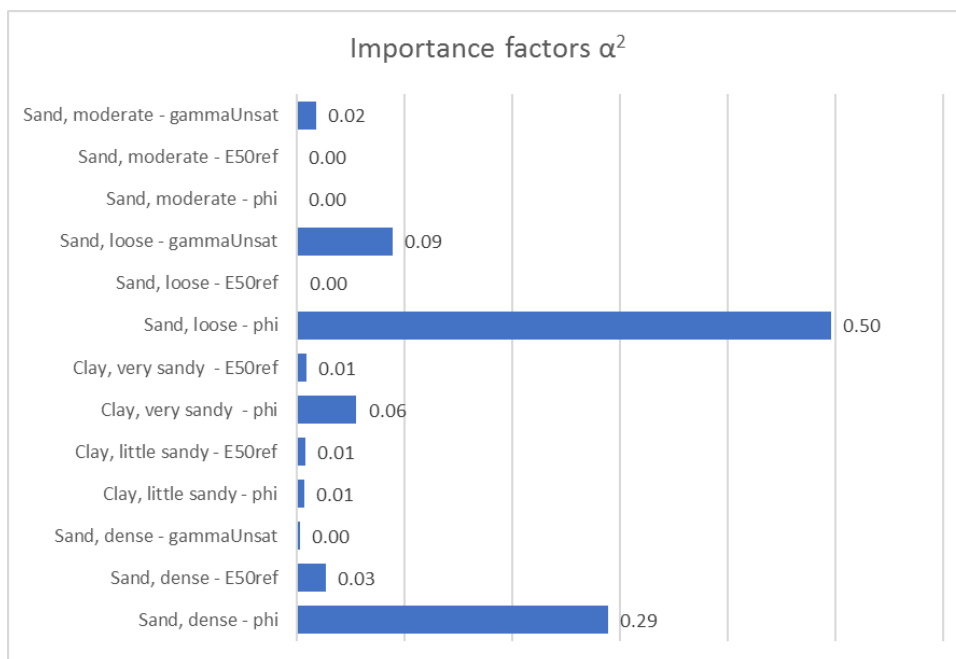


Figure 5.7 Importance factors wall failure, uncorrelated

Table 5.10 Calculation information, wall failure, uncorrelated

	Value
Reliability index β	6.9
Failure probability P_f	$2.2 \cdot 10^{-12}$
Number of iterations	31
Number of LSFE	547
Duration	18 hrs

The value for each parameter in the design point is given in Table 5.11.

Table 5.11 Design values vs mean values, wall failure, uncorrelated

Parameter	Unit	X_m	X^*	α^2
Sand, moderate - gammaUnsat	kN/m ³	18.0	18.8	0.02
Sand, moderate - E50ref	kN/m ²	45000	42862	0.00
Sand, moderate - phi	°	38.9	38.8	0.00
Sand, loose - gammaUnsat	kN/m ³	17.0	18.8	0.09
Sand, loose - E50ref	kN/m ²	30000	29792	0.00
Sand, loose - phi	°	32.9	16.9	0.50
Clay, very sandy - E50ref	kN/m ²	16000	12623	0.01
Clay, very sandy - phi	°	32.9	27.6	0.06
Clay, little sandy - E50ref	kN/m ²	16000	8002	0.01
Clay, little sandy - phi	°	25.6	24.1	0.01
Sand, dense - gammaUnsat	kN/m ³	19.0	18.7	0.00
Sand, dense - E50ref	kN/m ²	90000	61747	0.03
Sand, dense - phi	°	40.0	25.1	0.29

The obtained reliability index with this run is 6.9. This value is very high compared to the target reliability of 4.3. It must be noted that the uncertainty in the yield strength is not incorporated in the obtained value. Due to the significant uncertainty in this property and the direct contribution to the LSF it is expected that the reliability is therefore (slightly) lower. The influence of a lower yield strength on the reliability is determined hereafter.

Besides, due to financial and practical reasons there was chosen for thicker tubular piles than originally required. Another explanation for this high value is the fact that this quay wall is originally designed with D-sheet piling. In contrary to Plaxis, this program models the retaining wall as an uncoupled spring supported beam. Due to the uncoupled springs, vertical arching is not taken into account. Vertical arching causes that the horizontal load is transferred to the stiffer parts of the wall, being the support by the anchor and the fixation in the soil. This results in lower midspan maximum bending moments and higher anchor forces when modelling in Plaxis compared to D-sheet piling. For this quay wall, the bending moments in the wall are approximately 20% lower compared to a D-sheet piling calculation.

These two reasons make that a unity check of 0.78 was obtained in the reassessment of this quay wall performed by Witteveen+Bos (2017).

A fair comparison with the design guidelines is therefore not possible. Later on in this subchapter, a run is performed using a redesigned wall with a unity check of 0.99.

5.3.2 FORM with correlated parameters

Based on the results of the sensitivity analysis, a FORM calculation is performed with only six parameters but now including correlations to achieve a more realistic result. The incorrectness of the use of uncorrelated parameters can be shown on the hand of Table 5.11. The unsaturated unit weight of loose sand is a load parameter and is therefore increased whereas the friction angle is a resistance parameter and is largely decreased. This is contradictory to the general positive correlation between unit weight and friction angle. For

this kind of reasons it can be expected that the use of correlated parameters would result in a lower failure probability.

The performed calculation with correlated parameters did not converge within the 30 iterations that were set as a limit. By analysing the results of this run, the errors were reasonably close to their tolerances and therefore the results are accepted (Table 5.12).

The reliability index β found is 7.4, which is considerably higher than the value of 6.9 found with the uncorrelated parameters.

Table 5.12 Calculation results, wall failure, correlated

	Value	
Reliability index β	7.4	
Failure probability P_f	$6.0 \cdot 10^{-14}$	
Number of iterations	31	
Number of LSFE	315	
Duration	30 hrs	
Absolute error after 30 iterations:	0.09	Tolerance: 0.05
Relative error after 30 iterations:	0.01	Tolerance: 0.05
Residual error after 30 iterations:	0.28	Tolerance: 0.05
Constraint error after 30 iterations:	3.5 kNm	Tolerance: 20

The obtained importance factors are compared to the importance factors of the run with uncorrelated parameters (Figure 5.8). It can be seen that the differences in general are relatively small. Especially a significant change in the importance of the stiffness of the dense sand layer can be noticed. This change can be partly clarified by the correlation with the friction angle, but this is only a weak correlation (0.25) and therefore it does not fully explain this change. Apparently due to the reduction in the number of stochastic variables and the redistribution of importance, more importance is taken by the stiffness of the dense sand layer.

Another large relative change occurs in the volumetric weight of the loose sand (0.09 to 0.01). The correlation with the friction angle causes a reduction in weight instead of an increase which was the case for uncorrelated parameters. A comparison of the design point with correlated and uncorrelated parameters is given in Table 5.13.

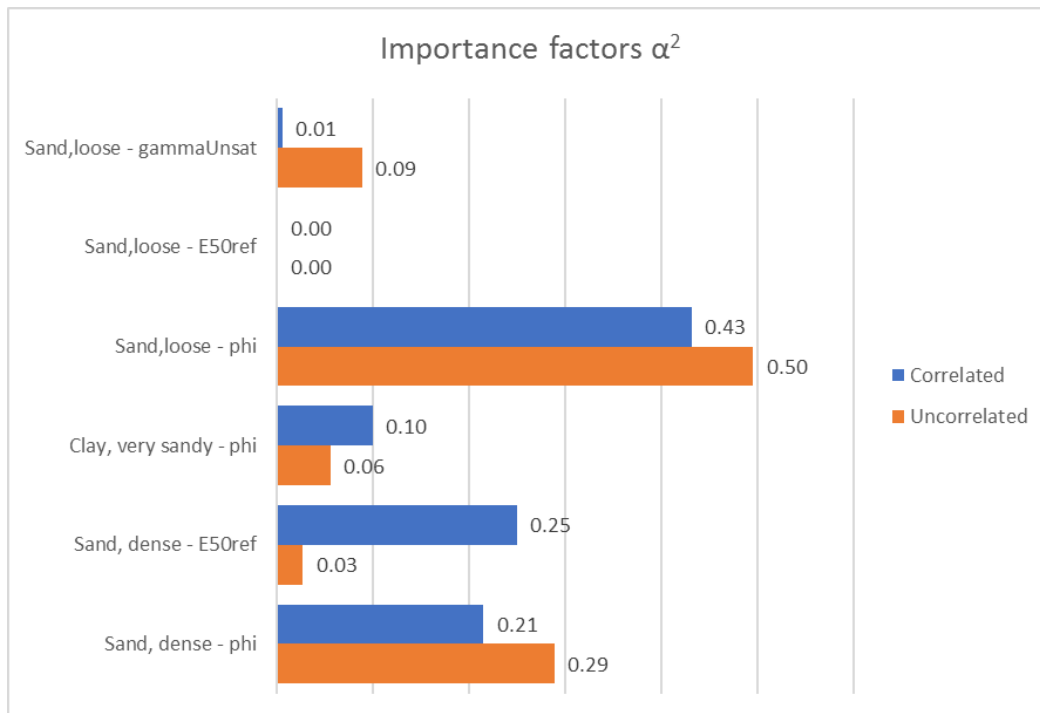


Figure 5.8 Importance factors of the uncorrelated and correlated run, wall failure

Table 5.13 Design point, wall failure, correlated

Parameter	Unit	X* (correlated)	X* (uncorrelated)	X _m
Sand, loose - gamma _{Unsat}	kN/m ³	16.5	18.8	17.0
Sand, loose - E50ref	kN/m ²	26948	29792	30000
Sand, loose - phi	°	18.1	16.9	32.9
Clay, very sandy - phi	°	25.2	27.6	32.9
Sand, dense - E50ref	kN/m ²	29065	61747	90000
Sand, dense - phi	°	21.0	25.1	40.0

The failure state of the soil in the design point for correlated parameters is shown in Figure 5.9. The red points in this figure are the most important as they indicate failure of the soil. The failure points clearly indicate that the structure is on the edge of soil mechanical failure. This is also confirmed by the fact that one of the runs actually did not finish due to soil mechanical failure.

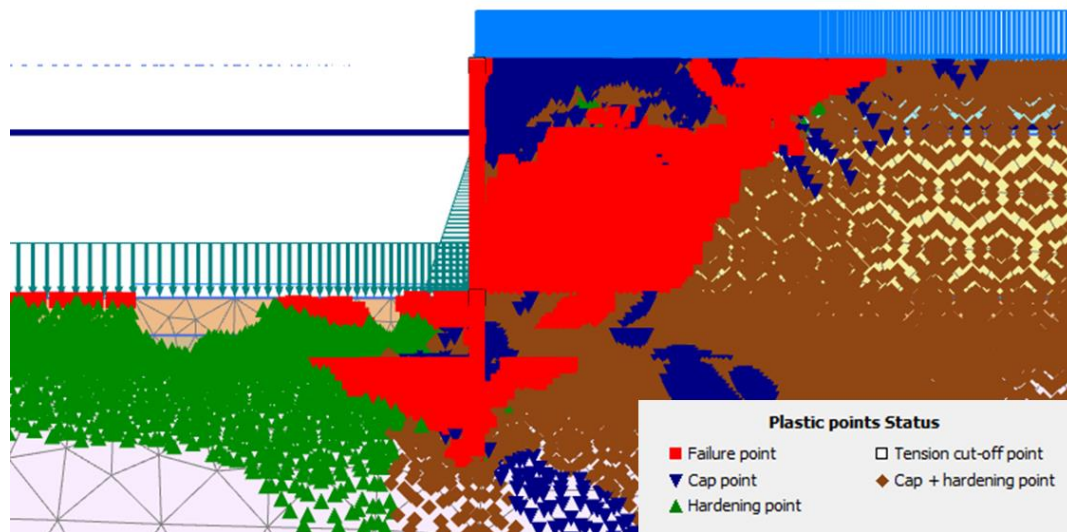


Figure 5.9 Plastic point status in the design point, wall failure

5.3.3 Run with characteristic yield strength

Up until now, the reliability is calculated with the mean value for the yield stress of the tubular pile. It can be expected that the yield stress has a significant importance in the limit state due to its explicit presence in the LSF (equation 5.4). When instead of the mean value ($f_y=548 \text{ N/mm}^2$), the characteristic value ($f_y=485 \text{ N/mm}^2$) is used for the yield stress, the bending moment threshold value in the LSF reduces from 4046 to 3495 kNm/m'. The limit state function then becomes:

$$Z = 3495 - M_{\zeta} \tag{5.6}$$

Using five of the six parameters of the previous run with correlated parameters, the reliability index found for this new LSF is 6.5 (Table 5.14). The unit weight was left out of the calculation due to its low importance in the previous run.

When comparing the β of both runs, it can be concluded that the yield stress is a dominant stochastic variable which should be included in the determination of the failure probability and the importance factors.

Table 5.14 Influence of the yield strength on the reliability index, wall failure, correlated

	$f_{y,kar}=485 \text{ N/mm}^2$	$f_{y,mean}=548 \text{ N/mm}^2$
Reliability index β	6.5	7.4
Failure probability P_f	$3.8 \cdot 10^{-11}$	$6.0 \cdot 10^{-14}$
Number of iterations	100	30
Number of LSFE	856	315
Duration	40 hrs	12 hrs

The significant difference in calculation time between both runs is mainly caused by a change in convergence settings and a bug in ProbAna as one of the three convergence rules was not obeyed correctly. When both the residual error and the constraint error are below their pre-set tolerances, the calculation should stop, which due to unknown reasons did not happen during this run.

The importance factors for both runs are shown in Figure 5.10. Comparing both runs, a significant change in importance factors can be noticed, predominantly a shift from the importance of the friction angle of the dense sand layer to the friction angle of the loose sand layer.

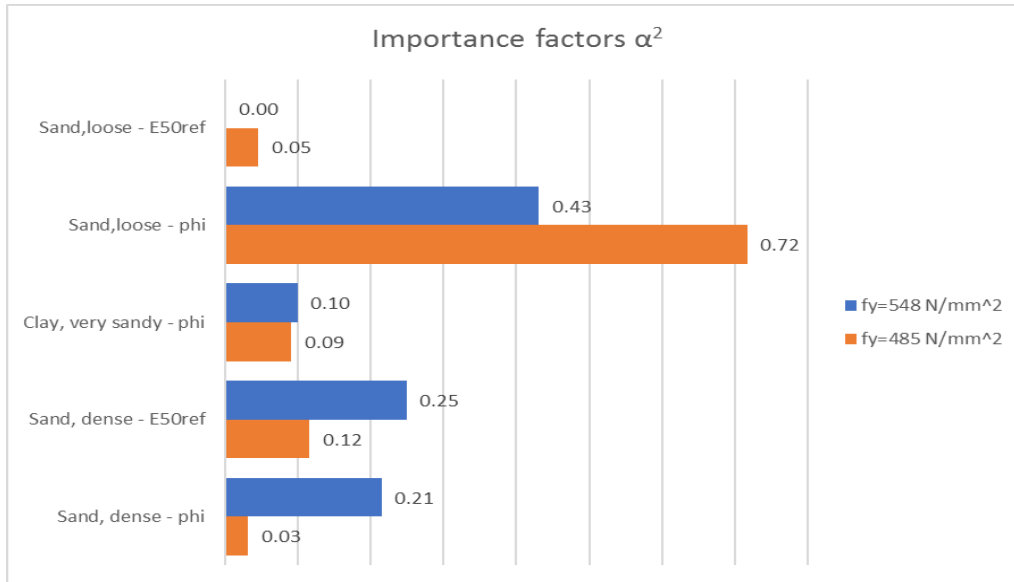


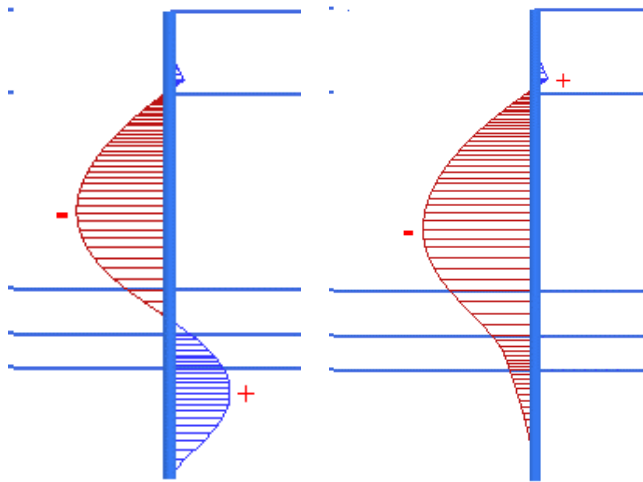
Figure 5.10 Importance factors for varying yield stress, wall failure, correlated

The soil properties in both design points are given in Table 5.15.

Table 5.15 Comparison of the design point for a changing yield stress. Due to the low importance of the unit weight of the loose sand this variable was left out of the calculation to reduce computational time.

Parameter	Unit	Design point ($f_{y,kar}=485 \text{ N/mm}^2$)	Design point ($f_{y,mean}=548 \text{ N/mm}^2$)	Mean X_m
Sand, loose - gammaUnsat	kN/m ³	Not included	16.5	17.0
Sand, loose - E50ref	kN/m ²	19112	26948	30000
Sand, loose - phi	°	14.2	18.1	32.9
Clay, very sandy - phi	°	26.5	25.2	32.9
Sand, dense - E50ref	kN/m ²	45021	29065	90000
Sand, dense - phi	°	33.3	21.0	40.0

Because of the difference in importance factors, the bending moment distribution in both design points is compared in Figure 5.11. The shape shown in A is as expected, whereas in B the fixed moment is completely disappeared. In case B, the bending moment capacity of the wall is that high that a further reduction of the friction angle of the loose sand could not enforce failure and hence the friction angle of the dense sand layer is getting more importance and is reduced from 40° to 21.0°.



A) $M_{max} = 3495 \text{ kNm}$
 $f_{y,kar} = 485 \text{ N/mm}^2$
 B) $M_{max} = 4045 \text{ kNm}$
 $f_{y,mean} = 548 \text{ N/mm}^2$

Figure 5.11 Comparison of bending moment distribution

Besides that, also the failure of the passive wedge is far less pronounced for this run ($f_{y,kar} = 485 \text{ N/mm}^2$, $M_{max} = 3495 \text{ kNm}$) as shown in Figure 5.12.

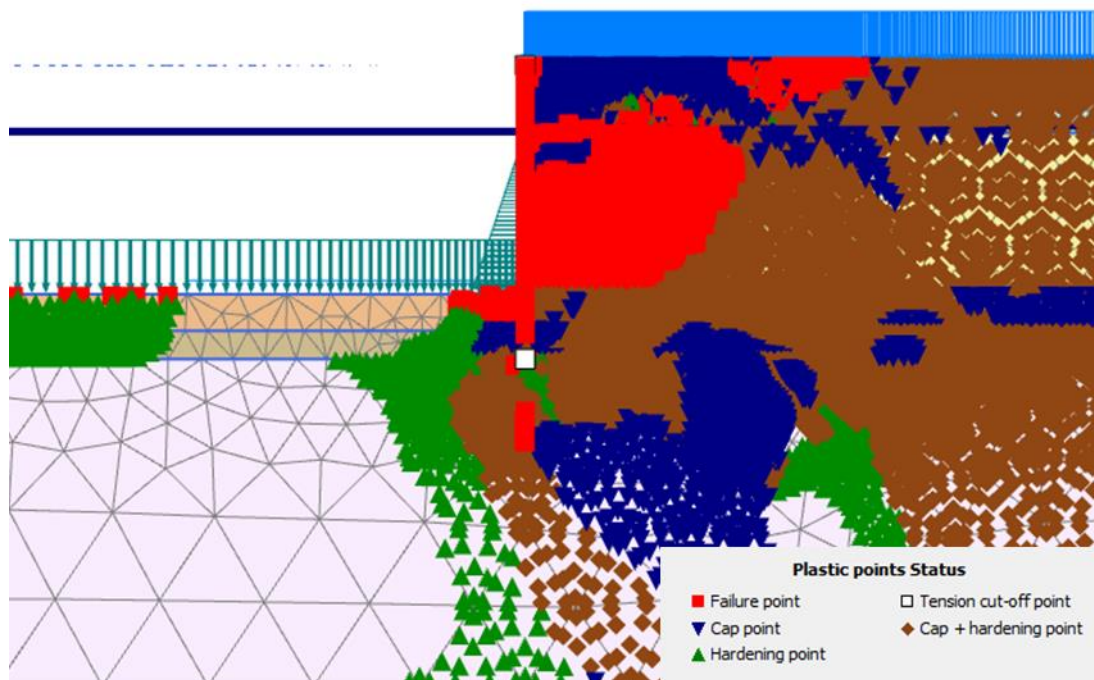


Figure 5.12 Failure points in the design point for LSF with $f_{y,kar} = 485 \text{ N/mm}^2 \rightarrow M_{max} = 3495 \text{ kNm}$

A rough graph of the correlation between yield stress and reliability shows that the yield stress has significant influence on the reliability. One can notice that no clear linear correlation exist between yield stress and β . This can therefore in the remainder of the case study characteristic values for the yield strength are used.

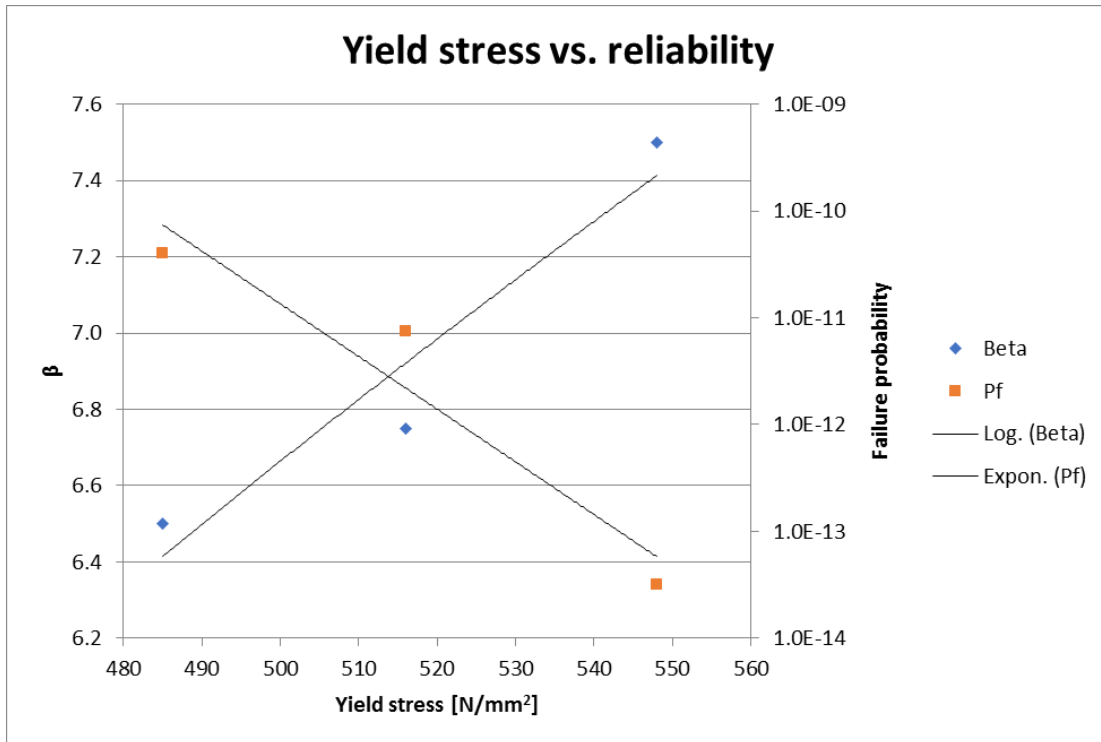


Figure 5.13 Yield stress vs. reliability

5.3.4 Influence of time-dependent loads

Until now only the soil is taken as random variable together with a deterministic normative load combination. To determine the influence of the water level difference and the surcharge load, a run is performed assuming both variables as stochastic.

The following distribution are assumed for the water level and the load:

Table 5.16 Distributions for the outer water level and the surcharge load

	Distribution	Mean	Standard deviation
OWL	Normal	-0.84 m	0.20 m
Surcharge load	Normal	40 kPa	8 kPa

To keep the number of variables limited, only the outer water level is taken as a variable, leaving the ground water level constant. Ground water level and outer water level have a relatively high correlation in case of a functioning drainage. Therefore assuming only one of the two as stochastic will most likely not lead to very different results than when assuming both as stochastic as long as this is taken into account in the standard deviation of OWL.

The standard deviations in Table 5.16 are based on an educated guess. For the distribution of the OWL the extreme water level distributions shown in Figure 5.14 were taken into consideration.

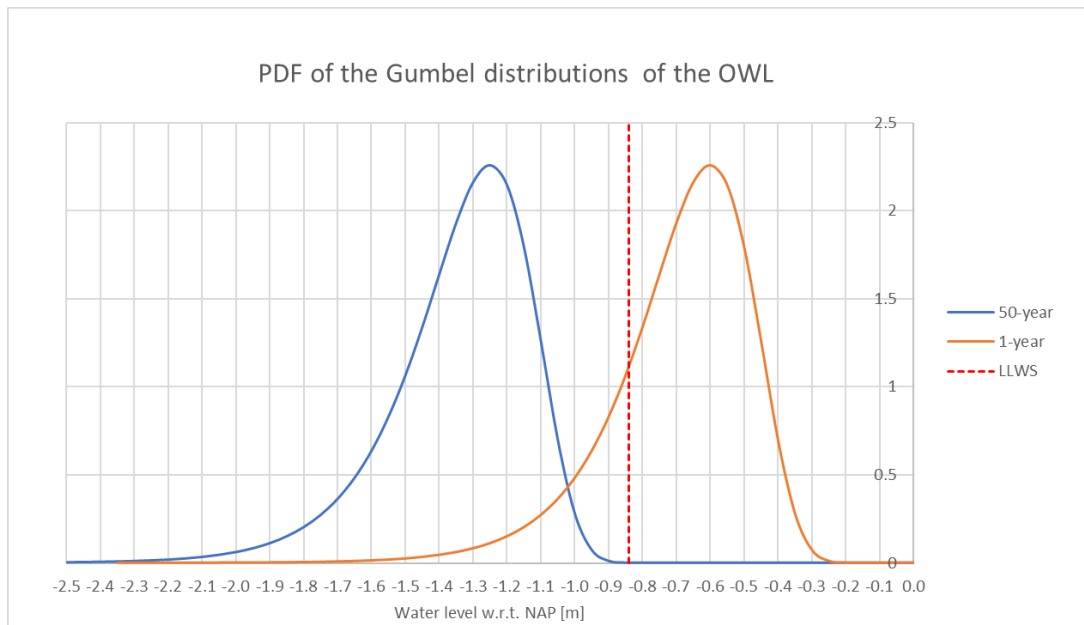


Figure 5.14 PDF of the extreme value distributions of the OWL of the Maasvlakte

Table 5.17 Calculation results, wall failure, including time dependent load variables

	Value			
Reliability index β	5.5			
Failure probability P_f	$1.8 \cdot 10^{-8}$			
Parameter	Unit	Design point ($f_{y,kar}=485 \text{ N/mm}^2$)	Mean X_m	Importance factor α^2
OWL	m	-1.11	-0.84	0.07
Surcharge load	kPa	-40.0	-40	0.00
Sand, moderate - gammaUnsat	kN/m ³	18.8	18.0	0.02
Sand, moderate - phi	°	41.3	38.9	0.01
Sand, loose - gammaUnsat	kN/m ³	16.6	17.0	0.01
Sand, loose - E50ref	kN/m ²	29538	30000	0.00
Sand, loose - phi	°	19.0	32.9	0.63
Clay, very sandy - phi	°	27.5	32.9	0.10
Sand, dense - E50ref	kN/m ²	41124	90000	0.11
Sand, dense - phi	°	35.3	40.0	0.05

Compared to the reliability index of the run with deterministic loads a slight decrease of 0.3 is obtained. A remarkable result here is that the surcharge load has no influence at all, whereas the uncertainty in the water level difference is not negligible. This comparison confirms the assumption that time dependent load variables are only of minor importance with regard to the reliability.

5.3.5 Validation of Abdo-Rackwitz algorithm

The validity of the obtained results using the Abdo-Rackwitz algorithm, are checked by performing the exact same run (wall failure with $f_{y,kar} = 485 \text{ N/mm}^2$) with the COBYLA-algorithm. Ideally, the results should be checked with a level III analysis like MC or DS, but this is outside of the possibilities due to their long calculation time compared to FORM. The results of both FORM runs are given in Table 5.18, Table 5.19 and Figure 5.15. No significant difference in reliability index can be noticed, while also the difference in design point is marginal except for the stiffness of the loose sand.

The calculation time with COBYLA is much shorter. This can be partly linked to the fact that COBYLA does not calculate gradients explicitly. Though the fact that the Abdo-Rackwitz calculation did not stop when both the residual and the constraint error were below their maximum tolerance is the most importance cause for this difference.

Table 5.18 Calculation results, Abdo-Rackwitz vs. Cobyla

	Abdo-Rackwitz	Cobyla
Reliability index β	6.5	6.6
Number of iterations	100	96
Number of LSFE	856	107
Duration	40 hrs	5 hrs

Table 5.19 Design point, Abdo-Rackwitz vs. Cobyla

Parameter	Unit	Abdo-Rackwitz	Cobyla	Mean X_m
Sand, loose - E50ref	kN/m ²	19112	12575	30000
Sand, loose - phi	°	14.2	15.7	32.9
Clay, very sandy - phi	°	26.5	25.5	32.9
Sand, dense - E50ref	kN/m ²	45021	40096	90000
Sand, dense - phi	°	33.3	31.4	40.0

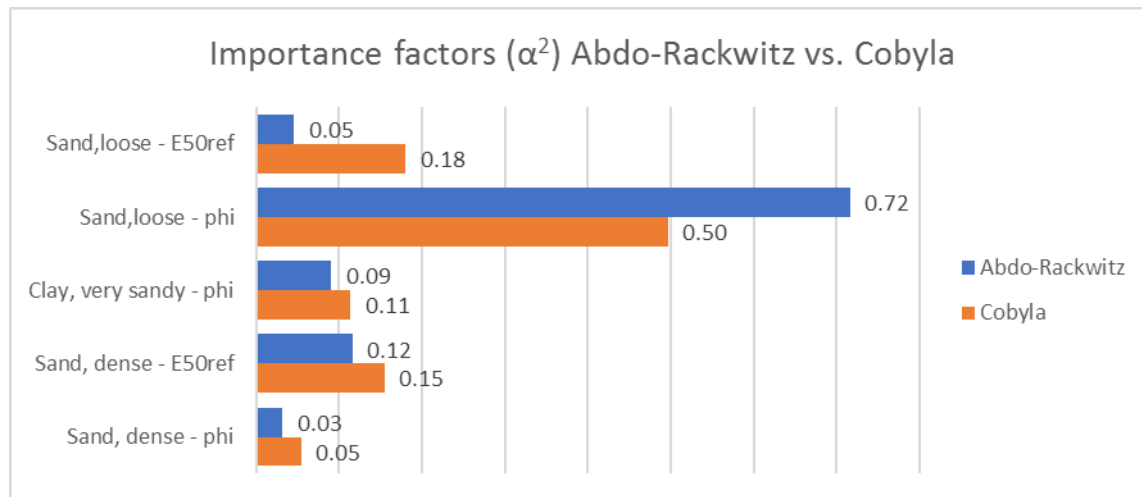


Figure 5.15 Comparison of importance factors (α^2), Abdo-Rackwitz vs. Cobyla

5.3.6 Redesign of the retaining wall

The overcapacity in the retaining wall makes a comparison with the target reliability useless. A unity check of 0.83 was obtained in the reassessment of the wall (Witteveen+Bos, 2017). For a fair comparison with the design guidelines a unity check of 1.0 should be realised. For this purpose, the wall properties are modified in this section.

For the determination of the design values of the structural forces, the approach described in CUR211 (2013) is followed. The design values for the bending moment, the normal force and the anchor forces are obtained after applying a ϕ -c reduction in Plaxis of 1.2 (RC3) on the representative values of the soil strength parameters. The outcomes should be compared with the sectional forces found in SLS * 1.2 after which the highest value should be taken:

Performing these steps results in:

$$M_d = 2842 \text{ kNm/m'}$$

$$N_d = 2058 \text{ kN/m'}$$

Subsequently the unity check on the wall is given by:

$$UC = \frac{\frac{M_d}{W_{el}} + \frac{N_d}{A}}{f_y} \tag{5.7}$$

To acquire a unity check of 1.0, the wall thickness of the tubular piles was iteratively reduced, which both affects the elastic section modulus W_{el} and the cross-sectional area A of the tubular piles. A reduction of the wall thickness from 19 to 16 mm eventually resulted in a unity check of 0.99.

The new properties of the wall are thus:

$$\begin{aligned} EA &= 4.49 \cdot 10^6 \text{ kN/m} \\ EI &= 9.79 \cdot 10^5 \text{ kNm}^2/\text{m} \\ w &= 2.52 \text{ kN/m/m} \end{aligned}$$

For this modified design of the combi-wall a new run was performed. The results of this run are shown in Table 5.20.

Table 5.20 Run with redesigned combi-wall profile

	Value		
Reliability index β	5.8		
Failure probability P_f	$2.8 \cdot 10^{-9}$		
Number of iterations	51		
Number of LSFE	701		
Duration	24 hrs		
Parameter	Unit	Design point ($f_{y, kar} = 485 \text{ N/mm}^2$)	Mean X_m
Sand, moderate - gammaUnsat	kN/m ³	19.0	18.0
Sand, moderate - phi	°	42.2	38.9
Sand, loose - gammaUnsat	kN/m ³	16.5	17.0
Sand, loose - E50ref	kN/m ²	27546	30000
Sand, loose - phi	°	17.1	32.9
Clay, very sandy - phi	°	27.7	32.9
Sand, dense - E50ref	kN/m ²	52913	90000
Sand, dense - phi	°	36.3	40.0

Despite the unity check of 0.99, still a relatively high reliability index of 5.8 is found compared to the target reliability index of 4.3. An exact match with the target reliability index cannot be expected due to the generality and conservatism of the design guidelines. However, this difference is relatively large. Although the obtained results are not per definition wrong, there are multiple explanations possible for this difference:

- The assumed mean values for the soil properties are not representative for the actual soil behaviour. The mean values in this case study are determined based on transformation of the characteristic values to mean values based on the standard values of NEN9997. Whether this results in the right values of the mean parameters is uncertain. A calibration with measurements would reduce this error/uncertainty. This will be the case in the second case study.
- The use of a limited amount of variables. Leaving out all the non-dominant variables results in a slight overestimation of the reliability. Also load variables are not included in this calculation and therefore their exact importance is unknown.
- Inaccuracies in the calculation method. FORM is a method that approximates the failure probability. Due to these approximations a deviation is possible with exact results that would be obtained using a level III method.

5.3.7 First conclusions

Based on the results of the runs performed for the failure of the retaining wall the following conclusions are drawn:

- The first calculations confirm the fact that runs should be performed with correlated parameters to prevent unrealistic combinations of soil parameters and to get a more realistic approximation of the failure probability.
- The retaining wall in this case is overdimensioned due to multiple reasons:
 - The use of D-sheet piling instead of Plaxis.

- The choice for a thicker profile due to practical and financial reasons (during construction, thicker tubular piles were better available and for a good price)
- The yield stress has significant influence on the limit state and therefore either a conservative value should be chosen or preferably it should be selected as stochastic variable and directly implemented in FORM.
- As already expected the computational times are long, usually in the order of a day.
- The results of COBYLA and Abdo-Rackwitz are comparable in this case. Therefore COBYLA might be useful when only a few random variables are of interest.
- The uncertainty in time dependent load variables have only minor contribution to the reliability index of the retaining wall

5.4 LS2: Yielding of the anchor rod

In this section the exceedance of yield stress in the anchor rod is considered. First, the reliability of the anchor is determined for the original design because in the reassessment it appeared that this element of the quay wall was critical due to the unity check of 1.12 (Witteveen+Bos, 2017).

The LSF for this failure criterion was given by:

$$Z = f_y A_{anchor} - N_s \quad (5.8)$$

Since the tubular piles are double anchored and both anchors have deviating structural properties, also two limit state functions can be formulated. However, during previous calculations it already became clear that the upper anchor is always the most critical one and therefore only this anchor is assessed.

Since a deterministic value for the yields stress f_y should be chosen, and given the significant importance of the yield stress in previous research (Teixeira et al. (2015), Wolters (2012)) the characteristic value is used here instead of the mean value. Also a deterministic value for A_{anchor} is assumed. Firstly, the reliability is calculated for an uncorroded cross-section:

$$f_y A_{anchor} = 500 \text{ N/mm}^2 * 5510 \text{ mm}^2 = 2755 \text{ kN}$$

Filling this into the LSF:

$$Z = 2755 - N_s \quad (5.9)$$

For the sensitivity analysis, again uncorrelated variables are used to determine the most important parameters. Besides γ_{unsat} , φ' and E_{50}^{ref} , also the interface strength R_{inter} is taken as stochastic. Given the fact that the soil adjacent to the retaining wall settles more than the wall itself, a smaller interface strength causes a smaller vertical load on the wall, which reduces the vertical downward force on the anchor rod resulting in a larger tension force.

The interface strength depends for a large part on the friction angle, therefore the same COV as for the friction angle is applied. A truncated normal distribution is used to prevent that values smaller than 0.0 or larger than 1.0 are used. The results of the sensitivity analysis are shown in Figure 5.16.

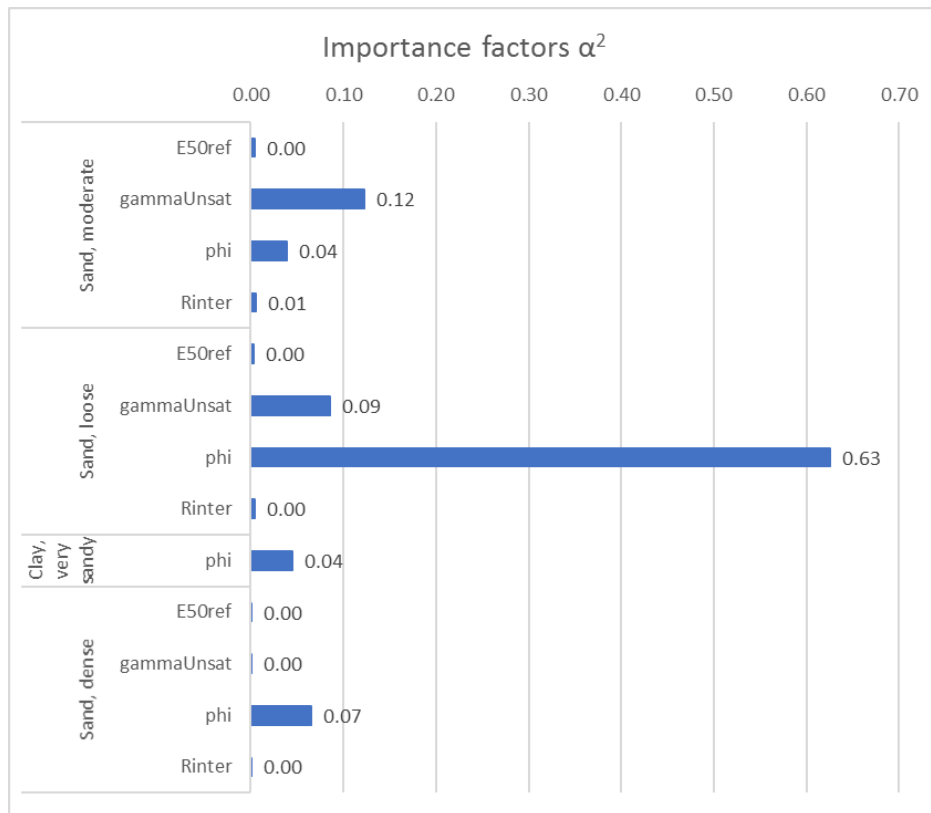


Figure 5.16 Importance factors sensitivity analysis anchor, uncorrelated

It can be noticed that this problem is mainly dominated by the friction angle and the unit soil weight, whereas the stiffness and the interface strength in total only have an influence of 1%. The friction angle of the loose sand layer is dominating this problem, as this was also the case for the retaining wall.

Based on this results the failure probability is determined with only 8 (correlated) parameters.

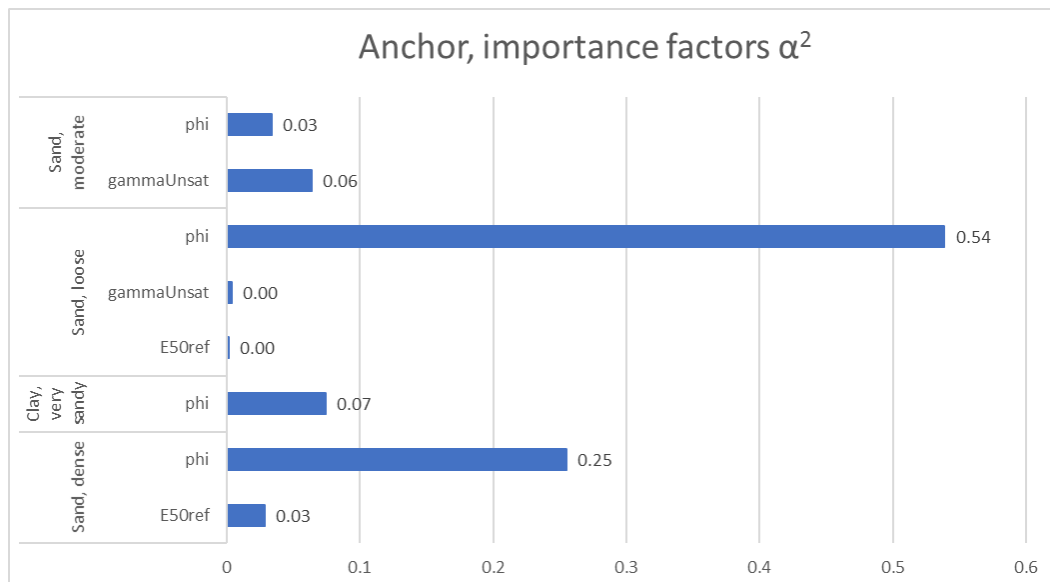


Figure 5.17 Importance factors anchor, correlated

The reliability index determined with this run is 7.6. When checking the results, it is remarkable that the saturated unit weight and the stiffness of the loose sand barely decrease, whereas the friction angle of this layer is heavily reduced. Due to the use of correlations one might expect that these two parameters are also

partly reduced. Whether this observation is caused by an error in the algorithm is hard to say based on only one observation.

When comparing the design point for wall failure with the design point of anchor failure, only slight differences can be noticed (Table 5.21). Mainly the stiffness of the dense and loose sand layer deviates between both points. The large similarity indicates a high degree of dependency between both failure mechanisms.

Table 5.21 Design point anchor, correlated

	Value			
Reliability index β	7.6			
Failure probability P_f	$1.4 \cdot 10^{-14}$			
Number of iterations	13			
Number of LSFE	169			
Duration	6 hrs			
Layer	Unit	Mean X_m	Design point anchor X^*	Design point wall X^*
Sand, moderate - gammaUnsat	kN/m ³	18.0	19.7	-
Sand, moderate - phi	°	38.9	37.6	38.5
Sand, loose - gammaUnsat	kN/m ³	17.0	16.6	-
Sand, loose - E50ref	kN/m ²	30000	28891	20278
Sand, loose - phi	°	32.9	16.3	17.5
Clay, very sandy - phi	°	32.9	26.1	27.1
Sand, dense - E50ref	kN/m ²	90000	58955	37411
Sand, dense - phi	°	40.0	23.8	26.0

It must be noted that in the calculation above no corrosion was taken into account. Corrosion rates for steel surrounded by soil are in the range of 0.02-0.05 mm/year (CUR211, 2013). For a 50-year lifetime, this results in a thickness reduction of +/-2.0mm and therefore a reduction in diameter of 4.0mm. The threshold for the maximum anchor force hence reduces from 2755kN to 2455kN.

The reliability index found for a threshold of 2455 kN is: $\beta = 6.5$

The reliability of the anchor bar decreases significantly (from 7.6 to 6.5) when taking into account corrosion. For the same reason, it can be concluded that again the yield strength is of importance. The anchor strength depends on both the steel cross sectional area and the yield strength. Therefore, the decrease in reliability can also be interpreted from the side of the yield stress. A yield stress of 445 N/mm² (instead of 500) combined with an uncorroded cross-section also gives a threshold value of 2455 kN for the LSF. So again the yield stress is of importance.

Given the fact that the anchor bar did not meet the safety requirements in the reassessment, the obtained $\beta = 6.5$ is a relatively high value compared to the target reliability index of 4.3. In the design procedure in guidelines usually effects of soil settlements and failure of a neighbouring anchor are taken into account. This can be an explanation for the obtained deviation.

5.5 LS3: Soil mechanical failure

The resistance against soil mechanical failure is mainly dominated by the shear resistance of the soil along the failure plane. Also the length of the tubular piles is of importance in the resistance to soil mechanical failure. Due to the relatively large installation depth of combi-walls, more passive resistance is activated and also the Bishop slip circle is enforced to go deeper.

When performing a ϕ -c reduction with mean values for all soil parameters, a Safety Factor of 1.94 is obtained. This already indicates that the occurrence of soil mechanical failure is not likely as all soil strength parameters

should roughly be divided by 2 before failure occurs. By analysing the failure points after the ϕ -c reduction in Figure 5.18 it seems that a combination of active and passive failure has triggered soil mechanical failure. However, this figure does not show the axial displacement of 0.9 m of the grout body. Hence, inadequate shear resistance of the grout body is probably the most dominant soil mechanical failure mode. This type of failure is not incorporated as a limit state in the ϕ -c reduction of Plaxis and should therefore be evaluated with a separate limit state function.

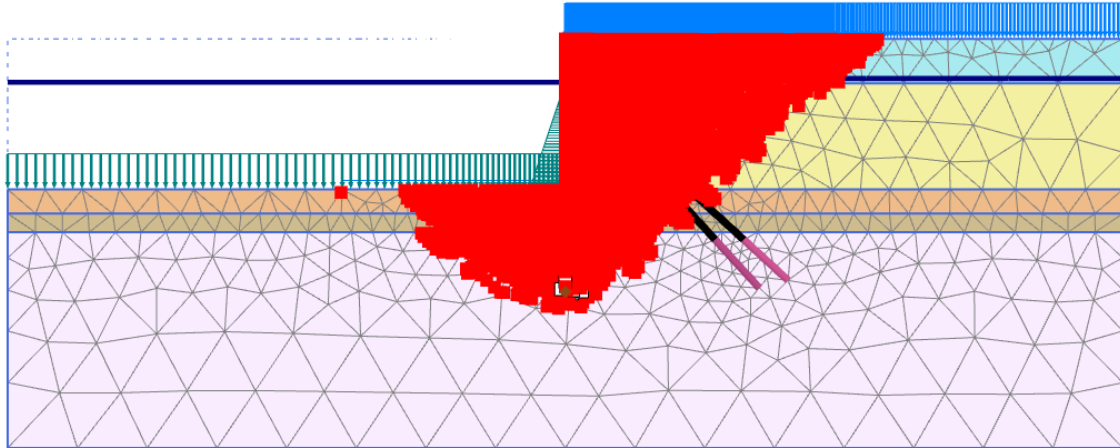


Figure 5.18 Failure points after applying a ϕ -c reduction

The LSF applied in the first run is:

$$Z = Msf - 1.0$$

For the first run only the soil strength parameters are taken as stochastic as they contribute directly to the shear resistance along the failure plane. The results of this run are given in Table 5.22. As expected a high reliability index of 7.9 is found.

Even with only six random variables the Abdo-Rackwitz algorithm showed difficulties in approaching a safety factor of 1.0 and finding the design point. The non-linearity of the soil in plastic state is probably the main cause for this. To reduce the computational time it can therefore be more convenient to use a Safety Factor of 1.1 or 1.05 as threshold or make use of wider tolerances for the convergence settings.

Obtaining a clearly defined safety factor also took quite some effort. Often an ever-increasing safety factor was obtained, which cannot be handled by ProbAna.

Table 5.22 Output results, soil mechanical failure

	Value		
Reliability index β	7.9		
Failure probability P_f	$9.5 \cdot 10^{-16}$		
Number of iterations	22		
Number of LSFE	256		
Duration	40 hrs		
Parameter	Unit	Mean X_m	Design point X^*
Sand, moderate - phi	°	38.9	26.8
Sand, loose - phi	°	32.9	17.7
Clay, very sandy - phi	°	32.9	26.2
Clay, little sandy - cref	kN/m ²	28.3	29.0
Clay, little sandy - phi	°	25.6	22.1
Sand, dense - phi	°	40.0	16.5

The two thickest layers get the most importance, which seems to make sense given their larger contribution to the shear resistance along the failure plane.

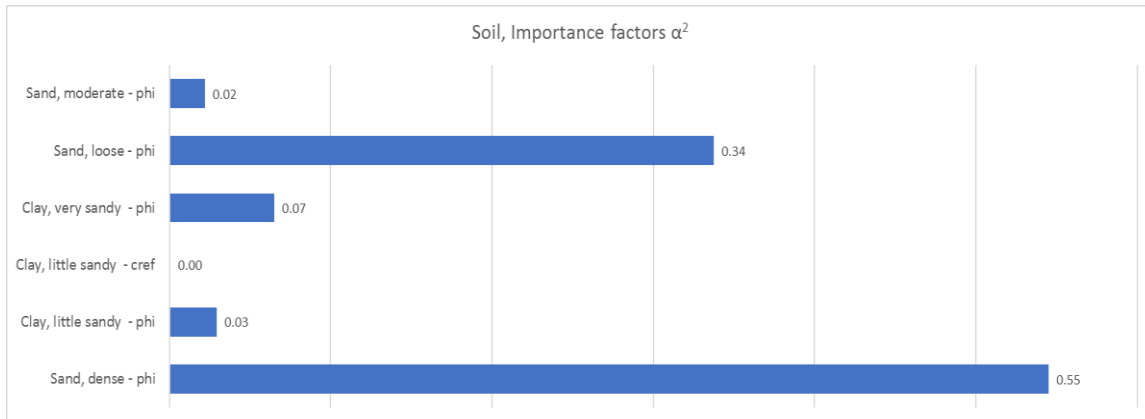


Figure 5.19 Importance factors, soil mechanical failure

Given the strong correlation between phi and unit weight, it is desirable to include the unit weight as a variable for at least the two dominant sand layers. Due to the long computational times and the low susceptibility for soil mechanical failure, this run will not be performed.

5.6 Intermediate conclusion

After the three considered failure mechanisms have been assessed, some first conclusions can be drawn. The conclusion has been subdivided into a part about the reliability of the considered structure and a part about the functioning of the Plaxis-FORM coupling.

5.6.1 Reliability of the structure

Regarding the limit states yielding of the wall, yielding of the anchor profile and soil mechanical failure, the structure can be considered very safe. Whether the overall reliability of the structure is sufficient cannot be concluded as not all failure mechanisms are checked. Especially the failure mechanism 'Shear resistance of the grout body inadequate' should be checked as this was a critical failure mode in the reassessment of this quay wall (Witteveen+Bos, 2017).

Table 5.23 Obtained reliability indices for the as-built LBBR quay wall

Limit state	Reliability index β
Yielding of the retaining wall	6.5
Yielding of the anchor steel profile	6.5
Soil mechanical failure	7.9

For the failure mechanism yielding of the combi-wall, a clear comparison with the design guidelines was performed by reducing the wall thickness compared to the as-built wall thickness to acquire a unity check of 0.99. Subsequently, the obtained reliability index when including both soil and variable loads as stochastic was:

$$\beta_{yielding,wall} = 5.5$$

This confirms the expectation that a semi-probabilistic design generally results in a higher reliability index than required by design codes. However, more structures should be assessed to be able to give a more sound conclusion about this assumption.

For the LBBR quay wall, the uncertainty in the soil parameters is the most dominant uncertainty of which furthermore the friction angle is the most dominant soil property. The uncertainty in the friction angle is reducible by performing measurements and apply this in a Bayesian update. In this way an increase in reliability can be obtained, making way for a possible load increase.

The strong correlation between yield stress and reliability for both the anchor and wall yielding implies that also the yield stress is a dominant uncertainty.

The influence of uncertainty in variable loads seems only minor for the limit state yielding of the wall. Whether this also holds for other failure mechanisms should be investigated.

5.6.2 Plaxis-FORM coupling (ProbAna)

The goal of this case study was also to gather experience with probabilistic calculations and to test the applicability of FORM for the three considered limit states. In general it can be concluded that for failure of the structural elements, FORM performed reasonably well. Whether convergence is reached highly depends on the maximum convergence errors. For convergence of structural elements the following errors are dominant:

- Absolute error
- Residual error

At first a maximum error of 1% was used. However, this resulted several times in non-convergence. Therefore the maximum error was increased to 5%. With this value convergence was reached most of the time, whereas it is still considered a reasonable tolerance to obtain accurate results.

Other problems that were encountered are:

- Plasticity in the initial phase
- Problems with the input restrictions of Plaxis for E_{oed} and K_0^{nc}

The first problem was only encountered when using the K_0 -procedure in Plaxis to determine the initial stresses in the soil and was caused by a bug in ProbAna. To tackle this, gravity loading was used instead.

Regarding the second bullet, this is not a flaw of ProbAna, but more a consequence of the use of probabilistic methods in combination with Plaxis. When Plaxis does not accept the input values determined by the FORM algorithm, the calculation is stopped and no results are available. The calculation should be started all over again from the start.

To limit the occurrence of this error, the ratio between E_{50} and E_{oed} , was slightly adapted from 1 : 1 to approximately 1 : 0.8 whereas also very high mean values of E_{50} were reduced to 80 MPa. As the importance of the stiffness was in general not very large, these adjustments are assumed to not influence the reliability index by much.

With these adjustments, results were obtained in most cases.

Regarding soil mechanical failure, at first difficulties were encountered in reaching a clearly defined safety factor using the ϕ -c reduction method. Thereafter the convergence to a safety factor of 1.0 took considerably more iterations compared to a limit state for a structural element. This is also caused due to the fact that the starting point ($M_{sf} = 1.94$) was far away from the threshold (1.0) and a different approach in the line-search algorithm of AR compared to other limit states. Unfortunately, the starting point cannot be adjusted with the current package.

Also the Cobyla algorithm was tested for this failure mechanism. This algorithm converged two times to a wrong design point (a M_{sf} of 1.4) and was therefore not used further throughout this thesis.

In general, with the Abdo-Rackwitz algorithm convergence can be reached, although taking quite some effort and computation time.

Change in software package

At this point, it was decided to upgrade the version of ProbAna to a more advanced custom version of ProbAna, from now on referred to as ProbAna2018, as the version used up till now is from 2017. The main reason/advantages of this upgrade are:

- Intermediate results are saved and available in case of an unfinished calculation.
- The algorithm can start at a starting point given by the user instead of the standard starting point (median values). This allows to continue a calculation after an error has occurred or when Plaxis has frozen or when previous knowledge about the design point is available.
- Properties of structural elements can be considered as stochastic.
- More freedom in the definition of the limit state function and more choice in distribution types.

The first two advantages save a lot of calculation time, whereas the last two can increase the validity of the results. All calculations in the remainder of this thesis are performed with the upgraded toolkit.

Additional calculations

After the change in toolkit and the experience gathered with performing probabilistic calculations, additional calculations are performed for this quay wall to achieve the following two objectives:

- 1 Determine the reliability index for the limit state: shear resistance of anchorage inadequate
- 2 Deriving a set of partial factors

These objectives are treated in the next two paragraphs.

5.7 LS4: Shear resistance of anchorage inadequate

The assessment of the reliability regarding soil mechanical failure showed that slipping of the grout body is the most dominant soil failure mode. However, in that calculation the shear resistance of the grout body itself is not considered stochastic, whereas there is quite some uncertainty in the resistance of a grout body and the modelling in Plaxis. With ProbAna2018, the strength of the grout body can be assessed individually, which is treated in this chapter.

In general, the strength of a grout body is calculated with:

$$F_{res,grout} = \alpha_t * q_c * L * O \quad (5.11)$$

In which

$F_{res,grout}$	Resistance of the grout body [kN]
α_t	Pile class factor [-]
q_c	Cone resistance [MPa]
L	Length of the grout body [m]
O	Circumference of the grout body [m] ($O = \pi * D$)

This results in the following LSF:

$$Z = \alpha_t * q_c * L * O - N_s \quad (5.12)$$

In which N_s is the normal force in the steel anchor bar.

The empirical value α_t describes the ratio between the cone resistance at the location of the grout body and the shear resistance τ along the grout body and is derived by:

$$\alpha_t = \frac{\tau}{q_c} \quad (5.13)$$

For self-boring grout injection piles in sand, the design value of α_t ranges from 0.008 as lower bound in case no in-situ tests are performed, up to a value of 0.012 when in-situ tests are performed (CUR236, 2011). Two important notes regarding these values are:

- 1 The cone resistance should be cut off at 20 MPa (in Dutch: afsnuiten), which implies that when a higher cone resistance than 20 MPa is measured at the location of the grout body, still 20 MPa should be used in equation 5.11.
- 2 The value of 0.012 is a design value, the expected value is generally higher.

These two remarks will become more clear when looking at the results of several in-situ test loadings shown in Figure 5.20. The dashed line in this figure illustrates the safe design value of $\alpha_t = 0.012$. All test loading results are above this line. The solid line represents $\alpha_t = 0.015$, which seems to represent the expected value quite well, especially for a cone resistance up to 20 MPa.

The results of the test loading at the location of LBBR are shown as green dots in Figure 5.20. Although the results indicate a good fit with an $\alpha_t = 0.015$, it must be noted that the grout body is not tested up till failure because the yield strength of the steel bar was limiting a further load increase. Taking this into consideration together with the test results for a cone resistance of 34 MPa, one might argue the validity of a complete cut-off at 20 MPa. In these cases with high cone resistance, a value of $\alpha_t = 0.015$ seems conservative. However, too few test results are available here to give a sound argumentation for this presumption.

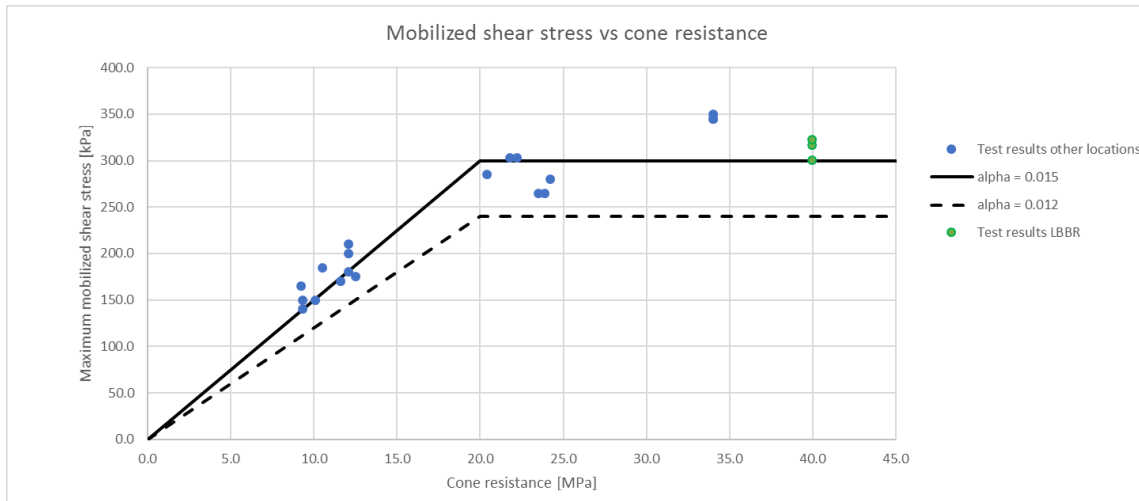


Figure 5.20 Results of in-situ test in self boring grout injection piles in sand. Adapted from: Acécon (2015)

The test results at LBBR are given in Table 2.3. Regarding the last column, failure of the grout body is defined as the exceedance of a creep measure of 2.0mm.

Table 5.24 Test results at the location of LBBR

Test nr.	τ [N/mm ²]	α_t [-] (with cut-off)	Creep measure [mm]
1	316	0.0158	1.38
2	300	0.0150	1.59
3	322	0.0161	1.23
Average	312.7	0.0156	

Based on these test results, assumptions for the distribution of the random variables are made, which can be found in Table 5.25. It was decided to apply a deterministic value of 20 MPa for the cone resistance and put all the uncertainty regarding shear resistance into the parameter α_t . In this way, the results can be compared easier with the current design approach. However, it also means that the outcomes are only valid for sand layers with an average cone resistance above 20MPa.

The average value of α_t is rounded up to 0.016 as failure didn't occur during the tests. The COV has been derived based on the test results of Figure 5.20

Regarding the geometrical parameters L and O , their uncertainty is assumed rather small. The screw has a diameter of 0.38m, which is considered to be a lower bound. With an upper bound taken at 0.40m, the average diameter is 0.39m, resulting in a circumference of 1.225m.

Table 5.25 Random variables regarding the resistance of the grout body

Variable	Symbol	Unity	Distribution	μ	COV
Pile class factor	α_t	-	Normal	0.016	0.10
Cone resistance	q_c	kPa	Deterministic	20,000	-
Length grout body	L	m	Normal	8.1	0.01
Circumference grout body	O	m	Normal	1.225	0.01

The distributions of the soil parameters are kept the same as they were for previous limit states and are therefore not repeated here.

With the expected value of each variable, the resistance of the grout body is:

$$E(F_{res,grout}) = \alpha_t * q_c * L * O = 0.016 * 20,000 * 8.1 * 1.225 = 3175 \text{ kN}$$

Which is higher than the expected yield limit of the steel anchor rod: 2774 kN.

Results

The results of the calculation for this limit state are given in Table 5.26 and Figure 5.21. The calculated reliability index for this limit state is 4.9, which is considerably lower than the value found for soil mechanical failure (4.9 vs 7.9). The main reason for this deviation is the large difference in limit state functions.

As Figure 5.21 shows, the problem is mainly dominated by the uncertainty in the parameter α_t , which has a value of 0.009 in the design point.

It is therefore worthwhile to consider the validity of the assumed distribution of α_t .

Table 5.26 Calculation information for limit state 4

	Value		
Reliability index β	4.9		
Failure probability P_f	$5.0 \cdot 10^{-7}$		
Number of iterations	1		
Number of LSFE	20		
Duration	0.4 hrs		
Parameter	Unit	Design point X^*	Mean X_m
Sand, moderate - ϕ'	°	38.25	38.9
Sand, loose - ϕ'	°	26.89	32.9
Clay, very sandy - ϕ'	°	30.77	32.9
Sand, dense - ϕ'	°	38.93	40.0
Sand, moderate - E_{50}^{ref}	kN/m ²	48715	45000
Sand, loose - E_{50}^{ref}	kN/m ²	26925	30000
Clay, very sandy - E_{50}^{ref}	kN/m ²	14521	16000
Sand, dense - E_{50}^{ref}	kN/m ²	70369	70000
Sand, moderate - γ_{unsat}	kN/m ³	18.46	18.0
Sand, loose - γ_{unsat}	kN/m ³	16.59	17.0
Clay, very sandy - γ_{unsat}	kN/m ³	17.53	18.0
Sand, dense - γ_{unsat}	kN/m ³	18.89	19.0
α_t	-	0.009	0.016
L	m	8.056	8.1
q_c	kPa	20000	20000
O	m	1.222	1.225

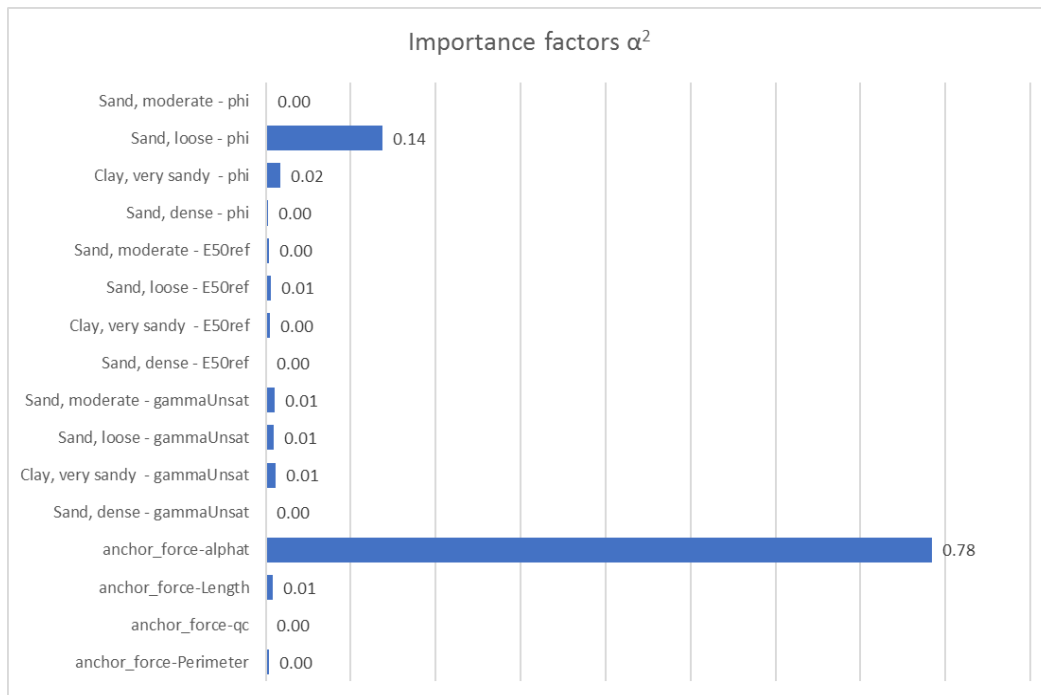


Figure 5.21 Importance factors limit state grout body

The parameters of the distribution of α_t are determined based on only a few test results that were all in the range of 0.013-0.018. It is therefore questionable whether the chosen normal distribution is also valid for values that lie far away from this range, such as the value of 0.009. Besides, in practice it is obliged to perform in-situ

suitability tests on at least 3 grout piles. In this way, the occurrence of an extreme low value of α_t is more or less excluded.

The impact of the choice for the distribution type is therefore investigated. A calculation is performed for which 0.012 is assumed to be the lower bound for α_t , as shown by the truncated normal distribution in Figure 5.22. However, FORM showed convergence problems with the truncated normal distribution. Therefore the parameters of the normal distribution were transformed to parameters for the Beta distribution. With this distribution convergence was reached.

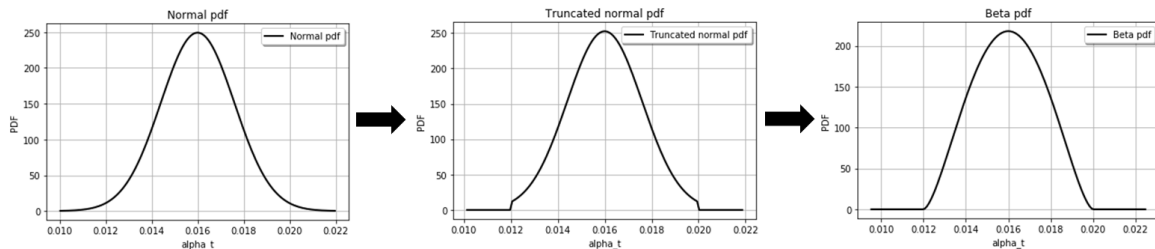


Figure 5.22 Normal vs truncated normal vs Beta distribution for α_t

The lower bound for α_t results in a shift of importance to the soil parameters. This results in an increase in reliability index to 6.8. The complete calculation results of this run are given in Appendix F.

Table 5.27 Calculation information

	Value
Reliability index β	6.8
Failure probability P_f	$4.5 \cdot 10^{-12}$
Number of iterations	24
Number of LSFE	499
Duration	9 hrs

Conclusion

The calculations showed that the pile class factor in α_t is the most dominant parameter regarding the reliability of the grout body. However, not much is known about the statistical distribution of this parameter. Therefore two types of distributions are tested for this parameter. With a normal distribution the reliability index is 4.9, whereas when extreme values are prevented for by the use of a beta distribution, the reliability index is 6.8. The choice for the distribution of this parameter determines for a large part the outcome. Whether the distribution of α_t should be truncated or not and at which value is at this moment difficult to determine. It is advised to gather more test results for α_t to get a better insight in the uncertainty in this parameter.

The required reliability index for this failure mechanism is 4.3. Thus, the reliability of the grout body is sufficient.

5.8 Derivation of partial factors

The calculations in the previous paragraphs showed the overcapacity in the design even when the unity check for a certain failure mechanism is larger than 1.0. This is for a large part caused by the conservatism in the design codes regarding partial factors. The code takes into account modelling uncertainty and is developed in such a way that roughly 95% of the designs has the same or a higher reliability index than required.

In this paragraph the partial factors are derived on this quay structure to be able to have a discussion about the magnitude of the current partial factors.

5.8.1 Approach

For this purpose, the reliability index and sensitivity factors for the failure mechanisms yielding of the combi-wall and yielding of the anchor bar are calculated again. The main reason for a recalculation is the fact that structural properties formerly could not be included. Next to that, ProbAna2018 is better capable of handling large amount of variables. Therefore more soil parameters could be included compared to the initial calculations, which is preferable with respect to the correlations between soil parameters.

The calculations are performed using the adjusted design (see Chapter 5.3.6), because the original design has too much overcapacity with respect to the failure mechanism 'yielding of the wall'. This can result in an inaccurate representation of the sensitivity factors. The only adjustment that was made, was a reduction in wall thickness from 19mm to 16mm. For the failure mechanism soil mechanical failure no additional calculations were performed as this would be too time-consuming.

The structure is designed for RC3, so the partial factors will also be derived for this class. The target reliability at component level for this class is 4.3 .

For the derivation of the partial factors with the results of a FORM calculation ideally each partial factor is derived by:

$$\gamma_i = \frac{X_{k,i}}{X_i^*} = \frac{\mu_i - k\sigma_i}{X_i^*} \quad (5.14)$$

In which

- μ_i Mean value of variable X_i
- σ_i Standard deviation of variable X_i
- $X_{k,i}$ Characteristic value of parameter X_i
- X_i^* Design value of parameter X_i obtained from FORM
- k factor representing the distance from the mean to the characteristic value in units of standard deviation. ($k = 1.645$ for a 5% under exceedance value)

With this method the partial factors are derived for the reliability index β_{FORM} that is obtained with the FORM calculation. However, this reliability index is not always equal to the desired reliability index of the design code (referred to β_{RC3} from now on). In this thesis, the obtained reliability indices are often higher than the required reliability indices. Therefore, when applying equation 5.14 the partial factors would result in too high partial factors. It would be time consuming to create a design that almost exactly approaches the required reliability index such that: $\beta_{FORM} \approx \beta_{RC3}$. This is also not per definition needed. To derive the design point for the required β_{RC3} , the following equations are used:

For normal distributions:

$$X_{i,RC3}^* = \mu_{Xi} - \alpha_i \beta_{RC3} \sigma_{Xi} \quad (5.15)$$

For lognormal distributions:

$$X_{i,RC3}^* = \frac{\mu_{Xi}}{\sqrt{1+COV_i^2}} \exp\left(-\alpha_i \beta_{RC3} \sqrt{\ln(1+COV_i^2)}\right) \quad (5.16)$$

The partial factor for a resistance parameter is then derived by:

$$\gamma_{R,i} = \frac{X_{k,i}}{X_{i,RC3}^*} = \frac{\mu_i - k\sigma_i}{\mu_i - \alpha_i \beta_{RC3} \sigma_i} = \frac{\mu_i(1 - kV_i)}{\mu_i(1 - \alpha_i \beta_{RC3} V_i)} = \frac{1 - kV_i}{1 - \alpha_i \beta_{RC3} V_i} \quad (5.17)$$

In which

- α_i Sensitivity factor of random variable X_i obtained from a FORM calculation
- β_{RC3} Required reliability index for RC3
- $X_{i,RC3}^*$ Design value corresponding to β_{RC3}
- V_i Coefficient of variation of random variable X_i
- k factor representing the distance from the mean to the characteristic value in units of standard deviation. ($k = 1.645$ for a 5% under exceedance value)

The most important assumption with this method is that the sensitivity factors (α_i) do not significantly change for a slightly different reliability index. It is assumed that this is the case for this quay wall. The obtained reliability indices are in general one point higher than the required reliability indices. It should be checked with an additional calculation whether the assumption is valid.

OpenTURNS provides two types of sensitivity factors: Sensitivity factors in the U-space and sensitivity factors in the Y-space. The sensitivity factors in the U-space are decorrelated, therefore the ordering of the variables influences the magnitude of the sensitivity factors. For the importance factors in the Y-space, this problem does not occur as these factors are derived from the design point in the physical space (X-space) and therefore correlations are taken into account correctly. These factors should therefore be used to derive the partial factors.

5.8.2 LS1: Yielding of the wall

The applied LSF for wall failure (yielding) is:

$$Z = f_y - \max \left[\frac{|M(z)|}{W_{el}} + \frac{|N(z)|}{A_{wall}} \right] \quad (5.18)$$

The values of A_{wall} and W_{el} are automatically calculated based on the input for the pile diameter D and the wall thickness t . The applied distributions D , t and f_y for are given in chapter 4.3. The characteristic values of the unit weight, the wall thickness and the tube diameter are assumed to be equal to the mean values.

The results of the FORM run and the derivation of the partial factors are shown in Table 5.28. The partial factors on φ given in this table should be applied on $\tan(\varphi_k)$. In this section, less attention will be given to the geotechnical explanation of the obtained results as this was already described in detail for each failure mode earlier on in this chapter. When a partial factor should be applied on a mean, the characteristic value is taken equal to the mean value.

Table 5.28 Partial factors for LS1: Yielding of the wall

Parameter	Unit	α_i	μ_i	COV_i	$X_{k,i}$	X_i^* (FORM)	$X_{i,RC3}^*$	$\gamma_{i,calculated}$ (RC3)	γ_i (EC7)
β_{FORM}		5.73							
β_{RC3}		4.3							
Sand, moderate - φ'	°	0.125	38.9	0.1	32.5	41.74	40.98	0.55	1.2
Sand, loose - φ'	°	0.588	32.9	0.1	27.5	21.70	24.59	1.14	1.2
Clay, very sandy - φ'	°	0.227	32.9	0.1	27.5	28.51	29.68	0.91	1.2
Sand, dense - φ'	°	0.001	40	0.1	33.42	39.98	39.98	0.79	1.2
Sand, moderate - E_{50}^{ref}	kN/m ²	0.038	45000	0.3	69859	47772	45206	0.65	1.0
Sand, loose - E_{50}^{ref}	kN/m ²	0.181	30000	0.3	17729	22052	22864	0.78	1.0
Clay, very sandy - E_{50}^{ref}	kN/m ²	0.143	15000	0.3	8864	12547	11998	0.74	1.0
Sand, dense - E_{50}^{ref}	kN/m ²	0.075	70000	0.3	41368	61651	61025	0.68	1.0
Sand, moderate - γ_{unsat}	kN/m ³	0.160	18	0.05	18.00 (μ)	18.85	18.62	1.03	μ
Sand, loose - γ_{unsat}	kN/m ³	0.117	17	0.05	17.00 (μ)	16.42	16.57	0.97	μ
Clay, very sandy - γ_{unsat}	kN/m ³	0.194	18	0.05	18.00 (μ)	16.97	17.25	0.96	μ
Sand, dense - γ_{unsat}	kN/m ³	0.033	19	0.05	19.00 (μ)	18.82	18.86	0.99	μ
OWL*) **)	m	0.011	-0.84	0.24	-0.84	-0.83	-0.83	0.99	-
Surcharge load	kPa	0.193	-40	0.1	-40.0	-44.51	-43.31	1.08	1.25
t_{tube}	m	0.194	0.016	0.03	0.0160 (μ)	0.0155	0.0156	1.03	μ
D_{tube}	m	0.038	1.42	0.007	1.42 (μ)	1.418	1.42	1.00	μ
f_y	kPa	0.611	548000	0.07	485000	411497	447262	1.08	1.0

*) Results obtained from a similar FORM calculation

**) The partial factor should be on the water level difference instead of the water level itself, however the GWL is not considered here, so no sound conclusion can be given about this partial factor

The two most dominant parameters in this calculation are the yield strength and the friction angle of the loose sand layer. Especially the yield strength is of mayor importance in this problem. It is worth noticing that the distribution of the yield strength was truncated at 388 MPa (=0.8*485MPa) based on the test results of Peters et al. (2017). However, in this run the lower bound was not reached in the design point. In some test calculations the design point did reach the boundary.

In practice, the yield strength of the tubular piles is tested beforehand and piles are rejected in case of bad test results, making this assumption of a lower bound more valid.

The partial factors for most parameters are around or below 1.0. When comparing them with the partial factors of EC7 (last column of Table 5.28), the most important (slight) differences can be found in the partial factor on the yield strength, the partial factor on the load and the partial factor of the friction angle.

5.8.3 LS2: Yielding of the anchor bar

The LSF for yielding of the anchor bar is:

$$Z = f_y A_{anchor} - N_s \quad (5.19)$$

The partial factors for this limit state are given in Table 5.29.

Table 5.29 Partial factors for LS2: Yielding of the anchor bar

Parameter	Unit	α_i	μ_i	COV_i	X_{ki}	X_i^* (FORM)	$X_{i,RC3}^*$	$\gamma_{i,calculated}$ (RC3)	γ_i (EC7)
β_{FORM}		5.25							
β_{RC3}		4.3							
Sand, moderate - φ'	°	0.045	38.9	0.1	32.5	37.96	38.14	0.81	1.2
Sand, loose - φ'	°	0.554	32.9	0.1	27.5	23.25	25.07	1.11	1.2
Clay, very sandy - φ'	°	0.165	32.9	0.1	27.5	30.02	30.57	0.88	1.2
Sand, dense - φ'	°	0.046	40	0.1	33.42	39.03	39.21	0.81	1.2
Sand, moderate - E_{50}^{ref}	kN/m ²	0.123	45000	0.3	69859	54153	50350	0.72	1.0
Sand, loose - E_{50}^{ref}	kN/m ²	0.111	30000	0.3	17729	25296	24986	0.71	1.0
Clay, very sandy - E_{50}^{ref}	kN/m ²	0.083	15000	0.3	8864	14084	12944	0.68	1.0
Sand, dense - E_{50}^{ref}	kN/m ²	0.029	70000	0.3	108670	73226	70159	0.65	1.0
Sand, moderate - γ_{unsat}	kN/m ³	0.169	18	0.05	18.00 (μ)	18.81	18.65	1.04	μ
Sand, loose - γ_{unsat}	kN/m ³	0.146	17	0.05	17.00 (μ)	16.34	16.47	0.97	μ
Clay, very sandy - γ_{unsat}	kN/m ³	0.133	18	0.05	18.00 (μ)	17.36	17.49	0.97	μ
Sand, dense - γ_{unsat}	kN/m ³	0.009	19	0.05	19.00 (μ)	18.95	18.96	1.00	μ
OWL	m	0.007	-0.84	0.25	-0.84	-0.83	-0.83	0.99	-
Surcharge load	kPa	0.156	-40	0.1	-40.00	-43.32	-42.69	1.07	1.25
f_y	kPa	0.712	565000	0.07	500000	417205	443880	1.13	1.0
A_{anchor}	m ²	0.167	0.0049	0.02	0.0049 (μ)	0.0048	0.00484	1.01	μ

The results show similar partial factors as for the failure mechanism yielding of the wall. Again the yield strength and the friction angle of the loose sand are the most dominant parameters and obtain safety factors above 1.0, whereas for most other parameters a partial factor of 1.0 or lower is obtained. Worth mentioning is that the current design approach prescribes next to the partial factors of the last column, also an additional partial factor of 1.25 on the design load in the anchor bar. This value is not taken into consideration here.

5.8.4 LS3: Soil mechanical failure

The structure is very safe regarding soil mechanical failure ($\beta = 7.9$) due to its large embedded depth. The assumption that the influence factors obtained for a quay wall with a β of 7.9 are the same as for a (shorter) quay wall with $\beta_{RC3} = 4.3$ would be very rough. For an accurate result, a new calculation should be performed with a shorter combi-wall. Due to time limitations this calculation is not performed here.

To still get some insight in the required partial factors, they are approximated from the results of $\beta = 7.9$ and shown in Table 5.30.

Table 5.30 Approximation of partial factors for LS3: Soil mechanical failure

Parameter	α_i	μ_i	COV _i	X _{k,i}	X _i *	X _{i,RC3} *	Y _{i,calculated} (RC3)	Y _i (EC7)
β_{FORM}	7.9							
β_{RC3}	4.3							
Sand, moderate - ϕ'	°	0.149	38.9	0.1	32.5	26.78	0.86	1.3
Sand, loose - ϕ'	°	0.581	32.9	0.1	27.5	17.71	1.13	1.3
Clay, very sandy - ϕ'	°	0.255	32.9	0.1	27.5	26.21	0.93	1.3
Clay, little sandy - ϕ'	°	0.171	25.6	0.1	21.4	22.11	0.89	1.3
Sand, dense - ϕ'	°	0.738	40	0.1	33.4	16.52	1.28	1.3
Clay, little sandy - c'	kPa	0.028	28.3	0.2	19.0	29.00	0.66	1.6

As it concerns soil mechanical failure and only soil parameters are taken into account in this calculation, it is logical that higher partial factors for the friction angle are obtained for this failure mode. This is also the reason why EC7 prescribes higher partial factors for this failure mode, 1.3 instead of 1.2.

The two thickest sand layers, the dense sand (Pleistocene) and the loose sand layer get the most importance and would require a safety factor of respectively 1.28 and 1.13. Note that soil stiffness and density are not included as random variable in this calculation.

5.8.5 Differentiation between Reliability Classes

The partial factors derived above are related to RC3, whereas it is also possible to derive partial factors for the classes RC2 and RC1. Table 5.31 shows the steps in partial factors between reliability classes for several soil parameters according to EC7. For now, we only focus on the friction angle, as for the density no differentiation is made and the effective cohesion and the undrained shear strength were less relevant for this case study.

Table 5.31 Partial factors for soil parameters for simple quay walls according to Table A.4b of NEN 9997-1:2012

Soil parameter	Reliability Class		
	RC1	RC2	RC3
Friction angle	1.15	1.175	1.20
Effective cohesion	1.15	1.25	1.40
Undrained shear strength	1.50	1.60	1.65
Density	1.00	1.00	1.00

For this case study, the derived partial factors on the friction angle for all three reliability classes are given in Table 5.32. One can notice that the steps between reliability classes are in the range of 0.04-0.07, depending on the magnitude of the sensitivity factor. These steps are much larger than the steps of 0.025 prescribed by EC7. From this you can conclude that the steps of EC7 are most likely too small and will result in only a minor differentiation between the reliability classes.

Table 5.32 Partial factors on the friction angle for the three limit states and for a standardized α -value

Limit state	α_ϕ	Reliability Class		
		RC1	RC2	RC3
Wall	0.59	1.04	1.09	1.14
Anchor	0.55	1.03	1.07	1.11
Soil	0.74	1.13	1.20	1.28
Standardized (EC7)	0.70	1.10	1.16	1.22

Figure 5.23 provides a better overview of the correlation between the partial factor and the reliability index β . The coloured lines show the required partial factor for multiple values of the sensitivity factor α_i . Considering this graph, the current partial factors (the black markers in Figure 5.23) seems to be based on a sensitivity factor of $\alpha = 0.70$. This factor is most likely derived from probabilistic calculations on multiple quay walls and

is more or less in line with the results found in this case study. For this standardized sensitivity factor, the steps between reliability classes should be approximately 0.06 instead of the current 0.025. The corresponding partial factors are added in the last row of Table 5.32. The main differences with respect to the currently prescribed partial factors is that the partial factor for RC1 decreases from 1.15 to 1.10, whereas the partial factor for RC3 would slightly increase from 1.20 to 1.22.

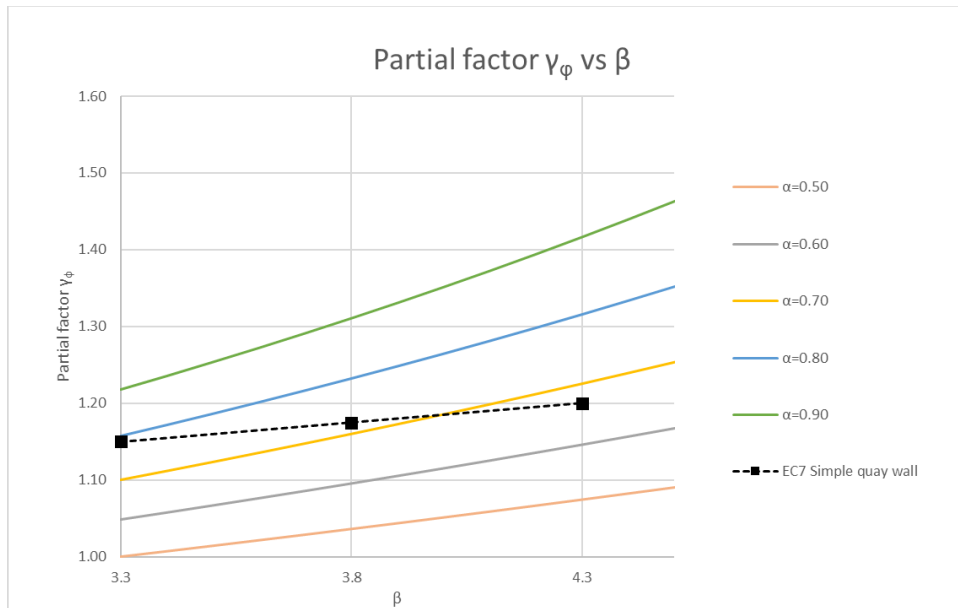


Figure 5.23 Partial factor on the friction angle as function of the reliability index, for multiple values of α

5.8.6 Overall conclusion partial factors

The overall impression is that for all parameters lower partial factors are derived than prescribed by EC7, only for the yield strength higher partial factors are found. This impression is as expected, as with the current set of partial factors, higher β 's than required were obtained. To obtain designs with a lower β , so closer to the required β , consequently lower partial factors should be prescribed.

Table 5.33 gives an overview of the partial factors per failure mode. In the fifth column the overall partial factor is derived by taking a conservative value for each factor. For clarity only the partial factors for RC3 are presented here.

Some general conclusions with regard to the obtained results are:

- Often one soil layer is dominant for a certain limit state and requires partial factors, whereas for all other layers a characteristic value would be sufficient. Applying the partial factor on all layers can result in an overdesign of the structure as proved by the calculations in this chapter.
- The surcharge load on the quay wall receives a slightly lower partial factor than EC7.
- Partial factors on stiffness are all lower than 1.0, indicating that a characteristic value is already conservative. For the LS anchor failure, both low and high stiffness can be normative.

Table 5.33 Derived partial factors per failure mode and overall partial factors (RC3)

Parameter	Limit State				EC7 (RC3)
	Wall	Anchor	Soil	Derived	
Density	1.03	1.04	-	μ	μ
Friction angle*	1.14	1.11	1.28	1.15 (1.30 for GEO)	1.20 (1.30 for GEO)
Stiffness	0.78	0.72	-	1.00	1.00
Surcharge load	1.08	1.07	-	1.10	1.25
Water level difference (Δ)**	1.0	1.0	-	1.0	1.0
Tube diameter / Wall thickness / Area anchor bar	μ	μ	-	μ	μ
$f_{y,tube}$	1.08	-	-	1.1	1.0
$f_{y,anchor}$	-	1.13	-	1.15	1.0

*) applied on $\tan(\varphi)$

**) GWL is not considered here

Some remarks regarding the validity of the derived partial factors are:

- No model uncertainty is taken into account, which would result in slightly higher partial factors than derived here.
- No geometrical variations are taken into account.
- The calculation is based on a slightly simplified soil profile, in which two sand layers are merged. In the discussion of chapter 7, the effect of this merging is investigated.
- Discrepancy between the required β and the obtained β makes that the applied sensitivity factors are an approximation, especially for the case of soil mechanical failure. Besides, the calculation of the sensitivity factors can be performed in multiple ways. Ideally, a perfect match should be obtained between a manually calculated design point (with the α and β of FORM) and the FORM design point itself, but this is not always the case here. This is predominantly caused due to the use of correlations and non-normal distributions. Slight deviations between both design points are in the order of 1% for normal distributions. The error in the partial factor is therefore relatively small.
- More quay structures should be considered to check whether this set of partial factors is in line with other results.

6

CASE STUDY 2: QUAY WALL WITH RELIEVING PLATFORM

In this chapter, a quay wall with a relieving platform is considered, which is equipped with measuring equipment since the construction in 2012. First a general description of the quay wall is given together with its monitoring system. Thereafter the calibration process is described in more detail. With the calibrated model the reliability of the failure mechanisms yielding of the combi-wall and geotechnical failure is determined. The outcomes are compared with the target reliability and the influence of deepening is determined for the mechanism geotechnical failure.

6.1 General description of the structure

The quay wall used for the case study is located in the Mississippi haven as shown in Figure 6.1. The quay wall is in use by one of the largest dry bulk transshipment companies in Europe, called EMO B.V. (Dutch abbreviation for Europees Massagoed Overslagbedrijf). In 2017, the terminal handled 25.4 million ton of dry bulk consisting of coal and iron ore.



Figure 6.1 Location of EMO quay wall. Source: Adapted from Google (2018)

The quay wall used for this case study is constructed in 2012 and has a total length of 485m. The drawing is presented in Figure 6.2.

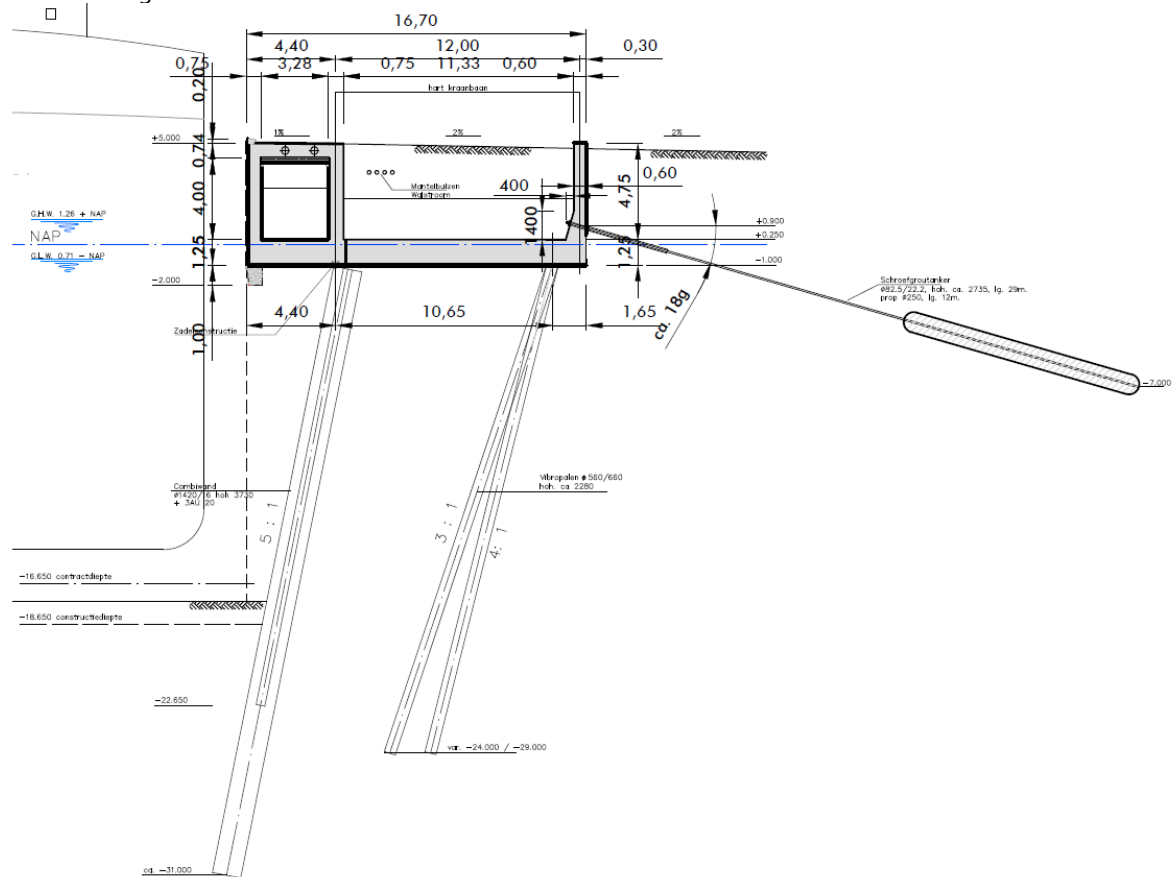


Figure 6.2 EMO quay wall

The quay wall is designed for a retaining height of 23.65m and consists of a concrete superstructure with relieving platform founded on a combi-wall and Vibro piles. At the back of the concrete superstructure grout anchors are installed. The combi-wall is installed with an inclination of 5:1 and consists of steel tubular piles with a diameter of 1420mm with three AU20 sheet pile elements in between. The combi-wall is connected with the superstructure by a cast iron saddle. In this way the bending moments in the superstructure are not transferred to the combi-wall, allowing for a lighter profile.

The concrete Vibro piles are placed with an inclination as well, alternating between 4:1 and 3:1 and are thus providing horizontal support to the superstructure. The diameter of the piles ranges between 560 and 660mm, and the installation depth varies between NAP-24.00m and NAP-29.00m.

The most important geometric parameters are:

- Top level structure: NAP +5.0m
- Construction depth: NAP - 18.65m
- Contract depth: NAP - 16.65m
- Current depth: NAP - 17.15m

The properties of the combi-wall are given in Table 6.1.

Table 6.1 Properties of the combi-wall

	Description	Symbol	Value	Unit
Sheet piles	type		AU20	-
	Amount		3	-
	Steel grade	f_y	S355GP	N/mm ²
	Tip level		-22.65	m NAP
Tubular piles	Outer diameter	D	1420	mm
	Thickness	t	16	mm
	Steel grade	f_y	X65 (445 MPa)	-
	Pile tip level		-31.0	m NAP
	c.t.c. distance		3.73	m
Properties per m'	Bending stiffness	EI	0.979*10 ⁶	kNm ² /m'
	Axial stiffness	EA	3.97*10 ⁶	kN/m'
	Weight	w	2.26	kN/m/m'
	Cross-sectional area	A	1.892*10 ⁻²	m ² /m'
	Section modulus	W_{el}	6.57*10 ⁻³	m ³ /m'

The specifications of the anchors are given in Table 6.2.

Table 6.2 Anchor properties

	Symbol	Value	Unit
Angle w.r.t. horizontal		18	°
Anchor type		82.5 x 22.0mm	-
Cross-sectional area	A	4181	mm ²
Steel grade		AC 600D	
Minimum yield stress	f_y	600	N/mm ²
Minimum tensile stress		750	N/mm ²
Connection with superstructure		+0.9	m NAP
Top level grout body		-4.35	m NAP
Length grout body		12	m
Diameter grout body		250	mm
c.t.c. distance		2.755	m
Axial stiffness per m'	EA	319*10 ³	kN/m'

6.2 Description of the measurement program

The quay wall is equipped with fibre optic measuring sensors already in the construction phase in 2012. Most of the sensors measure every 3 hours and send their data via a computer on location to a webserver. This server is accessible for the Port of Rotterdam authority, who can use the measurements for asset management and research. The sensors measure the following:

- Air pressure
- Temperature:
 - Air
 - Harbour water
 - Ground water
- Water level:
 - Harbour water.
 - Ground water, 4 sensors
- Anchor strains, 4 sensors
- SAAF (Shape Accel Array/Field) (=inclinometers), 4 sensors
- DSS (Distributed Strain Sensor) to monitor the erosion below the concrete relieving platform, 2 sensors.
- Deformation bolts, 25 units (measured by Fugro BV.).

Not all sensors measure continuously, in Table 6.3 a division is made between continuous measurements and manual measurements. The position of the sensors in the cross section is shown in Figure 6.3, while Figure 6.4 shows the location of the sensors. The sensors for measuring the groundwater level, the anchor force and the deformations (SAAF) are installed at four locations along the quay and are accessible for maintenance in the corresponding pit (referred to as P1, P2, P3 and P4).

Table 6.3 Types of measurements

Continuous measurements (every 3 hours)	Manual measurements
Temperature; groundwater, harbour water and near anchorage	SAAF Inclinometers in combi-wall (19 measurements until date)
Water level; groundwater, harbour water	Deformation bolts (6 measurements until date)
Anchor strains	
DSS	

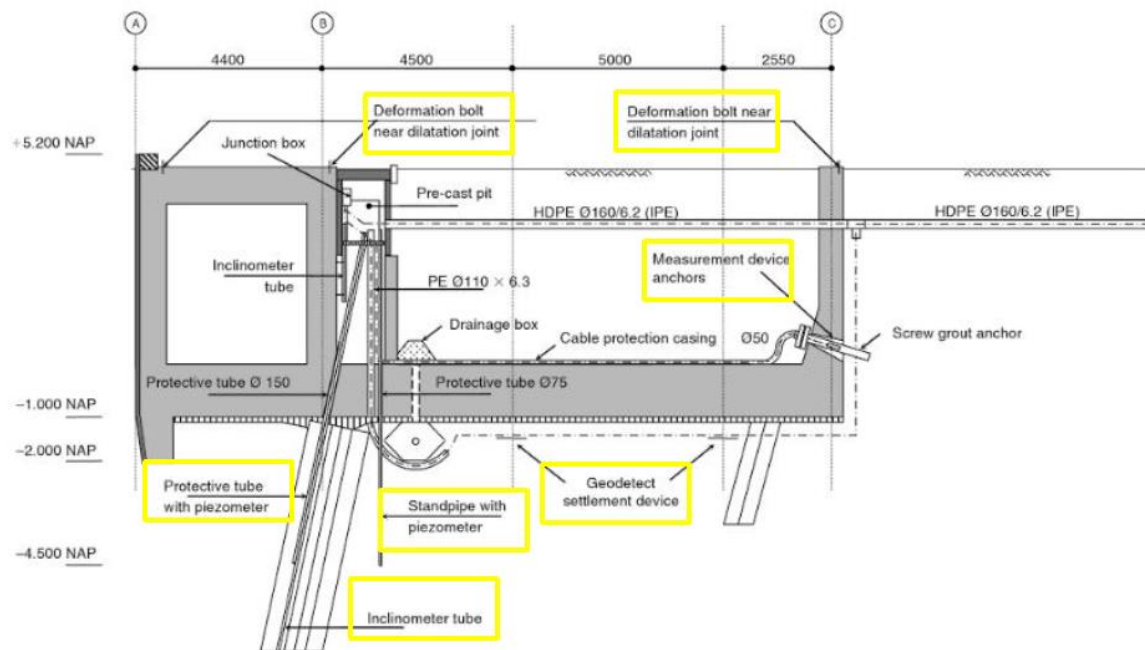


Figure 6.3 Position of the sensors (bounded in yellow)

All these measurements over multiple years result in a huge amount of raw data, which needs to be processed to get usable results. The raw data can be corrupted due to multiple causes:

- Power failure
- Maintenance (once every three months)
- Corroded or defect sensors
- Other causes (For example: rainwater entering the measurement pit and subsequently raising the water level in the standpipe of the ground water level)

During the data analysis, it turned out that quite a lot of sensors are defect or corrupted, either for a small period or forever.

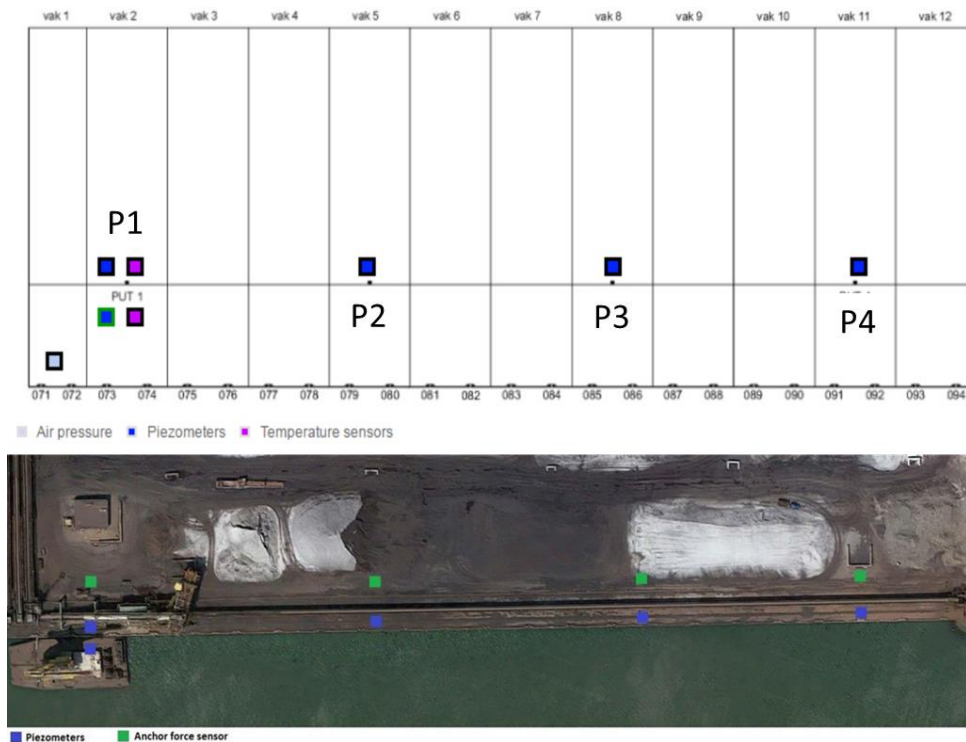


Figure 6.4 Top view of the location of the sensors pits

Besides the above described measurement system, also the surface loading is monitored by EMO since July 2016. Every half an hour a screenshot of the surface loading is captured. An example of such an image is shown in Figure 6.5.

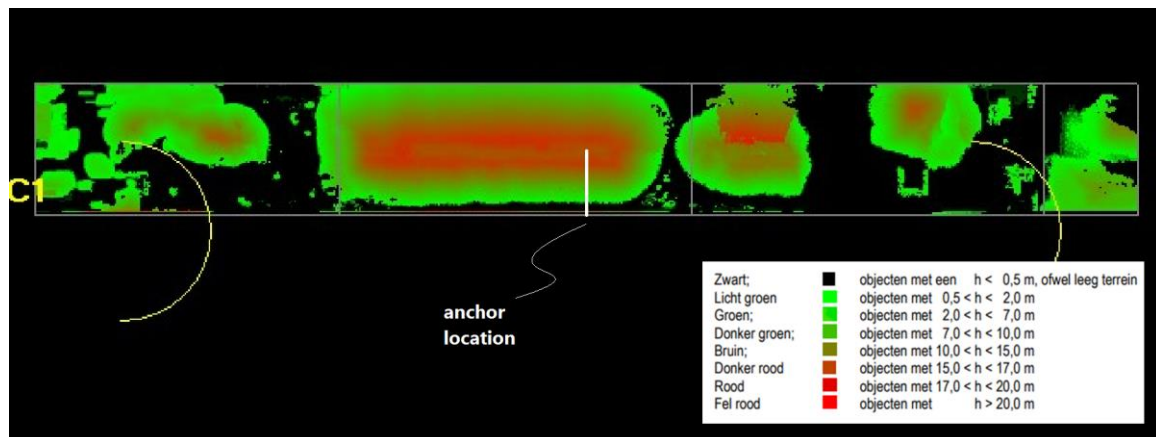


Figure 6.5 Example of surface loading of the EMO-quay wall

6.3 Approach for calibration and reliability analysis

As proven in the previous case study, the dominant uncertainty for a quay wall are the soil properties, although depending on the considered failure mechanism. When the aim is to use monitoring data to update the reliability for a certain failure mechanism, you therefore need a method which makes use of the data to reduce the uncertainty in the soil properties. The main difficulty in the case of quay walls is that the monitoring data only implicitly provides information regarding the soil parameters.

The monitoring data of the anchor strains and the wall deformations contains information about the actual in-situ soil properties. Whereas the following monitoring data provide information about the loading conditions on the quay at a certain moment in time:

- Water levels
- Surcharge information
- Temperature

For a calibration, both types of measurement sources should be combined. To do this, basically two types of calibrations can be distinguished:

- 1 Deterministic calibration
- 2 Full probabilistic calibration using Bayesian updating

With a deterministic calibration, the parameters are adjusted in such a way that a fit between measurements and calculations is obtained. It can be performed by manually adjusting parameters or in a more structured way using for example sensitivities (Calvello & Finno, 2004). In this way, only information about the mean value of each parameter is obtained and nothing about the standard deviation. Whereas predominantly a change in standard deviation affects the reliability.

With a full probabilistic update, usually a Bayesian update, the calibration process is performed in a more elaborate way. This method takes into account prior information about the uncertainty in each parameter and samples multiple sets of parameters to determine the most likely combination of parameters that fits the measurements. With this method not only the mean value of a parameter is updated but also the standard deviation, thus resulting in a more comprehensive update of the reliability. Den Adel (2018) proved that this method can be applied on quay walls modelled with Plaxis. The main downside of this method is the computational effort that is required for such an update.

Due to time limitations, it was decided to choose for the first type of calibration in which the soil (and structural) parameters are manually adjusted to fit model outcomes with measurements.

The calibration is consisting of the following (iterative) steps:

- 1 Determine mean properties of the soil parameters
- 2 Calibrate on five periods in time

The calibrated model is subsequently used in the reliability analysis. Thus, only the mean values are updated whereas the COV remains unchanged. Only the most critical failure mechanisms are assessed in this case study to have a useful comparison with the target β and to explore for possibilities for an increase in retaining height. The choice for the failure mechanism is partly based on results of the reassessment report of Witteveen+Bos (2018).

Table 6.4 Results reassessment of EMO quay wall.

Limit state	Critical limit state in reassessment?	Applicability FORM
Yielding of the anchor profile	No, large overcapacity	+
Yielding of the combi-wall	No, there is some bending moment capacity left	+
Geotechnical failure	Yes, structure is very susceptible for a Kranz-type of failure	+/-
Resistance grout body	Not assessed	+

It is chosen to only assess the limit states yielding of the wall and geotechnical failure, as these are expected to be most critical.

6.4 Calibration of the model

The model is calibrated on the location of Pit 3 (P3 at Figure 6.4). This location was the most suitable because at other locations either sensors were corrupted or loading by a large coal pile was limited due to the existence of buildings.

The soil stratification is based on the stratification used in the report of (Witteveen+Bos, 2018) instead of the soil profile used in the original design by Volker InfraDesign (2011). The reason for this is that for the original design the soil parameters are determined based on the several correlations between cone resistance, relative density and friction angle. The soil parameters can therefore not be considered as characteristic values. This makes the transformation to mean values complicated.

The soil stratification used by Witteveen+Bos is based on the soil classes defined in the NEN9997. The used CPTs and an overview of the complete soil profile along the quay wall can be found in Appendix I.

The characteristic values of the soil parameters are given in Table 6.5. The Hardening soil parameters are given further on in Table 6.7.

Table 6.5 Characteristic values at Pit 3

Level [m w.r.t. NAP]	Description	Layer number [-]	q_c [MPa]	$\gamma_{unsaturated}$ [kN/m ³]	$\gamma_{saturated}$ [kN/m ³]	ϕ' [°]	c' [kN/m ²]
5.0	Sand, moderate, top	1	10	18.0	20.0	32.5	0
-3.0	Sand, dense	2	20	19.0	21.0	35.0	0
-7.8	Clay, w. sandy, moderate	3	2	17.0	18.0	25.0	7.5
-9.1	Sand, moderate, 2	4	22	18.0	20.0	32.5	0
-12.0	Sand, clay layers	5	21	18.1	18.7	27.5	0
-19.0	Sand, Pleistocene	6	40	19.0	21.0	35.0	0

The Plaxis model of the quay wall is shown in Figure 6.6.

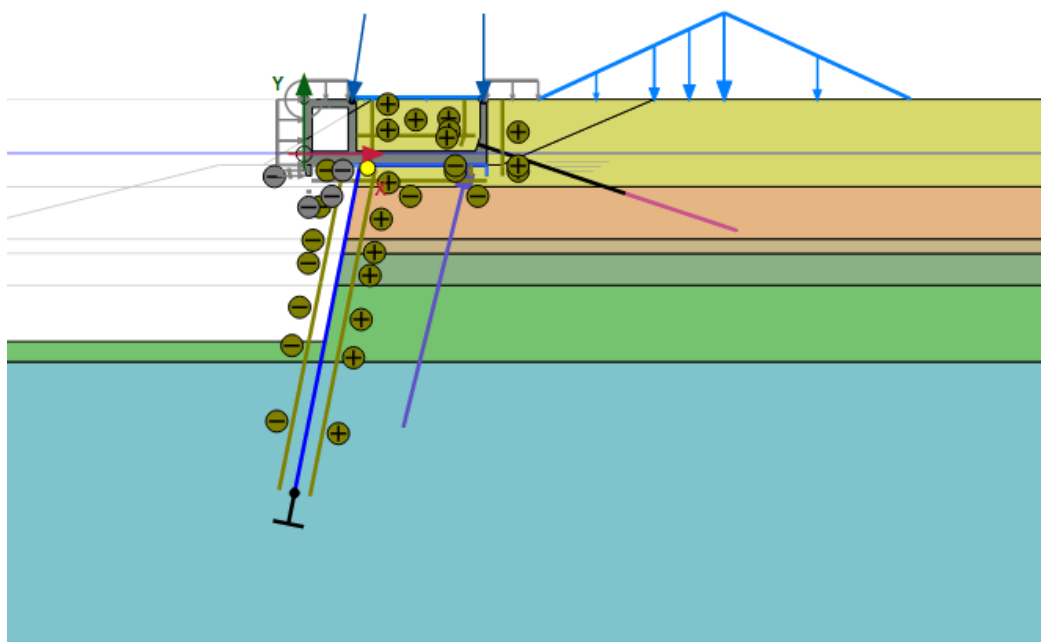


Figure 6.6 Plaxis model of the quay structure

6.4.1 Measured displacements versus calculated displacements

There are five points in time for which both SAAF measurements and surcharge information is available. All these five points are used in this paragraph.

Mean values of soil parameters can be derived by transforming the characteristic values with equation 6.1.

$$\mu_i = \frac{X_{i,k}}{1 \pm 1.64COV_i} \tag{6.1}$$

When using this transformation (only for the friction angle and the cohesion as all other parameters are already expected values) , quite a large misfit with the measurement data is found. Figure 6.7 shows the measured lateral combi-wall deformation over depth versus calculated combi-wall deformation. The same trend is found for the other four points in time.

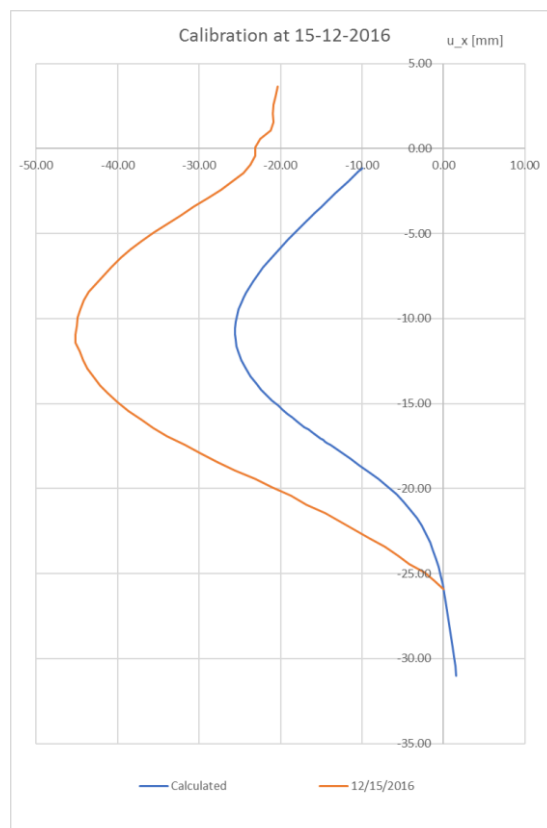


Figure 6.7 Measured lateral combi-wall deformation over depth (orange) vs calculated combi-wall deformations (blue)

A good fit was found (Witteveen+Bos, 2018) when increasing the characteristic friction angle of each layer by 2.5 ° instead of using equation 6.1 This can basically be considered as taking the average between the low and the high characteristic value of the friction angle of NEN9997. The results for the five calibration points in time shows quite a good match with the measurement data (Figure 6.8). The anchor forces were captured within a margin of 10% as well.

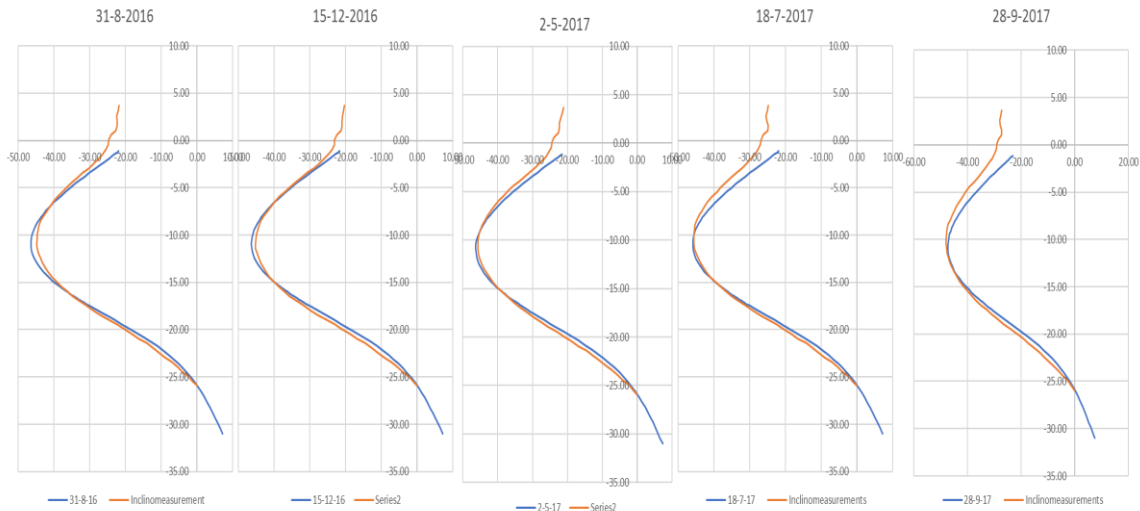


Figure 6.8 Measured lateral combi-wall deformation over depth (orange) vs calculated combi-wall deformations (blue) for five points in time

For this reason, these soil parameters are considered as the expected parameters. This results in the soil parameters of Table 6.6 and Table 6.7 which are used in the upcoming reliability calculations:

Table 6.6 Expected soil strength parameters

Level [m w.r.t. NAP]	Description	$\gamma_{unsaturated}$ [kN/m ³]	$\gamma_{saturated}$ [kN/m ³]	ϕ' [°]	c' [kN/m ²]
5.0	Sand, moderate, top	18.0	20.0	35.0	0
-3.0	Sand, dense	19.0	21.0	37.5	0
-7.8	Clay, w. sandy, moderate	17.0	18.0	22.5	7.5
-9.1	Sand, moderate, 2	18.0	20.0	35.0	0
-12.0	Sand, clay layers	18.0	19.0	29.8	0
-19.0	Sand, Pleistocene	19.0	21.0	37.5	0

The Hardening Soil parameters are determined based on the relation between relative density and cone resistance given by Lunne et al. (1997):

$$R_e = \ln\left(\frac{q_c}{61(\sigma'_v)^{0.71}}\right) \frac{100\%}{2.91} \quad (6.2)$$

The relative density is determined for three CPTs and is afterwards averaged. The stiffness parameters are determined with the following relations:

- $E_{50}^{ref} = 60 * R_e$
- $E_{50}^{ref} = E_{oed}^{ref} = 4 * E_{ur}^{ref}$

Table 6.7 Expected Hardening soil parameters

Description	Re [%]	E_{50}^{ref} [MN/m ²]	E_{oed}^{ref} [MN/m ²]	E_{ur}^{ref} [MN/m ²]	m [-]	ψ [°]	R_{inter} [-]
Sand, moderate, top	79	47	47	189	0.5	5.0	0.8
Sand, dense	78	47	47	186	0.5	7.5	0.8
Clay, w. sandy, moderate	-	3.1	1,6	11,1	0.9	0	0.8
Sand, moderate, 2	74	45	45	180	0.5	5	0.8
Sand, clay layers	68	41	41	163	0.5	0	0.8
Sand, Pleistocene	78	47	47	187	0.5	7.5	0.8

6.5 Probabilistic calculations

In this section, the results of the calculations for the two considered limit states are presented.

6.5.1 Starting points

The quay wall was originally designed for a maximum bulk load of 230 kPa. However this design was made in accordance with the old guidelines of the CUR211 (2005) and was modelled with a slightly different soil profile. Furthermore, it was modelled with an older version of Plaxis.

The assessment of the structure in accordance with the EC7, showed that the structure was not able to withstand the bulk load of 230 kPa. Moreover, EMO b.v. pointed out that, due to the limitations of the crane, the coal piles will not be stacked higher than 15-16 m, which corresponds to a load of +/- 170 kPa.

The dominant load combination that is considered here, is the surcharge load of 170 kPa together with a crane load of 600kN/m and a representative water level difference of 0.5m (OWL at NAP -0.84m and GWL at NAP - 0.34m)

The applied mesh size of the Plaxis Hardening Soil model is medium. Using a coarser mesh leads to an overprediction of +/-10% on the Plaxis safety factor and would hence result in a too optimistic value for the reliability index for geotechnical failure. Note in Figure 6.9 that the fixed-end anchor below the combi-wall is removed to keep all stresses in the model. This is only done for the limit state geotechnical failure.

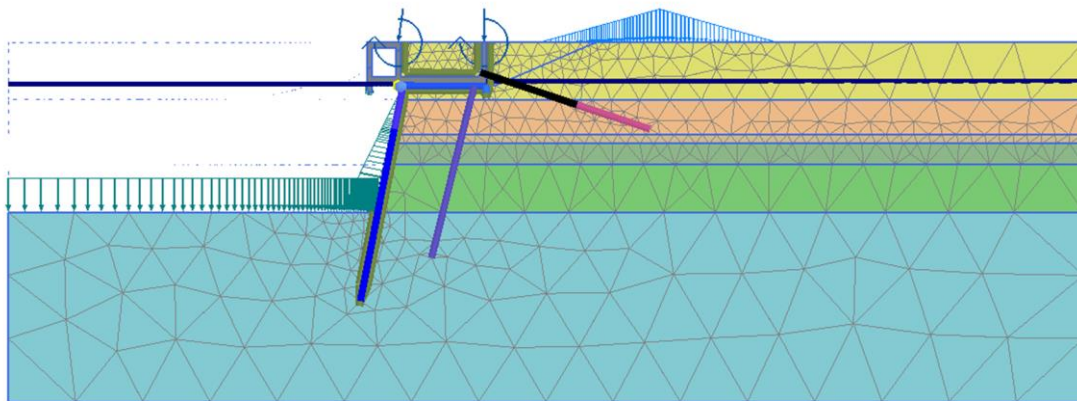


Figure 6.9 Applied mesh

The amount of construction stages has been decreased which has resulted in the following stages:

- 1 Initial phase (K0 -procedure)
- 2 Excavation till NAP -1.0 m
- 3 Installation of combi-wall and Vibro piles
- 4 Installation of superstructure and backfill behind structure
- 5 Installation and prestressing of grout anchors and sand fill inside structure
- 6 Dredging till construction depth
- 7 Load combination
- 8 (Safety phase)

6.5.2 LS1: Soil mechanical failure

For assessing the reliability with respect to soil mechanical failure the following LS is used:

$$Z = Msf - 1.05 \quad (6.3)$$

The assessment of this LS takes considerable computational effort, ProbAna2018 requires a stable safety factor and a current stiffness parameter (CSP) below 0.0005. If these requirements are not met, the number of calculation steps in the safety phase is increased in steps of 2000, until at least for 2000 steps a CSP below 0.0005 is found. This requirement can cause that a single LSFE takes more than 20 minutes.

For this reason the threshold was raised to 1.05, the amount of random variables were reduced as much as possible and the tolerances were set less strict (0.1, 0.1, 0.1, 0.05). With the medium mesh and without the fixed-end anchor, this problem was tackled for the main part. Increasing the threshold to 1.05 implies that there is some capacity left in the soil, meaning that the obtained reliability is an underestimation of the real reliability.

The parameters that are included in the calculation are the friction angle of each soil layer together with the unsaturated unit weight of the Pleistocene sand. The results are given in Table 6.8.

Table 6.8 Calculation results LS1: Soil mechanical failure

	Value				
Reliability index β	3.23				
Number of iterations	2				
Number of LSFE	21				
Constraint error	0.001				
Parameter	Unit	Design point X^*	Mean X_m	COV	Importance [%]
Sand, moderate, top - ϕ'	°	34.34	35.0	0.10	0.00
Sand, dense - ϕ'	°	36.66	37.5	0.10	0.00
Clay, w. sandy, moderate - ϕ'	°	24.62	25.0	0.10	0.00
Sand, moderate, 2 - ϕ'	°	34.63	35.0	0.10	0.00
Sand, clay layers - ϕ'	°	28.59	29.8	0.10	0.01
Sand, Pleistocene - ϕ'	°	25.78	37.5	0.10	0.68
Sand, Pleistocene - γ_{unsat}	kN/m ³	17.02	19.0	0.05	0.30

One can notice that only one iteration was needed. This is because the starting vector was chosen closer to the design point as a failed calculation already showed the large importance of the Pleistocene sand layer. The results indeed show that all importance goes to this layer. This is not strange as roughly 2/3th of the slip circle is located in this layer as shown in Figure 6.10.

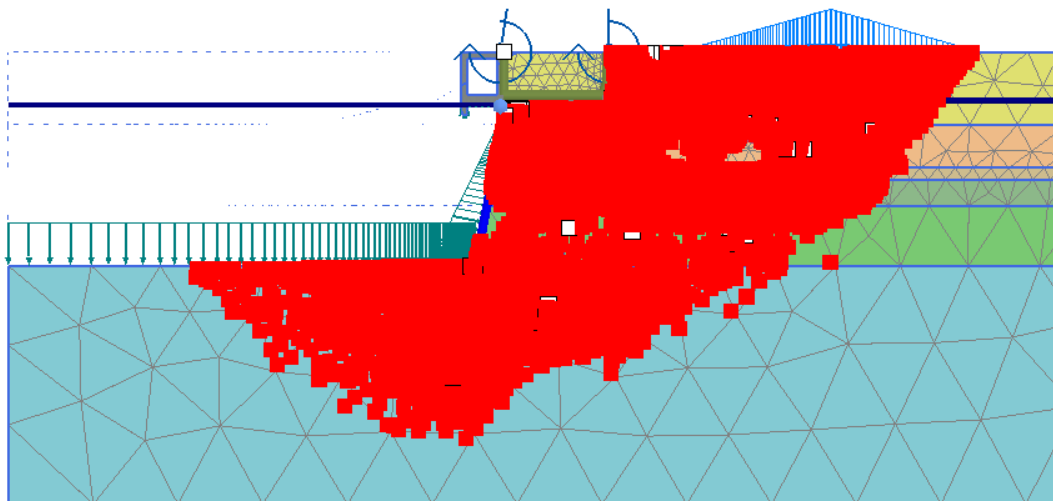


Figure 6.10 Failure points in design point LS Soil mechanical failure

The structure does not meet the requirements with respect to the target reliability of 3.8. However, it is still in the range of lifetime target reliability indices of 2.5-3.3 proposed by Roubos et al. (2018). With this in mind, the influence of a change in bottom depth / retaining height on the reliability index is investigated. The β is calculated for a bottom depth of 1.0 m lower and 1.0 m higher than the current design depth of NAP -18.65m. The results of Figure 6.11 show that a change in bottom height of 1.0 m roughly results in a change in β_{geo} of

0.4. This would imply that for the current dredging depth of NAP-17.15m the reliability is roughly 3.8, equal to the target reliability.

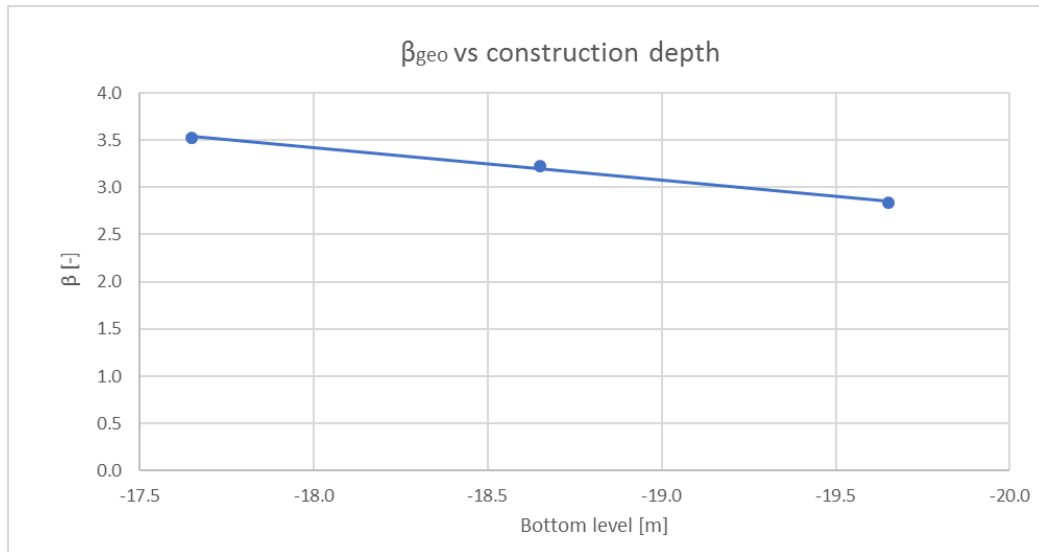


Figure 6.11 β vs construction depth for LS Soil mechanical failure

6.5.3 LS2: Yielding of the combi-wall

The LSF for yielding of the combi-wall is given by:

$$Z = f_y - \max \left[\frac{|M(z)|}{W_{el}} + \frac{|N(z)|}{A_{wall}} \right] \quad (6.4)$$

With a test run it turned out that around the FORM design point geotechnical failure occurs. Therefore, the combi-wall is elongated by 2.0 m. In general, a larger embedded depth is favourable for the bending moment in the wall. However, the quay wall has already a relatively large embedded depth. A deterministic calculation (with characteristic values) showed that the effect of a further increase in embedded depth is negligible on the obtained bending moment.

A sensitivity analysis with FORM (Appendix J) showed that only the two lowest layers have influence on the reliability index of the combi-wall. This is probably due to the relieving effect of the relieving platform as for the simple quay wall the middle layers had large importance. The result for the run with a limited amount of parameters is given in Table 6.9. Again the Pleistocene sand layer is dominant and the sandy clay layer above has only minor importance. Contrary to the results for the LBBR quay wall, the yield strength only has an importance of 1% for this quay wall.

Given the large importance of the Pleistocene sand layer in both limit states, it is interesting to investigate the effect of using different values for the COV of phi and to test other types of distributions. The results of these tests are discussed in chapter 7.

The obtained reliability index for this limit state does not meet the required reliability index of 3.8. Again, it is still in the range of lifetime target reliability indices of 2.5-3.3 proposed by Roubos et al. (2018).

Table 6.9 Calculation results LS2: Yielding of the combi-wall

		Value			
Reliability index β		3.12			
Number of iterations		4			
Number of LSFE		52			
Constraint error		4638 kPa (<1%)			
Parameter	Unit	Design point X^*	Mean X_m	COV	Importance [%]
Sand, clay layers - φ'	°	27.26	29.8	0.1	0.05
Sand, Pleistocene - φ'	°	26.84	37.5	0.1	0.53
Sand, clay layers - E_{50}^{ref}	kN/m ²	37075	41000	0.3	0.01
Sand, Pleistocene - E_{50}^{ref}	kN/m ²	31628	47000	0.3	0.11
Sand, moderate - γ_{unsat}	kN/m ³	18.24	18.0	0.05	0.00
Sand, clay layers - γ_{unsat}	kN/m ³	17.59	18.0	0.05	0.01
Sand, Pleistocene - γ_{unsat}	kN/m³	17.08	19.0	0.05	0.27
t_{tube}	m	0.0159	0.016	0.03	0.00
D_{tube}	m	1.4204	1.42	0.007	0.00
f_y	kPa	454462	470000	0.07	0.01

7

DISCUSSION

Several assumptions, simplifications and choices have been made throughout this research. It is therefore useful to discuss their validity and to check the impact of certain assumptions on the results. The main topics that are discussed here are:

- Influence of soil stratification
- Influence of the stochastic description of soil parameters
- Extreme values for soil parameters in FORM design points
- Influence of the use of monitoring data on the reliability
- Wider applicability of the results of both case studies

7.1 Influence of soil stratification

The results of the first case study showed that the friction angle of the loose sand layer (yellow layer in Figure 7.1) was the most important soil parameter for both yielding of the wall and yielding of the anchor bar. Herein the soil profile was simplified by merging two sand layers to one. However, this is a conservative assumption as in this way full dependency between both sand layers is assumed, which in reality is most likely not the case.

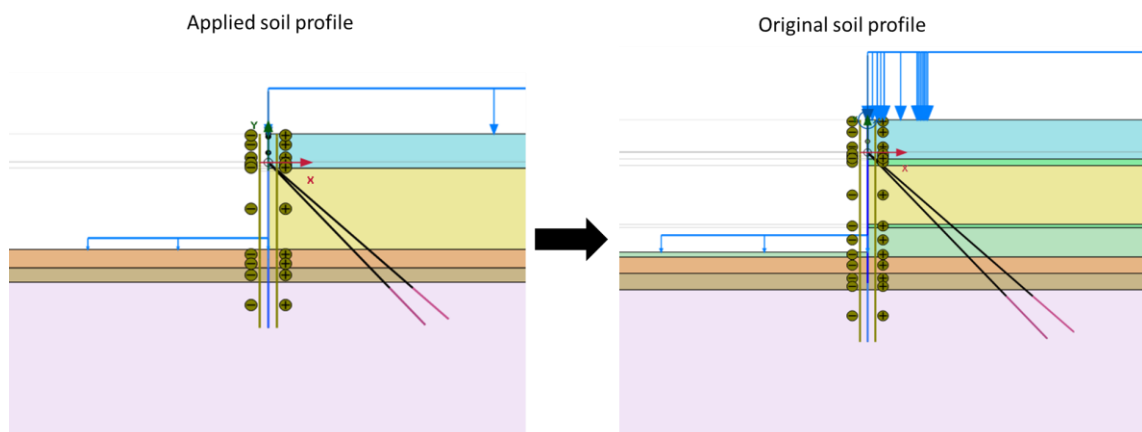


Figure 7.1 Applied vs original soil profile

For the applied soil profile, a reliability index β of 6.5 was found for the limit state yielding of the anchor bar. When performing the same calculation on the original soil profile (with the two very thin clay layers left out), the reliability index increases to 7.1. When splitting the layer even further up into a total of three equal layers, the reliability index increases even to 8.6. This demonstrates the importance of the soil stratification in a reliability analysis and raises questions about how many independent layers need to be modelled. Literature (e.g. Phoon and Kulhawy (1999)) prescribe a vertical scale of fluctuation in the range of 2 to 6 m, which implies that soil properties over a larger vertical distance are not correlated anymore. This would suggest that layers should not be thicker than ± 6 m. This is in large contrast with the thickness of the layers in both case studies, as layers with a thickness of 15 to 20m have been used.

7.2 Influence of the stochastic description of soil parameters

Relevant to this topic is the magnitude of the COV of the friction angle. In this research, for every layer the same value of 0.10 was applied independently of the layer thickness. CUR-C135 (2008) stated that the COV value given in NEN9997 should be interpreted as a spatially-averaged value. However, as already discussed in

chapter 4, the larger the vertical extent of a layer together with the vertical extent of a failure mechanism, the more spatial averaging is applicable (Schneider & Schneider, 2013). Thus in theory, the COV depends on the layer thickness and the vertical extent of the failure mechanism. This is an attractive concept in terms of reliability, but is considered doubtful by research of Ching et al. (2016) when using for a problem with homogeneous spatial-averaged soil layers in combination with reliability-based design. Nevertheless, it is still a topic that requires more attention.

Besides the discussion on the applicability of spatial-averaging, also the discussion on the choice for the friction angle is interesting to consider. With triaxial testing, three different value for the friction angle are distinguished (Figure 7.2) :

- 4 Friction angle at a an axial strain of 2%
- 5 Friction angle at a an axial strain of 5%
- 6 Peak friction angle

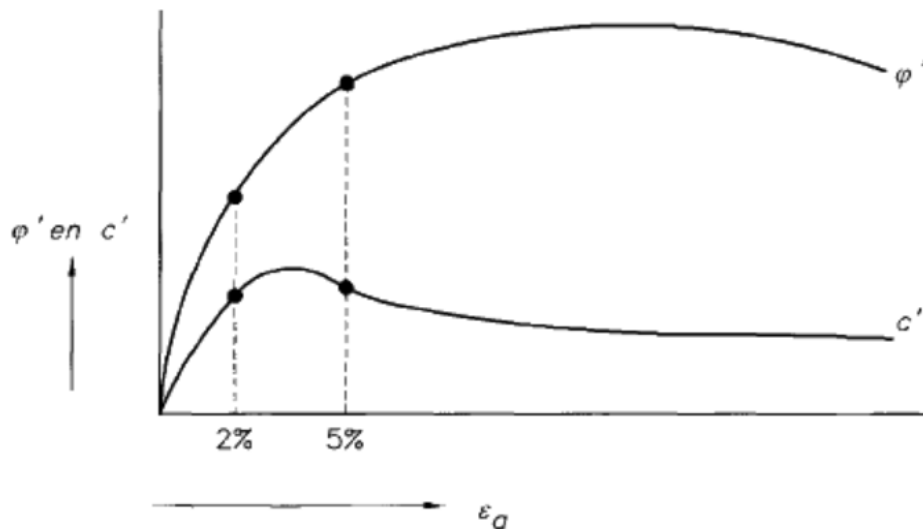


Figure 7.2 Friction angle vs axial strain. Source: CUR166 (2012)

In ULS calculations it is considered safe to use the friction angle belonging to a strain of 5%. Using the peak friction angle is also possible, but can be considered unconservative in case of layered soil. Differences in soil types can cause that certain layers reach failure earlier than others, causing that not all layers are at the same time on their peak strength (CUR166, 2012). When considering the research by Huijzer (1996) in which the triaxial test results for the Port of Rotterdam are described, a trend is visible in which the uncertainty in the friction angle decreases with increasing strain. The results for two layers of importance for the considered case studies in this thesis, are given in Table 7.1. It clearly shows a decrease in COV of 0.14 for 2% strain to ultimately 0.04 in case of maximum/peak friction angle. Furthermore, these values represent the point-to-point variation, implying that the spatially averaged variation is even lower.

Table 7.1 Triaxial test results. Source: Huijzer (1996)

	Holocene sand (NAP - 5m until NAP -20m)		Pleistocene sand (> NAP -20 m)	
	Mean	COV	Mean	COV
$\varphi'_{2\%}$	28.0	0.14	30.4	0.14
$\varphi'_{5\%}$	34.0	0.08	34.8	0.07
φ'_{max}	35.9	0.04	36.2	0.04

The COV at 5% strain for Pleistocene sand is lower than the currently applied value of 0.10. Given the large importance of this layer in the limit state geotechnical failure for the EMO quay wall, it is interesting to investigate the influence of different values for COV on the reliability index of this limit state. Besides the already performed calculations for COV = 0.10 also calculations for COV values of 0.075 and 0.05 are performed and shown in Figure 7.3. The figure shows a significant increase in reliability index from 3.2 (COV =0.10) to 5.4 (COV = 0.05). This shows the importance of the choice for an appropriate value of COV.

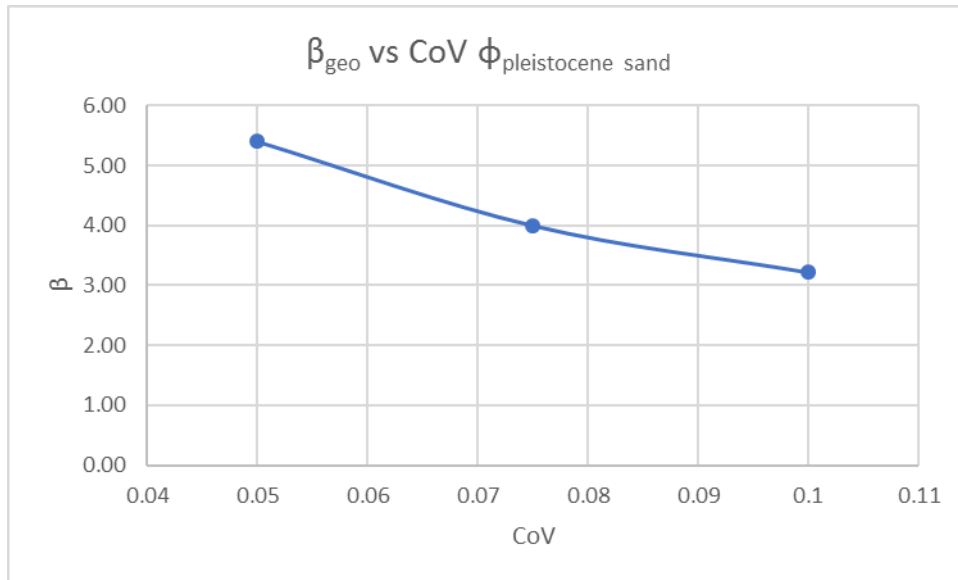


Figure 7.3 Influence of COV of β_{geo} of the EMO quay wall

7.3 Extreme values for soil parameters in FORM design points

Besides the discussion about the magnitude of the COV of the friction angle, also the validity of the normal distribution for extreme values of soil properties can be questioned. Sometimes a single soil parameter is completely dominant for the reliability of the considered limit state. A combination of a high sensitivity factor and high reliability index can cause that the FORM design point for the friction angle of the loose sand layer (yellow layer in Figure 7.1) reaches a value of 17° or even lower. It can be questioned whether it is physically possible for such a large sand layer (although mixed with clay) to reach such a low spatially averaged value. Triaxial test results of the database of Gemeentewerken Rotterdam (2003), which are shown in Figure 7.4, give an indication of the lower bound in test results.

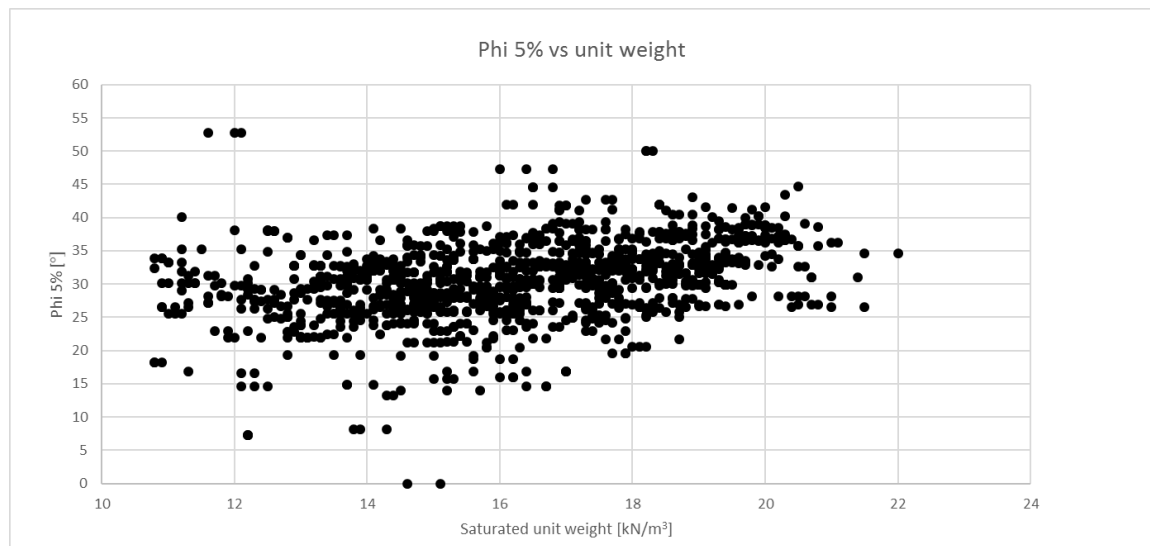


Figure 7.4 Triaxial test results

The unit weight of soil can be determined reasonably accurate, and therefore based on the unit weight, a lower bound for the friction angle could be estimated. The problem then shifts to what the ultimate lower bound for the unit weight of a certain layer should be. For a saturated unit weight larger than 17 kN/m^3 no values below $\pm 20^\circ$ can be found, whereas layer averaging is not even considered here.

To see the influence of a lower bound on the reliability index, for illustrational purposes a lower bound of 25° for the friction angle of the Pleistocene sand layer (which has a γ_{sat} of about 21 kN/m^3) is assumed and is

described by a shifted lognormal distribution (see Figure 7.5) . A truncated normal distribution could also be used but leads sometimes to convergence errors with FORM.

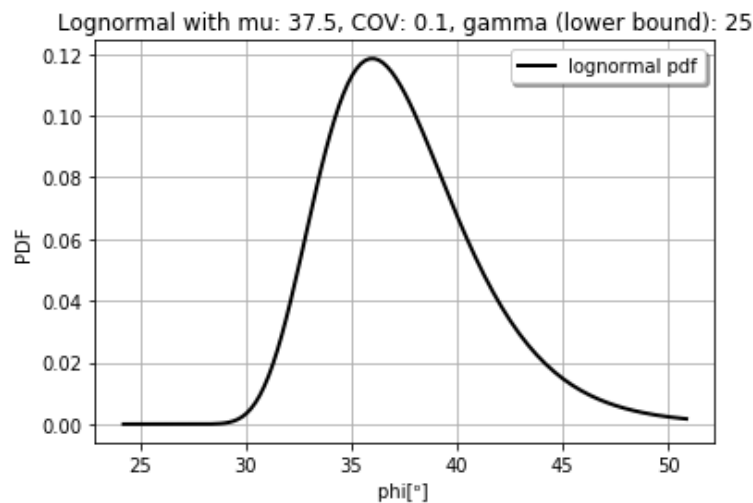


Figure 7.5 Lognormal distribution for ϕ' Pleistocene sand

The lognormal distribution is applied in the LS geotechnical failure of the EMO-quay wall. Compared to the results obtained with a regular normal distribution the reliability index increases from 3.2 to 5.0. The results of this run are shown in Table 7.2. Although it is only a hypothetical example, it illustrates the importance of the choice of the distribution. Especially for the Maasvlakte, where the soil profile is in general well known, the use of different types of distributions is worthwhile to further investigate.

Table 7.2 Results for geotechnical failure EMO with lognormal distribution for ϕ' Pleistocene sand

	Value				
Reliability index β	5.0				
Number of iterations	2				
Number of LSFE	27				
Parameter	Unit	Design point X^*	Mean X_m	COV	Importance [%]
Sand, moderate, top - ϕ'	°	32.93	35.0	0.10	0.01
Sand, dense - ϕ'	°	35.47	37.5	0.10	0.01
Clay, w. sandy, moderate - ϕ'	°	24.01	25.0	0.10	0.00
Sand, moderate, 2 - ϕ'	°	32.67	35.0	0.10	0.01
Sand, clay layers - ϕ'	°	25.72	29.8	0.10	0.05
Sand, Pleistocene - ϕ'	°	28.48	37.5	0.10	0.46
Sand, Pleistocene - γ_{unsat}	kN/m ³	15.40	19.0	0.05	0.37
Sand, Pleistocene - E_{50}^{ref}	kN/m ²	27614	48000	0.30	0.08
Surcharge load 1 (Left part of coal pile)	kN/m	-173	-170	0.05	0.00
Surcharge load 2 (Right part of coal pile)	kN/m	-173	-170	0.05	0.00

7.4 Influence of the use of monitoring data on the reliability

Until now the reliability of the EMO quay wall has only been determined for the calibrated model. Monitoring data is not available for every quay wall, therefore it is useful to investigate how large the impact of a calibration on the reliability can be. The main finding for the investigated case study was that the Pleistocene sand layer has the largest influence on the reliability. In case no calibration would be performed, the mean value of the friction angle of this layer would be taken at 41.9° (using equation 6.1) instead of the currently used value of 37.5°. This is roughly a difference of one standard deviation. This is a major difference what will largely affect the reliability index. Therefore, it can be expected that for the non-calibrated model, the reliability index for

both failure mechanisms is around one point higher. The results of the calculations for the non-calibrated design, given in Table 7.3, indeed shows that the reliability increases with 0.9 for both failure mechanisms. The parameters used for the non-calibrated together with the obtained FORM output are given in Appendix K.

Table 7.3 Comparison between the reliability index for the calibrated and the non-calibrated design

	Non-calibrated	Calibrated
Soil mechanical failure	4.1	3.2
Yielding of the combi-wall	4.0	3.1

So for this specific case study holds that the use of monitoring data is not ‘rewarding’ in terms of increase in reliability. As it concerns only one case study, it is not possible to draw sound conclusions about whether this will also be the case for other quay walls. It might be expected however, that also in other cases a mean friction angle of 41.9° (corresponding to a characteristic value of 35° for dense sand in NEN9997) will not be measured in reality.

It is also important to note that in the initial design of the contractor, optimistic soil conditions were used, resulting an optimistic design. This is a possible explanation for the low reliability indices that were found and the large difference between the calibrated and the non-calibrated design.

Besides, it’s good to mention that with the calibration only the mean values were updated. In case of a full-probabilistic update/calibration, also the standard deviation of each parameter is adjusted. Even in case higher displacements are measured than expected based on prior knowledge, the standard deviation of parameters still decreases due to fact that extra knowledge about the problem is attained. A decrease in standard deviation implies an increase in reliability index. So, If this would be applied here, the reliability would have turned out higher than calculated here.

7.5 Wider applicability of the results of both case studies

The results of both case studies showed deviating results for the reliability index and importance of parameters for the considered limit states. For the simple quay wall, the obtained reliability indices were in all cases higher than the target reliability, whereas for the quay wall with relieving platform the opposite was valid. This difference can be explained by the fact that it concerns different type of quay structures and different soil conditions. Furthermore, whether optimistic or pessimistic choices were made in the design, also influences the reliability. It is therefore not directly possible to generalize the findings of both case studies. However, considering the results from this thesis together with results obtained in previous probabilistic studies to quay walls, similarities can be noticed with respect to the importance of certain soil layers and soil parameters. In almost all cases the soil parameters have the most impact, followed by the structural properties.

Up to a certain degree, it can therefore be expected that for structures with almost the same composition and similar sandy soil conditions, the reliability will be in the same order of magnitude.

8

CONCLUSIONS AND RECOMMENDATIONS

In this chapter, the results of this research are discussed, followed by recommendations on the applicability and recommendations for further research. The objectives of this research were:

- 1 Establishing the actual reliability index of a quay wall in operation.
- 2 Exploring possibilities for an increase in retaining height, making use of probabilistic calculations.
- 3 Verifying the partial factors of the current design guidelines.

8.1 Conclusions

Four research questions have been set up at the start of this research. Following, each of them will be answered respectively. Besides this, more general conclusions are drawn about the applied methods and the obtained results.

1 What are the most suitable probabilistic methods to determine the reliability of a quay wall modelled with FEM?

In this thesis, the reliability of four failure mechanisms of quay walls has been investigated. These failure mechanisms were respectively: yielding of the combi-wall, yielding of the anchor bar, shear failure of the grout body and soil mechanical failure. By means of a literature review, the First Order Reliability Method (FORM) is considered to be the most suitable reliability method for assessing the Limit State Functions of these mechanisms. The main reason for this, is that the computational time using this method is much shorter compared to level III methods like Directional Sampling and Crude Monte Carlo simulation. With FORM, the calculation time is ranging from a few hours up to two days. The main disadvantage of FORM is its decrease in accuracy when using non-normal distributions and non-linear limit states. As this is the case in this thesis, the obtained failure probabilities are an approximation of the exact failure probability.

The probabilistic module ProbAna has been used for the coupling between the FORM-algorithms from the library of OpenTURNS and the Hardening Soil model of Plaxis. Two versions of ProbAna were used during the research, the second version is referred to as ProbAna2018. In the remainder of this chapter, conclusions about the applicability of FORM are referring to this version.

Based on the experience gathered during this research, it is concluded that for failure of the structural elements, FORM performed reasonably well. In most cases, the design point was reached within an error margin of 1% on all error types and was obtained after less than 10 iterations. Failed calculations were mainly caused by either soil body collapse, or were due to input restrictions in Plaxis on the values of E_{oed} and K_0^{nc} . To limit the occurrence of this second error, the ratio between E_{50} and E_{oed} , was slightly adapted from 1 : 1 to approximately 1 : 0.8 for the stiffness parameters that caused this problem. Soil body collapse was a problem that occurred for the quay wall with relieving platform, during the evaluation of failure of the combi-wall. This was solved by increasing the embedded depth of the combi-wall.

Regarding the limit state soil mechanical failure, difficulties were encountered in reaching a clearly defined safety factor using the phi-c reduction method. Furthermore, the mesh of the model needs to be finer than for the assessment of structural elements. Therefore, the computational effort for this limit state is significantly larger than for the other limit states. A preliminary calculation to find the direction of the design point and

thus the starting vector, highly reduces the calculation time. Due to the extra measures in ProbAna to increase the robustness for this limit state, it can be concluded that FORM is also applicable for this limit state.

2 What are the most sensitive parameters for each failure mode and for the overall system reliability?

In general, it can be concluded that, given a specified design, the uncertainty in the soil parameters have the largest influence on the reliability of the considered failure mechanisms. Of the three types of soil parameters included within this research (E_{s0}^{ref} , φ' , γ), the friction angle has the most influence in the investigated limit states. Time-dependent loads such as water level differences and surcharge loads are only occasionally included in the evaluations as they turned out to be of minor influence on the reliability.

Findings simple quay wall (double anchored combi-wall)

From the probabilistic calculations with respect to yielding of both the combi-wall and the anchor, it can be concluded that the friction angle of the loosely packed sand layer together with the yield strength have a large influence on the reliability. The obtained reliability indices (Table 8.1) for the as-built structure are all higher than the target reliability of 4.3. This was partly caused by the low unity check for the combi-wall. The results of Table 8.1 were obtained with calculations in which only the soil parameters were considered random.

Table 8.1 Obtained reliability indices for the as-built quay wall (RC3: $\beta_{target}=4.3$)

Limit state	Yielding combi-wall	Yielding anchor bar	Soil mechanical failure
β	6.5	6.5	7.9

For a slightly adjusted quay wall design with unity checks around 1.0, extensive calculations have been performed, including variable loads and structural parameters as random variables. Reliability indices (Table 8.2) obtained for this design show that also for this structure there is some overcapacity.

Table 8.2 Obtained reliability indices for the adjusted quay wall (RC3: $\beta_{target}=4.3$)

Limit state	Yielding combi-wall	Yielding anchor bar	Resistance grout body
β	5.7	5.3	4.9

Findings quay wall with relieving platform

The two failure mechanisms evaluated for the quay wall with relieving platform are yielding of the wall and soil mechanical failure. For both limit states, the friction angle of the dense Pleistocene sand layer is of major influence on the reliability. Most probably the relieving platform causes that only the deeper soil layers have influence on the reliability with respect to failure of the combi-wall. In contrast to the results of the simple quay wall, the yield strength was only of minor influence in the limit state.

Table 8.3 Obtained reliability indices for the as-built quay wall (RC2: $\beta_{target}=3.8$)

Limit state	Yielding combi-wall	Soil mechanical failure
β	3.1	3.2

The obtained reliability indices (Table 8.3) for the two failure mechanisms are lower than the target reliability of 3.8. It is important to note that in the initial design by the contractor, optimistic soil conditions were used, especially for the Pleistocene sand layer, which might have resulted in a too optimistic design. A second explanation is that in this case one soil parameter is extremely dominant with respect to the reliability. A semi-probabilistic design method is not developed for such an extreme case. This can cause that the reliability index is lower than the target reliability index.

3 How can monitoring data be used for model calibration and parameter distribution updating ?

There is still quite some uncertainty in the modelling of the behaviour of a quay wall. The monitoring data, consisting of anchor strains, wall deformations, water levels and temperature, helped with reducing the uncertainty in the modelling of the quay wall with relieving platform. A good fit was found between the measured and the calculated combi-wall deformations and anchor forces by performing a manual calibration. The obtained set of soil parameters were used as mean values in the probabilistic calculations. The calibration

turned out to have a significant impact on the reliability compared to the non-calibrated model. For the non-calibrated model, the reliability indices for both failure mechanisms were 0.9 higher than the values in Table 8.3. The main cause of this difference is the significant change in friction angle of the most dominant soil layer.

The downside of a manual calibration is that the acquired combination of parameters is just one possible combination, whereas there are many more parameter combinations that would fit the measurements. In the light of performing probabilistic calculations, the manual calibration does not provide information for a change in the standard deviation of each parameter and therefore it cannot be properly used as a measure to increase the reliability of the structure. For an update of the reliability, preferably a full probabilistic calibration should be performed. Den Adel (2018) proved with Bayesian updating that this is possible for quay walls modelled with Plaxis 2D. His results showed that in general, the standard deviations of the updated parameters decreased, resulting in an increase in reliability of the considered failure mechanisms.

4 How can this research contribute to an improvement of the current design guidelines?

Partial factors have been derived for the simple quay wall and are presented in Table 8.4. The first three columns show the partial factors obtained for each limit state. The last two columns respectively show the derived partial factors and the prescribed partial factors of Eurocode 7 (EC7). The overall impression here is that for most parameters, lower partial factors are derived than were prescribed by EC7. This is mainly caused by the fact that the obtained reliability indices were higher than required.

Only for the yield strength higher partial factors were derived. This can be explained by its large Coefficient of Variation (COV) and its direct presence in the limit states for both anchor and wall.

Table 8.4 Partial factors per failure mode and overall partial factors (RC3)

Parameter	Limit state			Derived	EC7 (RC3)
	Wall (Yielding)	Anchor (Yielding)	Soil		
Density	1.03	1.04	-	μ	μ
Friction angle*	1.14	1.11	1.28	1.15 (1.30 for GEO***)	1.20 (1.3 for GEO)
Soil stiffness	0.78	0.72	-	1.00	1.00
Surcharge load	1.08	1.07	-	1.10	1.25
Water level difference (Δ)**	1.0	1.0	-	1.0	1.0
Tube diameter	μ	μ	-	μ	μ
Wall thickness	μ	μ	-	μ	μ
Area anchor bar	μ	μ	-	μ	μ
$f_{y,tube}$	1.08	-	-	1.1	1.00
$f_{y,anchor}$	-	1.13	-	1.15	1.0

*) applied on $\tan(\varphi)$

**) variations in GWL were not considered here

***) GEO = Geotechnical failure, referring in this case to soil mechanical failure

Conclusions about the obtained results are:

- Often one soil layer is dominant for a certain limit state and requires partial factors, whereas for all other layers a characteristic value would be sufficient. Applying the partial factor on all layers can result in overdimensioning.
- Partial factors on stiffness are all lower than 1.0, indicating that a characteristic value is already sufficient. For anchor failure, both low and high stiffness can be normative.
- No model uncertainty is taken into account here, doing this would result in slightly higher partial factors than derived here. Also no geometrical variations are taken into account.
- The calculation is based on a slightly simplified soil profile, in which two sand layers are merged. As mentioned previously, this has significant impact on the reliability index. However, the deviation in influence factor α of the friction angle of that layer was small, implying only a minor deviation in the partial factors.
- Ideally a perfect match should be obtained between a manually calculated design point (with α and β of FORM) and the FORM design point, however this was not always the case here. This is predominantly

due to the use of correlations and non-normal distributions. Slight deviations between both design points are in the order of 1%. The error in the partial factor is therefore relatively small.

8.2 Recommendations

The main recommendations for further research are presented below.

Recommendations on model input

- The probabilistic calculations showed that often one soil layer is dominant for the reliability. In case of a high reliability index, the parameters of this layer are thus reduced to extreme low values for the design point, especially for the friction angle. It can be questioned whether this design point is physically realistic and whether the normal distribution is still valid for such extremes. Triaxial test results seem to show a lower bound given a certain unit weight. Probably a (shifted) lognormal distribution or a truncated normal distribution are more suitable, as with these distributions a lower bound can be set. Therefore research should be performed focussing on finding the possible lower bound for separate soil types. This might be beneficial for the reliability index.
- Soil stratification has a large influence on the reliability. Still not much guidance is available on how many (independent) soil layers should be used in a probabilistic calculation and on how spatial averaging is related to this. For all failure mechanisms, soil types and layer thicknesses, the same values for COV are used in general. In theory, the spatially averaged COV largely depends on the vertical extent of the failure domain and the vertical scale of fluctuation of the soil. This would imply case- and failure mode specific COV values. This concept needs to be further looked into, as a lower COV would result in lower partial factors and higher reliability indices.
- The stochastic distribution of the grout pile class factor α_t has been estimated in this thesis, as in the literature no information was found on this. As this parameter has a major influence on the reliability of the grout body, it is recommended to collect data of quality control checks and failure tests on grout bodies on a systematic basis to get a better insight into the stochastic nature of the factor α_t .

Recommendations on the use of probabilistic methods

- The applicability of FORM coupled with Plaxis for the case of quay walls, has only been verified by Teixeira et al. (2015) using Directional Sampling. To get a better insight into the accuracy of the results of FORM, more calculations with level III methods should be performed.
- For simple quay walls, probabilistic calculations can be performed relatively quickly. In the first stages of a design, it could therefore be very useful to perform probabilistic calculations as it gives insight into the parameters that are most influential. This can be used to increase the amount of tests on a specific soil layer.
- Information about the applied FORM algorithms of OpenTURNS is very scarce. It took quite some effort to exactly understand the working of the line search algorithm, and to find the most optimal settings for convergence. It would take much less time for new people to get familiar with FORM or other probabilistic methods if there would be a platform to share experience and knowledge.

Recommendations on partial factors

- The tubular piles of the combi-wall in both case studies are piles of class 4, which means they are susceptible for buckling before the yield limit in the outer fibre is reached. This failure mechanism is not addressed here. Therefore, it is advised to perform probabilistic calculations for this failure mechanism to check whether this results in different partial factors.
- In this research, partial factors are derived on only one quay wall. More quay structures, with different soil stratifications, should be considered to check whether the derived set of partial factors also holds for quay walls in different soil conditions.
- More quay structures, with similar soil stratifications, should be considered to check whether layer- and limit state specific partial factors could be defined for quay walls in the Port of Rotterdam. This would result in a more optimal design.

REFERENCES

- Acécon. (2015). *Rapportage bezwijkproeven op zelfborende groutinjectiepalen*.
- Andrianov, G., Burriel, S., Cambier, S., Dutfoy, A., Dutka-Malen, I., De Rocquigny, E., . . . Mangeant, F. (2007). *Open TURNS, an open source initiative to Treat Uncertainties, Risks' N Statistics in a structured industrial approach*. Paper presented at the Proceedings of the ESREL'2007 Safety and Reliability Conference, Stavanger: Norway.
- Bach, D. (2014). *Reliability-based design and quality control of bored piles*. PhD Thesis, Delft University of Technology
- Baecher, G. B., & Christian, J. T. (2003). *Reliability and Statistics in Geotechnical Engineering*. Chichester: Wiley.
- Brinkgreve, R. B. J., & Laera, A. (2017). *Probabilistic analysis*.
- Calle, K. O. F., & Spierenburg, S. (1991). *Veiligheid van damwandconstructies, onderzoeksrapportage deel I, Rapportnr. CO-316980/12*. Grondmechanica Delft
- Calvello, M., & Finno, R. J. (2004). Selecting parameters to optimize in model calibration by inverse analysis. *Computers and Geotechnics*, 31(5), 410-424.
- Ching, J., Hu, Y.-G., & Phoon, K.-K. (2016). On characterizing spatially variable soil shear strength using spatial average. *Probabilistic engineering mechanics*, 45, 31-43.
- CUR166. (2012). *Damwandconstructies, deel 1*: CUR Bouw & Infra.
- CUR211. (2005). *Handbook Quay walls*. Gouda, The Netherlands: CUR.
- CUR211. (2013). *Quay walls, 2nd edition*. Leiden, The Netherlands: SBRCURnet.
- CUR236. (2011). *Ankerpalen*.
- CUR-C135. (2008). *Van onzekerheid naar betrouwbaarheid; Handreiking voor geotechnisch ontwerpers*. Gouda, The Netherlands
- de Gijt, J. G. (2010). *A history of quay walls*. PhD Thesis, Delft University of Technology
- de Grave, P. (2002). *Validatie van partiële factoren uit "Probabilistische analyse damwandconstructies"*. MSc Thesis, Delft University of Technology
- Den Adel, N. (2018). *Load testing of a quay wall*. MSc Thesis, Delft University of Technology Delft.
- Gemeentewerken Rotterdam. (2003). *Alle triaxiaal proeven Rotterdam*.
- Google (Cartographer). (2018). Google Earth. Retrieved from <https://earth.google.com/web/>
- Griffiths, D. V., & Fenton, G. A. (2007). *Probabilistic methods in geotechnical engineering*: SpringerWienNewYork.
- Hasofer, A. M., & Lind, N. C. (1974). An exact and invariant first order reliability format. *Journal of the Engineering Mechanics division*, 111-121.
- Havinga, H. (2004). *Dossier Probabilistische berekeningen, onderdeel 7.1Bc*. Delft
- Hicks, M. A. (2013). An explanation of characteristic values of soil properties in Eurocode 7. In *In Advances in Soil Mechanics and Geotechnical Engineering* (pp. 36-45). Amsterdam: IOS Press.
- Huijzer, G. P. (1996). *Eindrapport probabilistische analyse damwandconstructies, Rapportnummer 94-168/B*.
- JCSS. (2006). *JCSS Probabilistic Model Code, Section 3.7: Soil properties*.
- Jonkman, S. N., Steenbergen, R. D. J. M., Morales-Nápoles, O., Vrouwenvelder, A. C. W. M., & Vrijling, J. K. (2016). *Probabilistic Design: Risk and Reliability Analysis in Civil Engineering*. Delft.
- Lemaire, M. (2009). *Structural reliability*. London: ISTE Ltd.

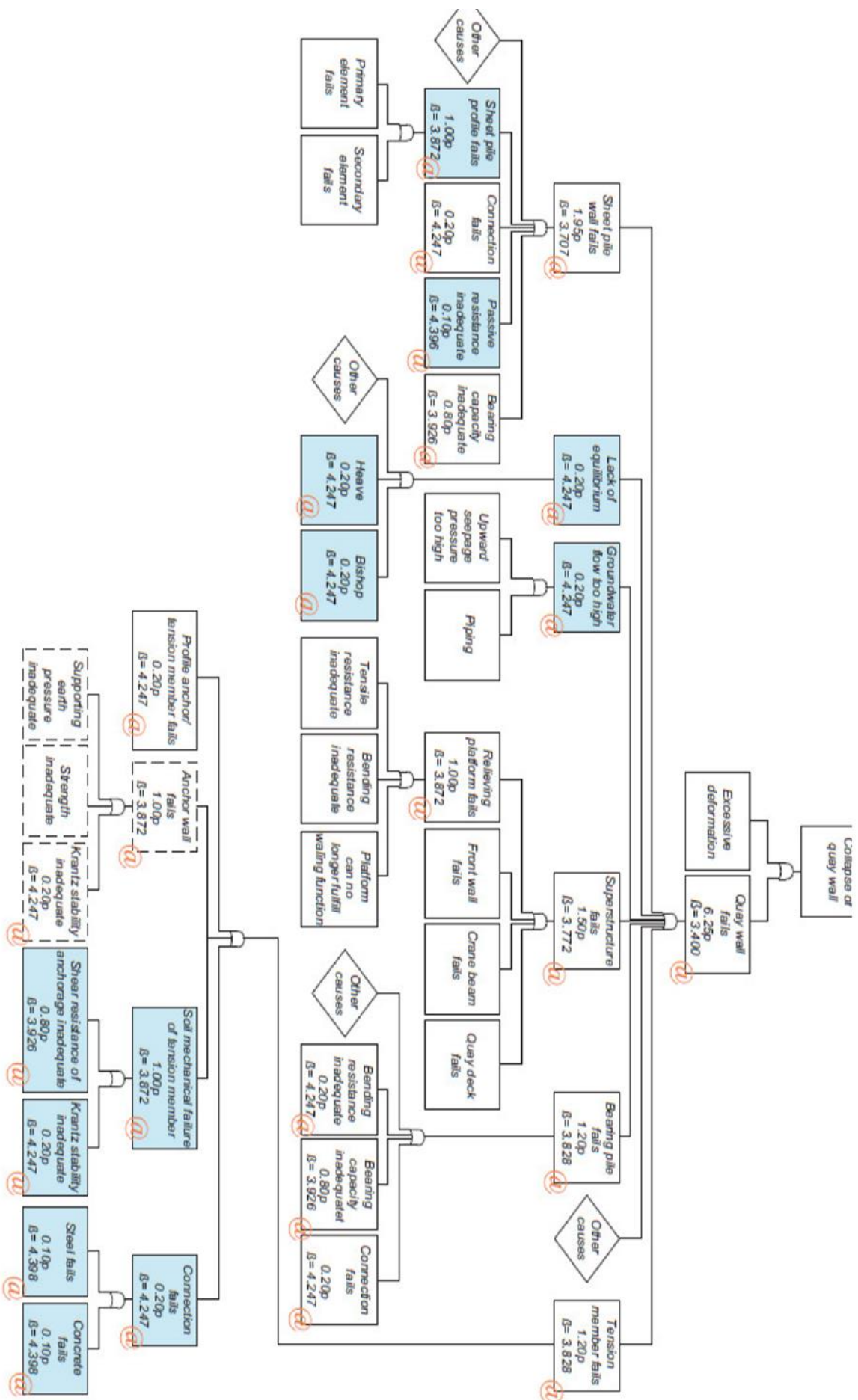
- Manoj, N. R. (2017). *Reliability based Ultimate Limit State Design in Finite Elements and compliance with Eurocode7*. MSc Thesis, Delft University of Technology.
- NEN-EN 1990. (2002). Eurocode - Basis of structural design. In.
- NEN-EN 10219-2. (2006). Cold formed welded structural hollow sections of non-alloy and fine grain steels - Part 2: Tolerances, dimensions and sectional properties. In.
- NEN 9997. (2017). Geotechnical design of structures. In.
- OpenTURNS. (2016). OpenTURNS 1.7 Reference Guide. Retrieved from http://autobuilder.openturns.org/openturns/tag/v1.8rc1/doc/commit/3b92f16bd65f582da0e34284f08bd27314ad5a53/squeeze-x86_64-doc/html/ReferenceGuide/
- Ou, C.-Y. (2013). *Deep Excavation, Theory and Practice*. Taipei, Taiwan: Taylor & Francis Group.
- Peters, D. J., Sadowski, A., Rotter, M., & Taras, A. (2017). *Calibration of Eurocode design models of thin-walled cylinder under bending with full scale tests*. Paper presented at the EUROSTEEL 2017.
- Phoon, K. K., & Kulhawy, F. H. (1999). Evaluation of geotechnical property variability. *Canadian Geotechnical Journal*, 36, 625 – 639.
- Plaxis. (2017). *Material Models Manual*.
- Port of Rotterdam. (n.d.). Rotterdam's Port development. Retrieved from <https://www.portofrotterdam.com/nl/files/history-port-of-rotterdam.png>
- Powell, M. J. D. (1994). A direct search optimization method that models the objective and constraint functions by linear interpolation. In S. Gomez & J.-P. Hennart (Eds.), *Advances in Optimization and Numerical Analysis* (pp. 51-67): Springer.
- Rippi, A. (2015). *Structural reliability analysis of a dike with a sheet pile wall: Coupling Reliability methods with Finite Elements*. MSc Thesis, Delft University of Technology
- Roubos, A. A., Steenbergen, R. D. J. M., Schweckendiek, T., & Jonkman, S. N. (2018). Risk-based target reliability indices for quay walls. *Structural Safety*, 75, 89-109.
- Schneider, H. R., & Schneider, M. A. (2013). Dealing with Uncertainties in EC7. In P. Arnold (Ed.), *Modern Geotechnical Design Codes of Practice* (pp. 87-100). Amsterdam: IOS-Press.
- Schrijver, I. J. M. (2016). *Reliability of flexible dolphins*. MSc Thesis, Delft University of Technology
- Schweckendiek, T. (2006). *Structural Reliability Applied To Deep Excavations Coupling reliability methods with finite elements*. MSc Thesis, Delft University of Technology
- Teixeira, A., Rippi, K., Schweckendiek, T., Brinkman, H., Nuttall, J., Hellebrandt, L., & Courage, W. (2015). *Soil-structure interaction: Reliability analysis of a retaining wall*. Natte Kunstwerken van de Toekomst
- van Gelder, P. H. A. J. M. (2000). *Statistical methods for the risk-based design of civil structures*. PhD Thesis, Delft University of Technology
- Vanmarcke, E., Shinozuka, M., Nakagiri, S., Schuëller, G. I., & Grigoriu, M. (1986). Random fields and stochastic finite elements. *Structural Safety*, 3(3), 143-166.
- Verruijt, A., & van Baars, S. (2009). *Grondmechanica: VSSD*.
- Volker InfraDesign. (2011). Geotechnische hoofdberekening EMO kade M5/M6 - 3796-R-0011 revisie 2.
- Vrijling, J. K., Bezuyen, K. G., Kuijper, H. K. T., van Baars, S., Molenaar, W. F., & Voorendt, M. Z. (2015). *Manual Hydraulic Structures*. Delft.

- Waarts, P. (2000). *Structural reliability using finite element analysis: an appraisal of DARS: Directional Adaptive Response surface Sampling*. PhD Thesis, Delft University of Technology
- Witteveen+Bos. (2017). *Rapport 'LBBR Reversed Engineering'*.
- Witteveen+Bos. (2018). *Quay Wall of the Future, Comparison report*.
- Wolters, H. J. (2012). *Reliability of Quay Walls*. MSc Thesis, Delft University of Technology

Appendices

A

APPENDIX: FAULT TREE FOR QUAY WALL WITH RELIEVING PLATFORM, CUR 211, FIRST EDITION



B

APPENDIX: PERFORMANCE OF ALGORITHMS OF OPENTURNS

In this appendix the working of the two available algorithms available in OpenTURNS is described together with their performance when coupled with Plaxis.

COBYLA

COBYLA stands for Constrained Optimization By Linear Approximation and does not make use the calculation of gradients. The exact working of this algorithm is quite difficult to understand and explain. According to Powell (1994), COBYLA constructs linear polynomial approximations to the objective and constraint functions by interpolation at the vertices of simplices (a simplex in n dimensions is the convex hull of $n+1$ points, n being the number of variables). This number of random variables should be limited to approximately 9 because otherwise the linear approximation can become highly inefficient. For further information reference is made to (Powell, 1994).

The algorithm follows approximately the following steps.

- 1 The calculations are carried out in the standard space and starts with a calculation with median values for all parameters.
- 2 After the mean value calculation, each individual parameter is varied by adding and subtracting $\rho_{beg} * \sigma$ to its mean value. The parameter ρ_{beg} should be provided by the user as input for the calculation.
- 3 After all parameters have been varied, the algorithm starts with searching to the design point.
- 4 After each iteration it is checked whether the convergence criteria are met. If this is the case the algorithm is stopped and the output is showed in the interface of ProbAna.

Abdo-Rackwitz

The Abdo-Rackwitz algorithm is based on the definition of gradients. Also this method is carried out in the standard space.

For every selected parameter the finite difference step (=step size) ϵ should be defined. This step size is used to calculate the gradient of the limit state function with respect to a certain parameter. The gradient can be calculated in two ways:

- Centered:

$$\frac{\partial Z}{\partial x_i} = \frac{Z(x + \epsilon_i) - Z(x - \epsilon_i)}{2\epsilon_i}$$

- Non-centered:

$$\frac{\partial Z}{\partial x_i} = \frac{Z(x + \epsilon_i) - Z(x)}{\epsilon_i}$$

For a centered gradient the LSF has to be evaluated two times, whereas for the non-centered only one evaluation is required. During every iteration the gradient is determined for every random variable, therefore it is desirable with respect to computational time to use a non-centered gradient. On the other hand it is known that the use of a centered gradient normally results in a more stable convergence.

For the step type a choice should be made between constant step size (the same step size for all iterations) or a blended step size (only a constant step size during the first iteration). From tests with blended step type it appeared that extremely unrealistic values are assigned to parameters (e.g. 90 degrees for the friction angle). This can result in the calculation of situations which are not within the physical boundaries for which Plaxis is

developed for and therefore give wrong results or errors. This is not desired as it can lead to an unstable FORM analysis. This problem can be partly prevented by the use of truncated normal distributions. By testing the algorithms, it appeared that the choice of the step size is causing this problem. The initial change of a parameter is determined as follows:

$$x_i = \begin{cases} \mu_i + \mu_i * \epsilon_i + \epsilon_i & \text{for } \epsilon_i \leq 1 \\ \mu_i * \epsilon_i + \epsilon_i & \text{for } \epsilon_i > 1 \end{cases}$$

So for a sand with $\varphi = 30^\circ$ and a finite difference step size of 3, the first step is not to $\varphi = 33^\circ$, but to $\varphi = 30 * 3 + 3 = 93^\circ$. This can cause problems within Plaxis. Also the use of a truncated normal distribution cannot prevent this step from being taken. Therefore it is very important to define the step size with attention. The main advantage of AR compared to COBYLA is the capability to handle a large number of random variables (up to 2000).

The convergence speed and the accuracy of the outcomes can be influenced by changing the default settings of the error tolerances. By default all values are set to 0.001. There are four types of error tolerances (OpenTURNS, 2016):

1 Maximum absolute error

This is the distance between two successive iteration points in the standard space:

$$|u_{n+1} - u_n|$$

2 Maximum relative error

This is the relative distance between two successive iteration points with respect to the second iteration point:

$$\frac{|u_{n+1} - u_n|}{|u_{n+1}|}$$

3 Maximum constraint error

This is the maximum distance between the constraint function and the threshold. Which is basically the maximum deviation in the calculated value for Z and the required value for Z (by definition Z=0). As the threshold value is given in the physical space (for example in kN) the value of this maximum error should be chosen with respect to this threshold (commonly 1% of the threshold value)

4 Maximum residual error

This is the orthogonality error, which describes the lack of orthogonality between the vector that links the standard space center to the point resulting from the iteration and the constraint surface

The iteration process is stopped when one of the three convergence criteria is met:

- 1 The absolute and the relative error are both below their pre-set value
- 2 The maximum constraint error and the maximum residual error are both below their pre-set value
- 3 The maximum number of iterations is reached

There is a difference between the terms iteration and evaluation. An evaluation is a single run in Plaxis to evaluate the prescribed LSF whereas an iteration is more related to a mathematical process and can contain multiple evaluations depending on the algorithm and the number of random variables.

As soil failure (or other failures) in Plaxis is not desired during the iteration procedure, several measures have been implemented in ProbAna to increase the robustness. The first measure is that when calculation failure occurs in a later phase than the considered phase for the LSF, it will be neglected and the iteration procedure is not interrupted.

If failure occurs in one of the parent phases of the considered phases, it cannot be neglected and therefore other measures are taken. As a first step some calculation features in Plaxis are adjusted. The *Max Load Fraction Per Step* is set to 0.1 and the option *Use gradual error* is enabled. If this is still not sufficient the strength parameters of the soil (φ and c') are increased by 20% in the case of a safety factor calculation. When this adjustment results in a successful calculation, the safety factor in the final answer is reduced by 20%. For other type of criteria such as exceedance of a threshold displacement other strategies are used.

Comparison of both algorithms

First the results of a performance test by Rippi (2015) are elaborated, whereafter the results of additional tests are described.

Rippi tested the performance of both algorithms on a Plaxis-model of an anchored sheet pile wall. The yield stress (450 kPa) of the anchor was chosen as the limit in the limit state function of the anchor.

For the Cobyla algorithm three test were carried out with respectively 3, 10 and 19 parameters. When the default values (0.001) of the error tolerances were used, no convergence was reached. Therefore it was required to increase the error tolerances significantly to the values of Table B.1. It must be noted that in the research of Rippi other convergence criteria are used than the ones in Probana. For convergence in the FORM analyses of Rippi, all four error tolerances should be met, whereas in Probana, only a combination of certain errors tolerances should be met.

Table B.1 Error tolerances COBYLA

	Default value	Adjusted value
Maximum absolute error	0.001	0.1
Maximum relative error	0.001	0.5
Maximum constraint error	0.001	0.2
Maximum residual error	0.001	0.1

Although convergence was reached with the adjusted values, the results of the calculation seemed incorrect as a very high failure probability of around 0.35 was obtained. Also in all of the three cases the algorithm stopped after 25 LSFE's while the maximum number of LSFE was set to 100. This is strange because as shown in Figure B.1, the maximum stress that was reached was around 375kPa which is significantly lower than the yielding stress limit of 450 kPa.

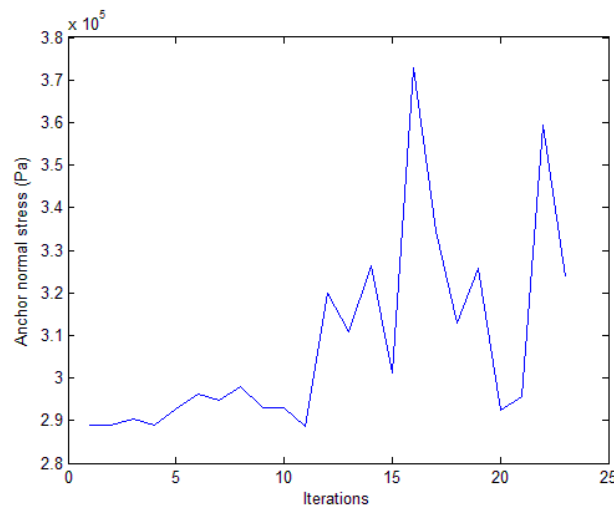


Figure B.1 Iteration values for the anchor stress using 3 random variables. Source: Rippi (2015)

For the case of 19 random variables the algorithm performed even worse; the maximum stress in the anchor did never surpass 267kPa. Also the algorithm was not able to variate its parameters properly. This is illustrated in Figure B.2, which shows that the friction angle is kept constant during almost the entire optimization.

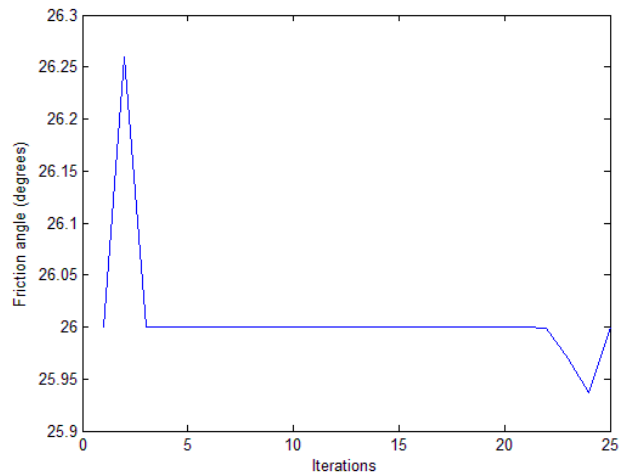


Figure B.2 Value of the friction angle during the iteration process with 19 random variables. Source: Rippi (2015)

The malfunctioning of the Cobyla algorithm for the case of 10 and 19 random variables is not remarkable. As already stated before, the algorithm becomes highly inefficient for more than 9 random variables according to the developer of the algorithm. However, this does not explain the malfunctioning of the algorithm for only 3 random variables. An explanation for this could be the apparent non-linearity of the anchor limit state function in the parameter space which cannot be handled by this linear optimization algorithm.

The only main advantage of this algorithm is the short computational time with respect to the AR algorithm.

The AR was also tested with 19 random variables and performed significantly better. It was able to vary the parameters consistently during the iteration process and convergence to the threshold of 450 kPa was obtained, see Figure B.3. The analysis resulted in a reliability index of 5.8 and the design point was also right. However, this analysis took 4 days and required 4151 LSFs. Another concern is that certain parameters received unrealistic values. For example negative values for the Poisson's ratio and extremely high values for the friction angle. This is problematic as it can result in soil body collapse during the iteration process.

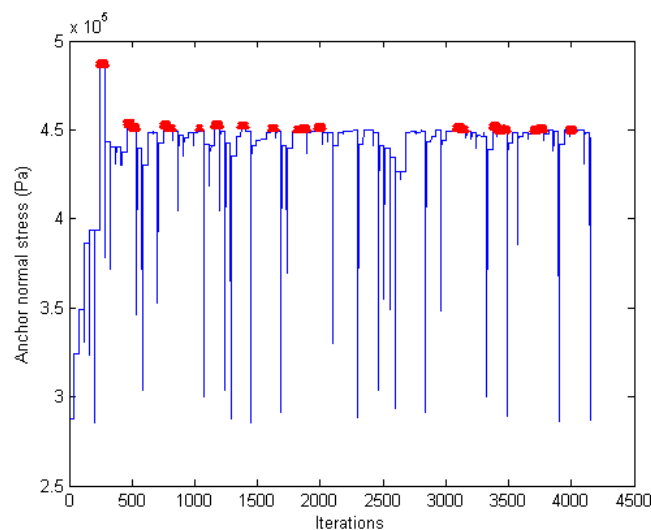


Figure B.3 Anchor stress during the FORM analysis using AR and 19 random variables. The red dots indicate when the threshold value of 450 kPa was exceeded

By increasing the error tolerances to values of around 1.0 and using truncated normal distributions instead of normal distributions it seemed to be solved. Another important change to prevent errors is the change of elastoplastic behavior of the anchor into elastic, as the plastic behavior is difficult to handle for the algorithm. With this setting the calculation time is around 10 hours.

By changing the starting point of the iteration more close to the design point the computational time can be decreased significantly. However, this requires prior knowledge of the design point, which is often not available.

Due to the difference in convergence criteria between Rippi's research and this one, extra tests were carried out to get a better understanding of the algorithms and the influence of the tolerance errors on the convergence of the FORM analysis. For this analysis the limit state function of the anchor of a combi-wall was used. The threshold for the tensile strength in the anchor was set at the yield strength of 2993 kN. First the performance of AR was tested. For the first run 6 parameters were selected as random variables. The convergence criteria settings were the following:

Table B.2 Convergence criteria

	Value
Maximum absolute error	0.05
Maximum relative error	0.05
Maximum constraint error	25 kN
Maximum residual error	0.05
Gradient type	Non-centered
Step type	Blended
Max. Iterations	50

With this settings convergence was reached after 27 iterations (273 LSFE's) which took 10 hours. All parameter distributions were chosen as Truncated normal to prevent physically unrealistic values. The obtained reliability index was 4.03 and also the design point seemed correct. When considering the development of the convergence error (Figure B.4), it can be concluded that the constraint error is already below its limit (25 kN) after two iterations.

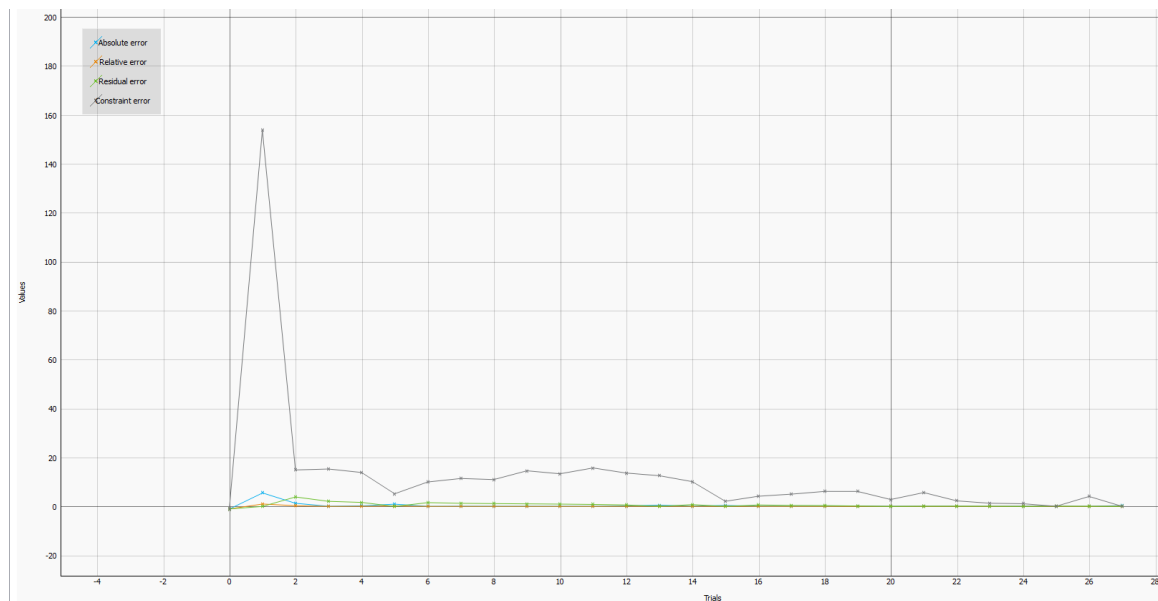


Figure B.4 Convergence errors

The three other errors required more iterations (Figure B.5). The algorithm was stopped because both the constraint and the residual error requirements were met.

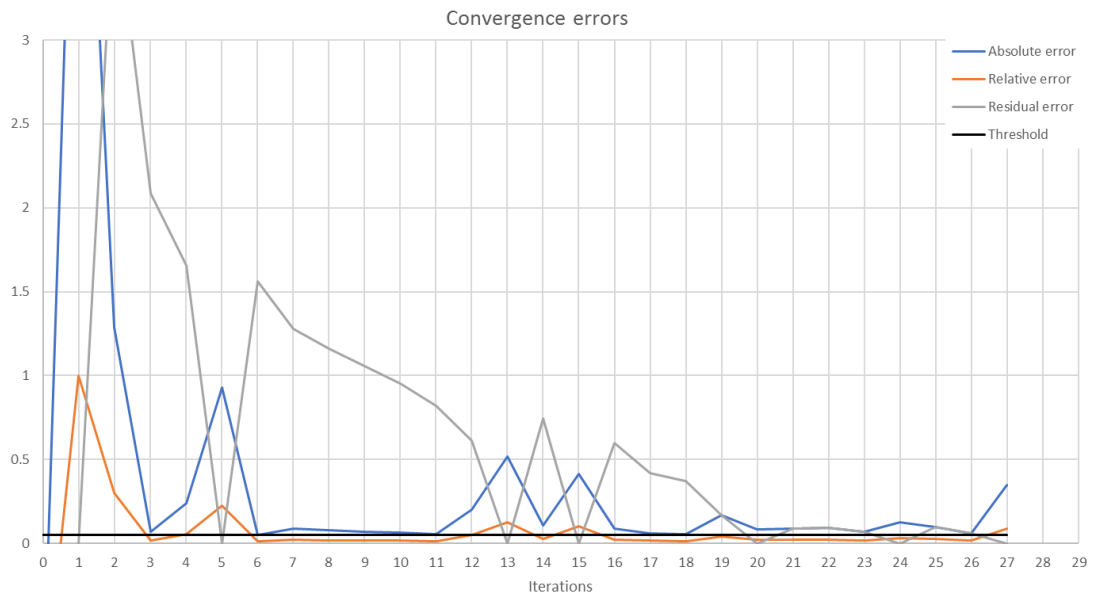


Figure B.5 Convergence errors



APPENDIX: MONTE CARLO SIMULATION FOR STRUCTURAL PROPERTIES

In this Appendix the statistical parameters of the composed structural properties are determined (e.g. the mean and COV of the bending stiffness EI). Besides, the correlation between parameters of the combi-wall are determined by a Pearson product-moment calculation. The python script contains a Monte Carlo Simulation and a function to determine the Pearson's correlation coefficients. Some figures are plotted to verify that the generated parameters follow a normal distribution and that the use of Pearson product-moment is allowed.

```
import math
import random
import numpy as np
import matplotlib.pyplot as plt

n = 100000

#properties of the tubular piles
A = np.zeros(n)
I = np.zeros(n)
t = np.zeros(n)
E = np.zeros(n)
EI = np.zeros(n)
EA = np.zeros(n)

#properties of the combi wall per meter
I_m = np.zeros(n)
A_m = np.zeros(n)
EA_m = np.zeros(n)
EI_m = np.zeros(n)
W_m = np.zeros(n)
w_m = np.zeros(n) # weight of the wall per meter length/depth

D_mean = 1420 # pile diameter
Tolerance_D = 10 #max tolerance in mm

t_mean = 16 # thickness of the tubular piles
Tolerance_t = 0.1* t_mean # tolerance of the thickness

length = 3.76 # length of the combi wall system in m
A_TSP = 37030 #mm2 Area of the triple sheet pile retrieved from tables Arcelor
#I_TSP = 92010e4 #mm^4

mean_E = 210E3 # MPa = N/mm2
cov_E = 0.03 # coefficient of variation E
std_E = cov_E*mean_E # standard deviation E

for i in range(n):
    #sampling of variables
    E[i] = random.gauss(mean_E,std_E)
    D = random.uniform(D_mean-Tolerance_D,D_mean+Tolerance_D)
    #t[i] = random.uniform(t_mean-Tolerance_t,t_mean+Tolerance_t)
```

```

t[i] = random.gauss(t_mean,Tolerance_t/2.0) # gaussian distribution for the wall
thickness
d = D-2*t[i] # inner diameter
I_TSP = random.gauss(92010e4,0.02*92010e4)
A_TSP = random.gauss(37030,0.02*37030) #mm^4
#properties of the tubular pile
A[i] = 0.25*np.pi*(D**2.0-d**2.0)
I[i] = np.pi*(D**4.0-d**4.0)/64
EI[i] = E[i]*I[i]
EA[i] = E[i]*A[i]
#properties of the system per running meter
I_m[i] = (I[i]+I_TSP)/length
EI_m[i] = (EI[i]+E[i]*I_TSP)/length
EA_m[i] = (EA[i]+E[i]*A_TSP)/length
W_m[i] = I_m[i]/float(D_mean)
A_m[i] = (A[i]+A_TSP)/length
w_m[i] = 78.5*(A_m[i]/1e6)

plt.plot(EA_m,EI_m,'ro')
plt.xlabel('EA per meter [N/m]')
plt.ylabel('EI per meter [Nmm^2/m]')
plt.title('MC simulation ')
plt.show()

#print ('mean I', np.mean(I))
#cov_I = np.std(I)/np.mean(I)
#print ('cov I' , cov_I)
#
#print ('mean A', np.mean(A))
#cov_A = np.std(A)/np.mean(A)
#print ('cov A' , cov_A)
#
#print ('mean EI', np.mean(EI))
#cov_EI = np.std(EI)/np.mean(EI)
#print ('cov EI' , cov_EI)
#
#print ('mean EA', np.mean(EA))
#cov_EA = np.std(EA)/np.mean(EA)
#print ('cov EA' , cov_EA)

print ('mean EI_m ', np.mean(EI_m))
cov_EI_m = np.std(EI_m)/np.mean(EI_m)
print ('cov EI_m' , cov_EI_m)

print ('mean EA_m =', np.mean(EA_m))
cov_EA_m = np.std(EA_m)/np.mean(EA_m)
print ('cov EA_m' , cov_EA_m)

print ('mean w_m', np.mean(w_m))
cov_w_m = np.std(w_m)/np.mean(w_m)
print ('cov w_m' , cov_w_m)

n, bins, patches = plt.hist(EI_m, 100, density=True, facecolor='g', alpha=0.75)

plt.xlabel('EI per meter [Nmm^2/m]')
plt.ylabel('Probability')
plt.title('MC simulation ')
plt.grid(True)
plt.show()

def average(x):
    assert len(x) > 0
    return float(sum(x)) / len(x)

def pearson_def(x, y):

```



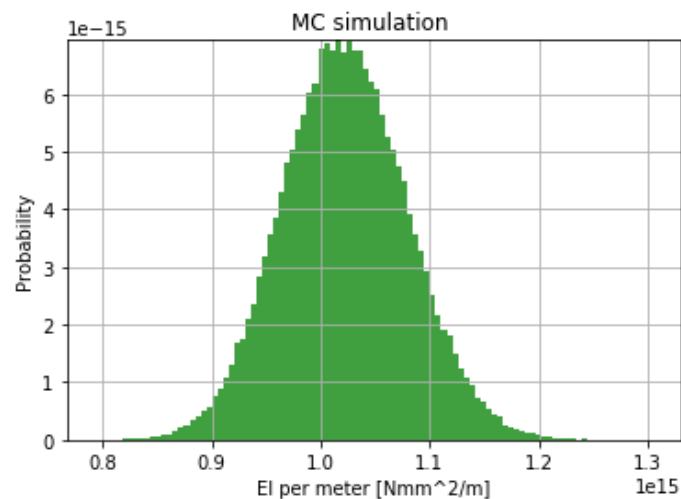
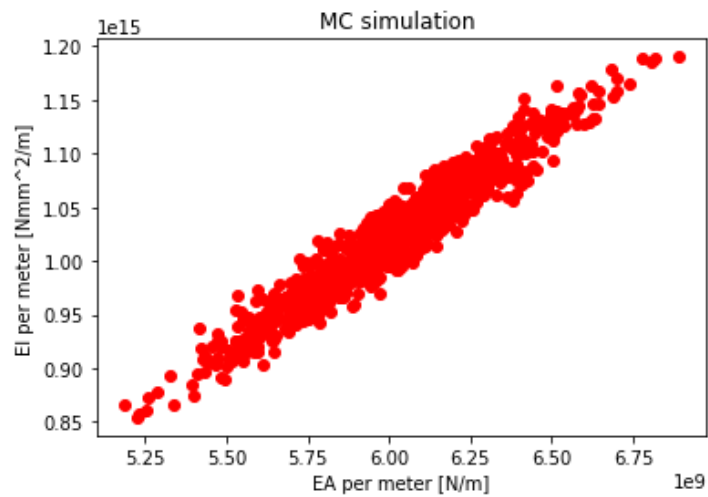
```

assert len(x) == len(y)
n = len(x)
assert n > 0
avg_x = average(x)
avg_y = average(y)
diffprod = 0
xdiff2 = 0
ydiff2 = 0
for idx in range(n):
    xdiff = x[idx] - avg_x
    ydiff = y[idx] - avg_y
    diffprod += xdiff * ydiff
    xdiff2 += xdiff * xdiff
    ydiff2 += ydiff * ydiff

return diffprod / math.sqrt(xdiff2 * ydiff2)

print ('p_EAm_wm = ',pearson_def(EA_m,w_m) )
print ('p_EAm_Am = ',pearson_def(EA_m,A_m) )
print ('p_Wm_wm = ',pearson_def(W_m,w_m) )
print ('p_Wm_Am = ',pearson_def(W_m,A_m) )

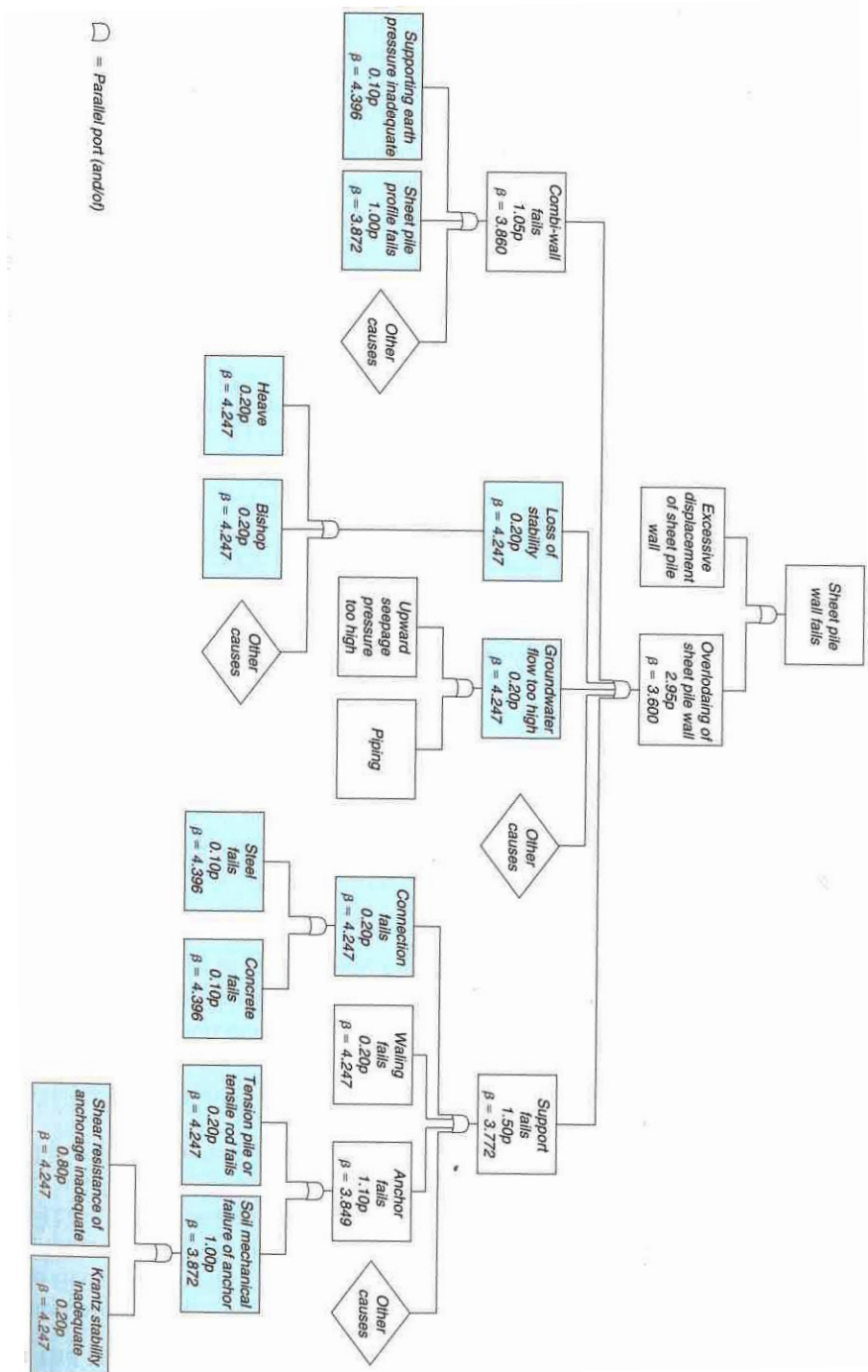
```



D

APPENDIX: FAULT TREE SIMPLE QUAY WALL

Below is the fault tree of CUR211 (2005) given, in which the failure space distributed is applied.



The division of the failure space for RC3 for simple quay walls according to (CUR211, 2005) is given in the table below:

Failure mechanism	allowable probability in p	Probability of failure	reliability index β
Quay wall fails	2.95p	8.540E-06	4.300
Combi-wall fails	1.05p	3.040E-06	4.524
Sheet pile profile fails (yielding)	1.00p	2.895E-06	4.534
Passive resistance inadequate	0.10p	2.895E-07	4.998
Loss of stability	0.20p	5.790E-07	4.863
Groundwater flow too high	0.20p	5.790E-07	4.863
Support fails	1.50p	4.342E-06	4.448
Soil mechanical failure of tension member	1.00p	2.895E-06	4.534
<i>Shear resistance of anchorage inadequate</i>	0.80p	2.316E-06	4.581
<i>Kranz stability inadequate</i>	0.20p	5.790E-07	4.863
Profile of anchor/tension member fails	0.20p	5.790E-07	4.863
Connection of tension member fails	0.20p	5.790E-07	4.863

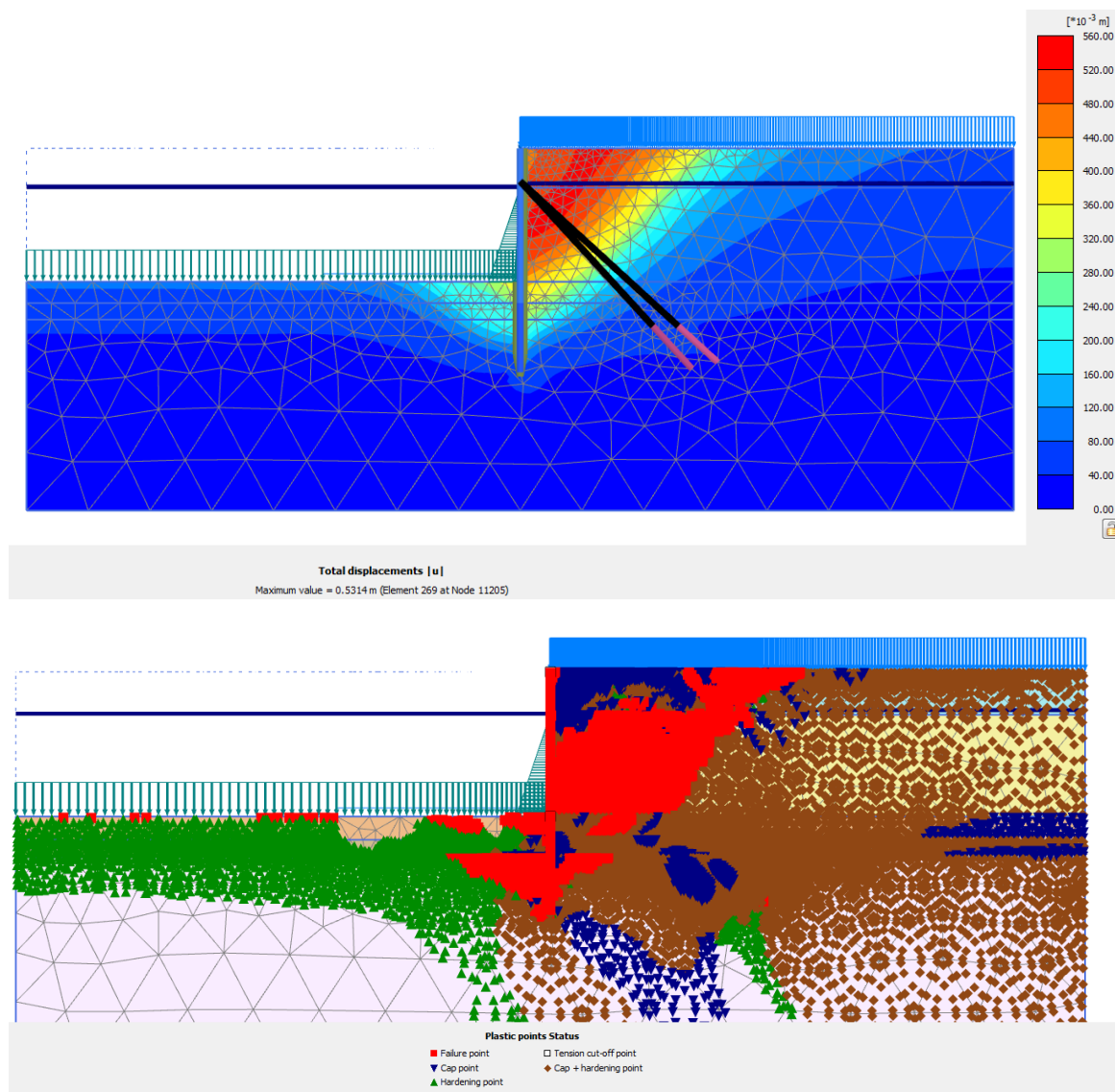
E

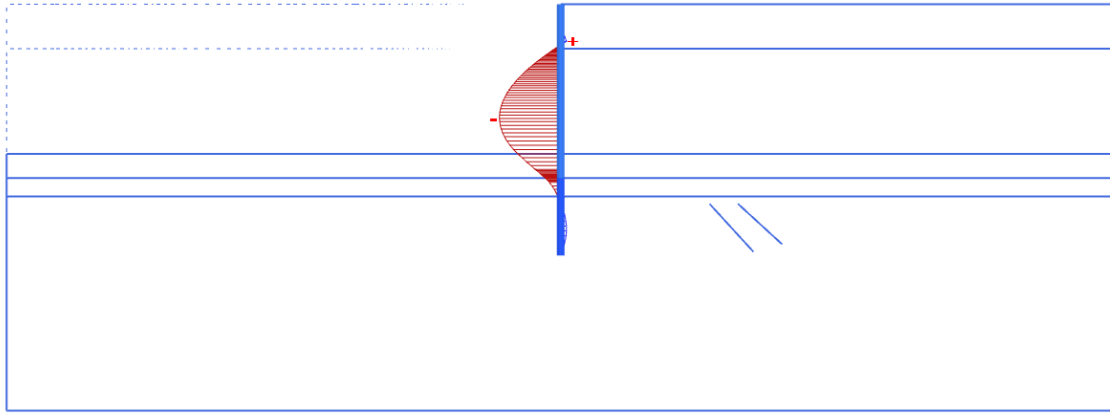
APPENDIX: PLAXIS OUTPUT RESULTS LBBR

In this appendix, the Plaxis output results in the design point of FORM is shown.

LS1: Yielding of the wall

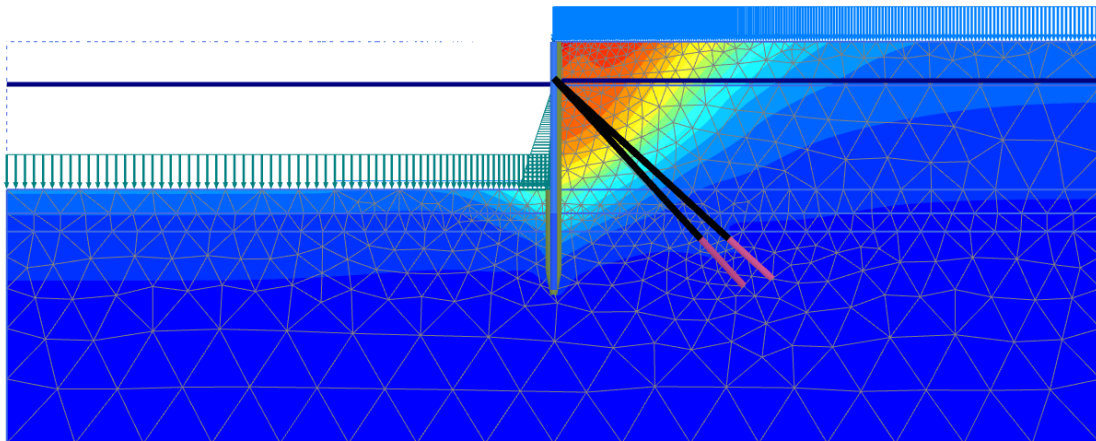
Output results for LSF: $Z = 4045 - M_S$



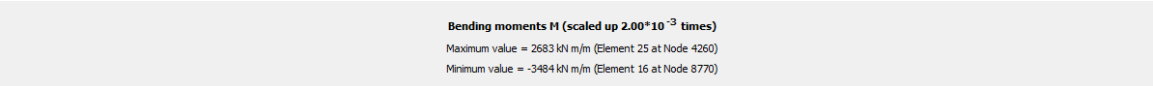
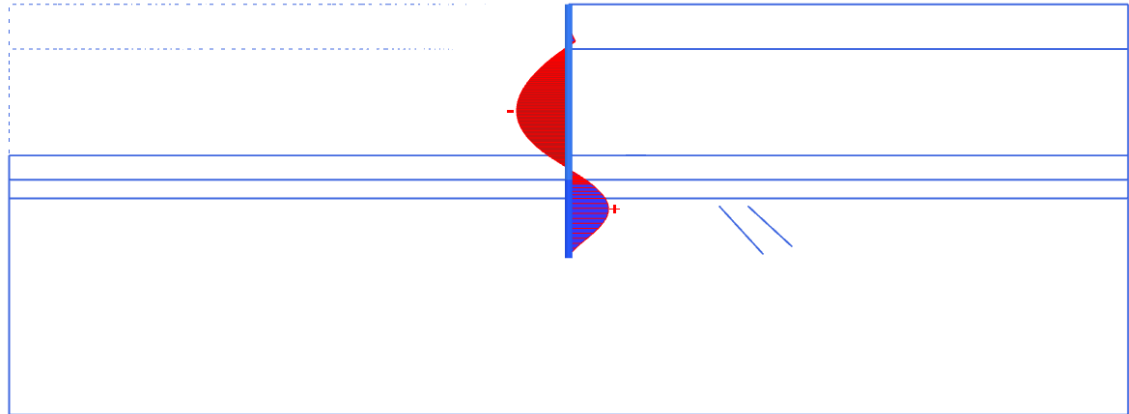
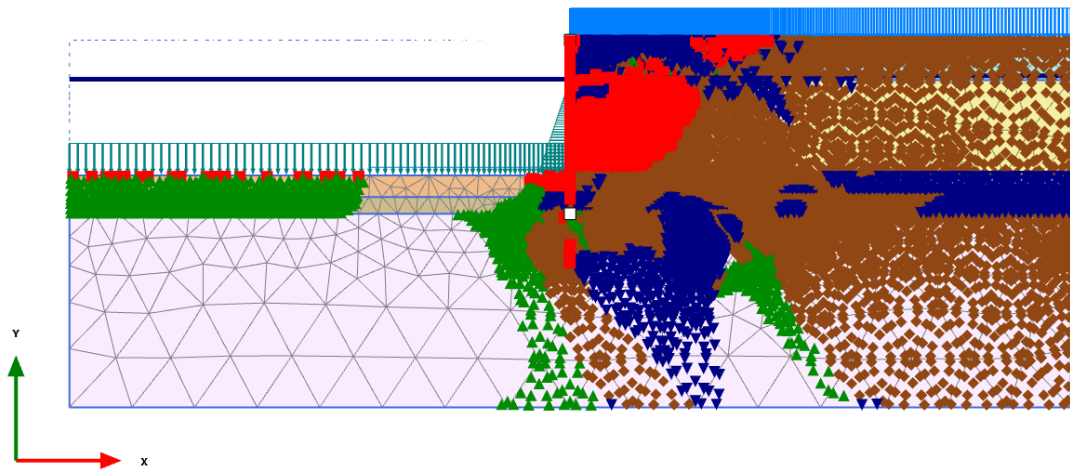


Bending moments M (scaled up $2.00 \cdot 10^{-3}$ times)
 Maximum value = 402.4 kN m/m (Element 5 at Node 10943)
 Minimum value = -4137 kN m/m (Element 17 at Node 8371)

Output results for LSF: $Z = 3495 - M_S$



Total displacements $|u|$
 Maximum value = 0.4097 m (Element 325 at Node 11893)



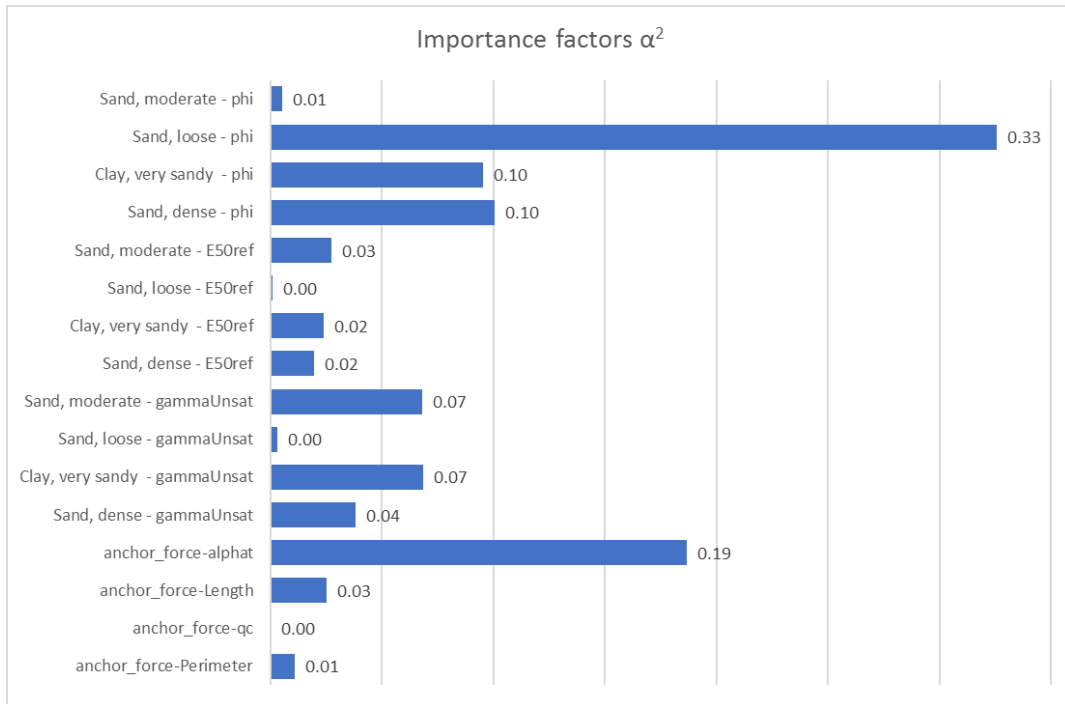
F

APPENDIX: FORM OUTPUT RESULTS SIMPLE QUAY WALL LS4: SHEAR RESISTANCE OF THE GROUT BODY

The results for the limit state shear resistance of the grout body of the simple quay wall are presented in this appendix. For the results below, the Beta distribution is used for the stochastic description of the parameter α_t , instead of a regular normal distribution.

Table F.1 LS: shear resistance of the grout body

	Value		
Reliability index β		6.8	
Failure probability P_f		$4.5 \cdot 10^{-12}$	
Number of iterations		24	
Number of LSFE		499	
Duration		9 hrs	
Parameter	Unit	Design point X^*	Mean X_m
Sand, moderate - phi	°	36.9	38.9
Sand, loose - phi	°	20.3	32.9
Clay, very sandy - phi	°	25.8	32.9
Sand, dense - phi	°	31.2	40.0
Sand, moderate - E50ref	kN/m ²	62529	45000
Sand, loose - E50ref	kN/m ²	28194	30000
Clay, very sandy - E50ref	kN/m ²	11704	16000
Sand, dense - E50ref	kN/m ²	52701	70000
Sand, moderate - gammaUnsat	kN/m ³	19.63	18.0
Sand, loose - gammaUnsat	kN/m ³	16.66	17.0
Clay, very sandy - gammaUnsat	kN/m ³	16.36	18.0
Sand, dense - gammaUnsat	kN/m ³	17.70	19.0
anchor_force-alphat	-	0.0123	0.016
anchor_force-Length	m	7.99	8.1
anchor_force-qc	kPa	20000	20000
anchor_force-Perimeter	m	1.218	1.225





APPENDIX: CALCULATIONS RESULTS FORM FOR DERIVING PARTIAL FACTORS SIMPLE QUAY WALL

The results of the limit state evaluations for the derivation of partial factors are given below.

Table G.1 LSI: Yielding of the wall

FORM event probability	4.9674E-09			
General reliability index	5.732			
Hasofer reliability index	5.732			
Number of evaluations	103			
Number of iterations	5			
The standard point origin is in the failure space	FALSE			
Parameter	Standard space design point	Physical space design point	Importance factors U-space	Importance factors Y-space
ZandSchoonMatig-E50ref	0.221	47771.61	0.001	0.001
ZandSchoonLos-E50ref	-1.061	22052.32	0.034	0.033
KleiSterkZandig-E50ref	-0.837	12547.40	0.021	0.020
ZandSchoonVast-E50ref	-0.437	61650.54	0.006	0.006
ZandSchoonMatig-phi	0.697	41.74	0.015	0.016
ZandSchoonLos-phi	-3.283	21.70	0.328	0.345
KleiSterkZandig-phi	-1.161	28.51	0.041	0.052
ZandSchoonVast-phi	0.107	39.98	0.000	0.000
ZandSchoonMatig-gammaUnsat	0.722	18.85	0.016	0.026
ZandSchoonLos-gammaUnsat	1.444	16.42	0.063	0.014
KleiSterkZandig-gammaUnsat	-0.350	16.97	0.004	0.038
ZandSchoonVast-gammaUnsat	-0.022	18.82	0.000	0.001
Surcharge-qy_start	-1.129	-44.51	0.039	0.037
Combiwall_redesign-t_tube	-1.136	0.02	0.039	0.038
Combiwall_redesign-d_tube	-0.224	1.42	0.002	0.001
max_stress_plate_plus_sign-fy_tube	-3.580	411497.07	0.390	0.373
Final absolute error	1.35			
Final relative error	0.23			
Final residual error	3.1032E-17			
Final constraint error	3456.7			

Table G.2 LS2: Yielding of the anchor bar

FORM event probability	7.55E-08			
General reliability index	5.25			
Hasofer reliability index	5.25			
Number of evaluations	147			
Number of iterations	7			
The standard point origin is in the failure space	FALSE			
Parameter	Standard space design point	Physical space design point	Importance factors U-space	Importance factors Y-space
ZandSchoonMatig-E50ref	0.654	54152.8	0.015	0.015
ZandSchoonLos-E50ref	-0.588	25296.5	0.013	0.012
KleiSterkZandig-E50ref	-0.439	14083.9	0.007	0.007
ZandSchoonVast-E50ref	0.156	73226.2	0.001	0.001
ZandSchoonMatig-phi	-0.418	38.0	0.006	0.002
ZandSchoonLos-phi	-2.884	23.3	0.302	0.306
KleiSterkZandig-phi	-0.791	30.0	0.023	0.027
ZandSchoonVast-phi	-0.291	39.0	0.003	0.002
ZandSchoonMatig-gammaUnsat	0.943	18.8	0.032	0.028
ZandSchoonLos-gammaUnsat	0.820	16.3	0.024	0.021
KleiSterkZandig-gammaUnsat	-0.233	17.4	0.002	0.018
ZandSchoonVast-gammaUnsat	-0.017	19.0	0.000	0.000
Borehole_1-Head	0.038	-0.8	0.000	0.000
Surcharge-qy_start	-0.830	-43.3	0.025	0.024
anchor_force-fy	-3.781	417205	0.518	0.507
anchor_force-A	-0.886	0.005	0.028	0.028
Final absolute error	0.758			
Final relative error	0.144			
Final residual error	0.000			
Final constraint error	7.737			

H

APPENDIX: PLAXIS SOIL MODELS

Soil models

Within Plaxis multiple material models are available for the description of the behaviour of the soil. The applicability of a model depends on the soil type and the required accuracy of the calculation. For soils in the Netherlands the constitutive models based on the criterion of Mohr-Coulomb are most relevant. A detailed description of the different models is given below:

Mohr-Coulomb model

The theory of Mohr-Coulomb divides the behaviour of soils into two parts: a linear elastic part and a perfectly plastic part (Figure H.1). The linear elastic part is described by Hooke's law. This law describes a linear relation between stresses and strains by the Young's Modulus E .

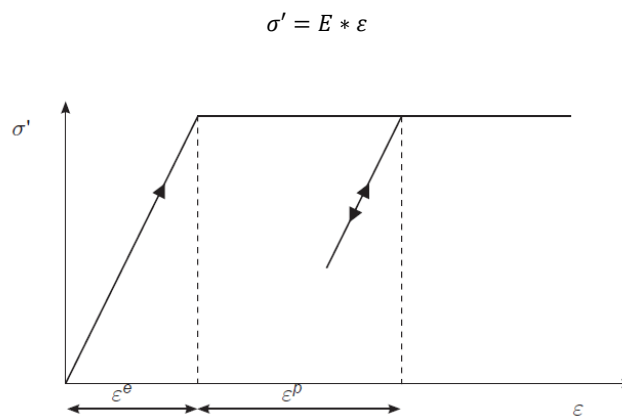


Figure H.1 Stress-strain relationship for an elastic perfectly plastic model. Source: Plaxis (2017)

The boundary between the elastic and the plastic part is determined by the failure criterion of Mohr-Coulomb. Coulomb derived his expression for the maximum shear stress with the analogy of a sliding block on a slope. In this way he stated that the maximum shear stress in a soil body is:

$$\tau_f = c + \sigma' \tan \varphi'$$

Where

- τ_f critical shear stress
- c cohesion
- σ' effective stress
- φ' friction angle

This line is presented in Figure H.2. The criterium of Mohr-Coulomb extends this theory for any plane within a material element by using principal stresses. The principle stresses σ_1 , σ_2 and σ_3 indicate the main stress directions on a considered element. They are acting on planes which are orientated in such a way that they are not loaded by shear stresses. σ_1 is the largest principle stress, which is normally in the vertical direction due to the weight of the soil above. σ_3 is the lowest principle stress. The radius of the Mohr circle is determined by the difference between the highest principle stress and the lowest principle stress, also known as the deviator stress.

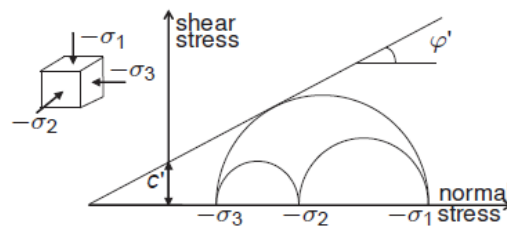


Figure H.2 Mohr-Coulomb failure criterion. Source: Plaxis (2017)

When the Mohr circle is crossing the failure criterion of Coulomb irreversible plastic deformations are assumed to occur as shown in Figure H.1. For stress combinations below the limit, the soil is assumed to behave linear with a fixed value for the stiffness. In reality the stiffness is far from a fixed value and depends on the stress. It is possible though to let the stiffness linearly increase with depth to partly account for the stress dependency of stiffness. Because other kinds of stiffness effects or not taken into account, the Mohr-Coulomb model is a rather rough and basic model and thus requires limited computational effort.

Hardening Soil model

The Hardening Soil model describes the relation between stress and stiffness much more accurate as the regular Mohr-coulomb soil model does not take into account shear hardening and compression hardening. When a soil is loaded for the first time the soil particles rearrange in position so that the soil skeleton becomes a denser structure. After unloading, the soil does not fully return to its zero strain level due to the irreversible plastic deformation. The next time the soil is loaded up till a previous load state the soil behaves much stiffer, which is expressed by the unloading / reloading stiffness. Another aspect that is not (or partly) taken into account in the regular Mohr-Coulomb models is the increase in stiffness with confining pressure. Due to this phenomena the soil tends to be stiffer at greater depth. These effect are taken into account in the Hardening Soil model by describing the stiffness with three different stiffness parameters:

E_{50}^{ref}	Secant stiffness in standard drained triaxial test
E_{oed}^{ref}	Tangent stiffness for primary oedometer loading
E_{ur}^{ref}	Unloading / reloading stiffness

The superscript *ref* is introduced to indicate that the stiffness parameter should be inputted for a reference value of the cell pressure of usually 100 kPa. The definitions of E_{50}^{ref} and the E_{ur}^{ref} are displayed in Figure H.3, whereas E_{oed}^{ref} is determined with an oedometer test. The FEM-model calculates for every element the actual stiffness based on the actual minor principal stress σ_3' .

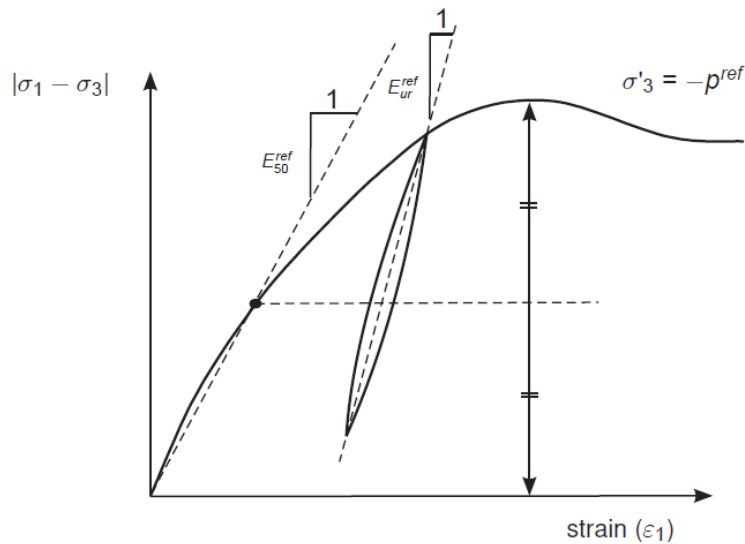


Figure H.3 Definition of the stiffness parameters. Source: Plaxis (2017)

Hardening Soil model with small strain stiffness

The Hardening Soil model with small strain stiffness is almost equal to the regular Hardening Soil model except for the addition to account for increased stiffness of soils at very small strains. This is especially important for the accurate determination of displacements during normal loading conditions. Figure H.4 illustrates the relation between the shear modulus and the shear strain and also indicates the range of retaining walls and conventional soil testing methods. It clearly shows that the range of retaining walls is mostly located in the small strain area. Therefore the addition of two parameters that describe the variation of stiffness with strain is needed. These are the very small strain shear modulus G_0 and the shear strain level $\gamma_{0.7}$.

The downside of this model is the extra computational time it takes to run the model compared to the regular Hardening Soil model. As this thesis is mainly focussed on checking of failure in ULS, this soil model seems to have not much additional value compared to the regular Hardening Soil model.

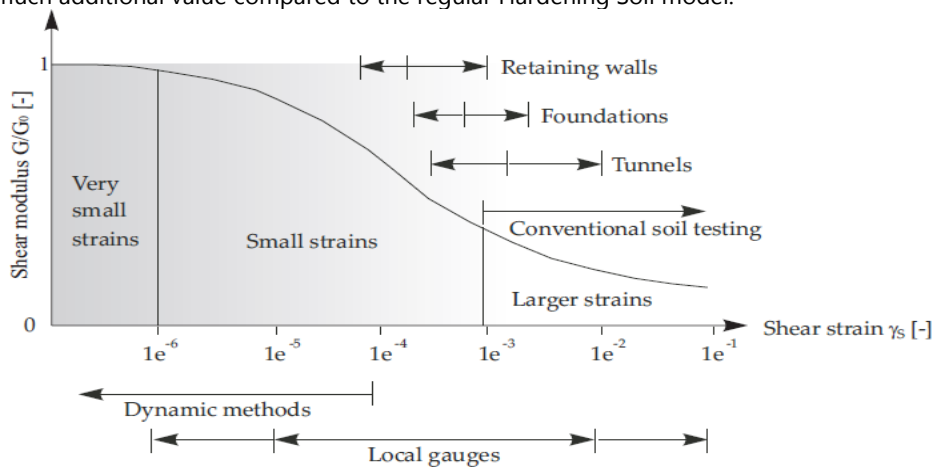
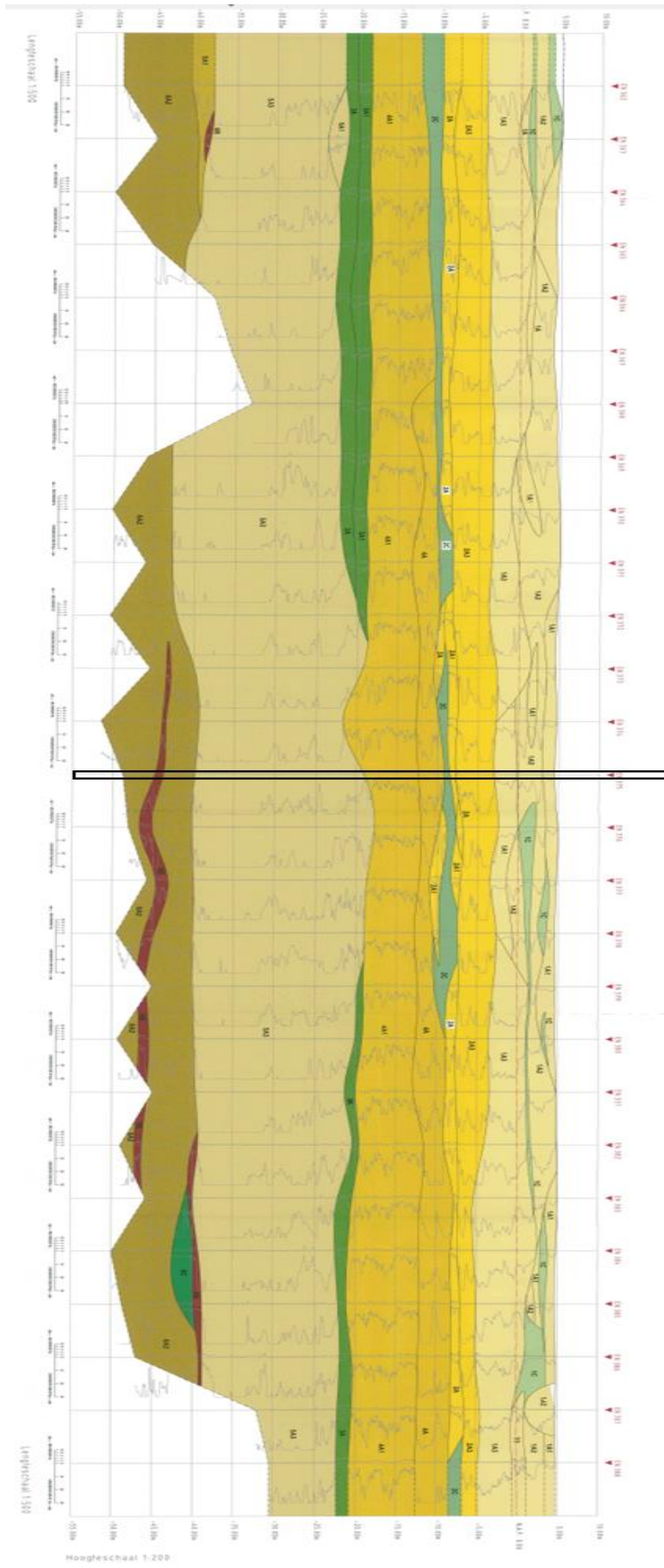


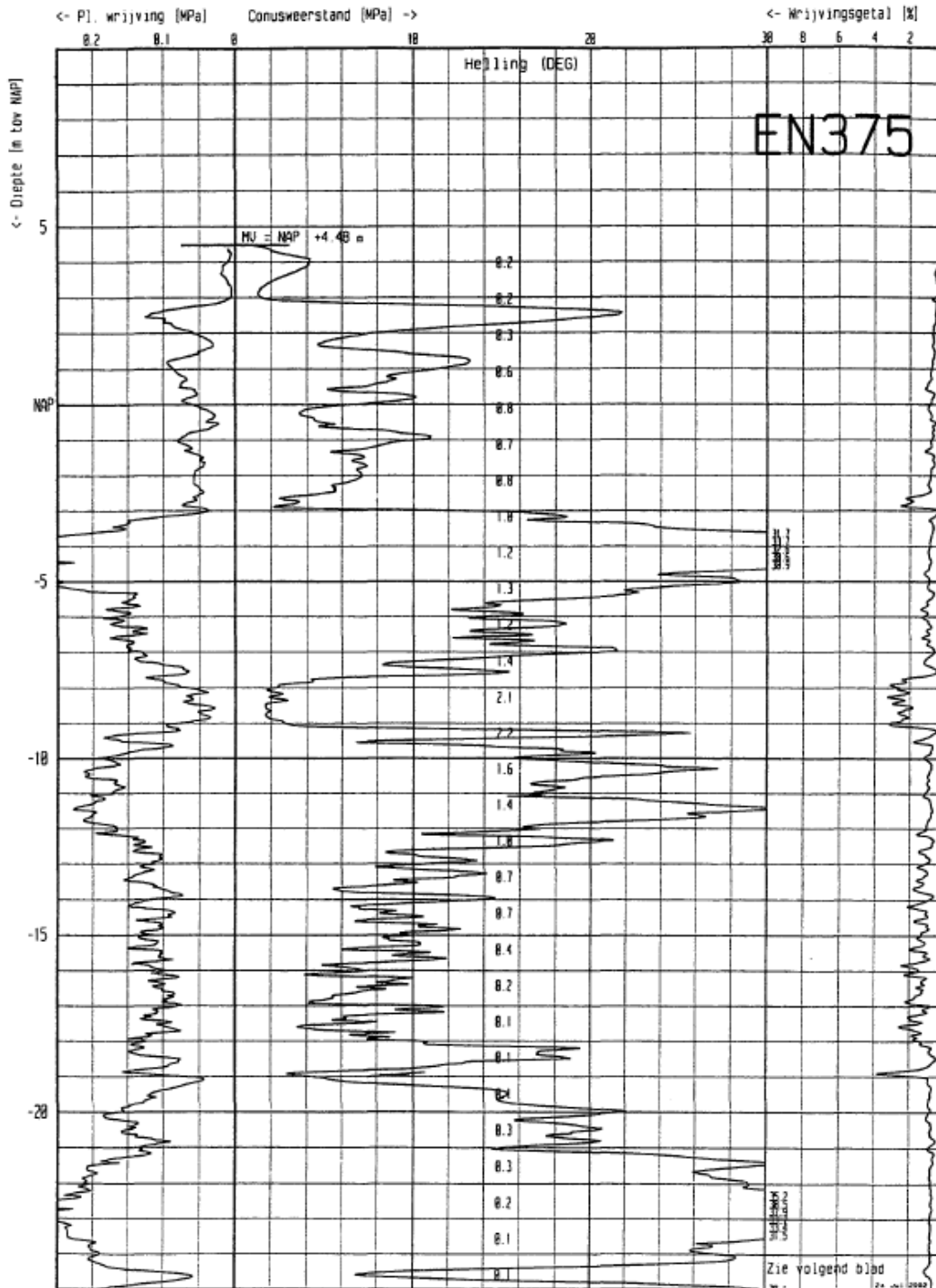
Figure H.4 Shear modulus versus shear strain. Source: Plaxis (2017)


I

APPENDIX: LONGITUDINAL SOIL PROFILE AND USED CPT

On the next page, the longitudinal soil profile for the EMO quay wall is shown. The black square indicates the location of the closest nearby CPT with respect to the measurement pit that is used in this research.



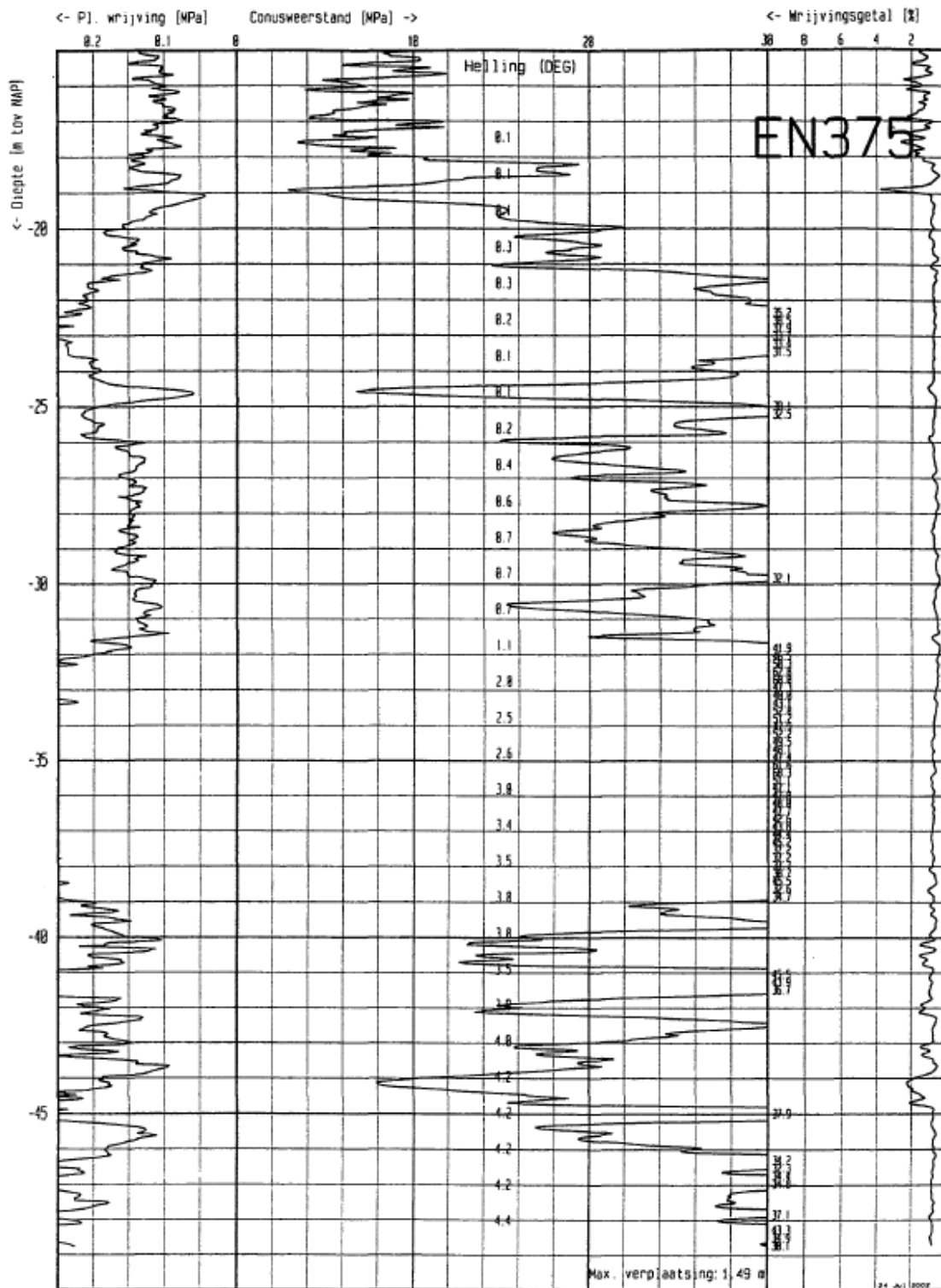



Project : mississippihaven
 Locatie : Rotterdam
 Paraaf 1:  2:

Conus : Cil.elec k1-piezo
 Nummer : CFPI 020709
 Bereik : 50 kN
 Sondering volgens NEN 5140 Klasse 2

MAP : 2002-033
 DATUM : 23-7-2002

Gemeentewerken
 ROTTERDAM
 Ingenieursbureau
 Geotechniek



Project : mississippihaven
 Locatie : Rotterdam
 Paraaf 1:  2:

Conus : Cil.elec k1-piezo
 Nummer : CFPI 020709
 Bereik : 50 kN
 Sondering volgens NEN 5140 Klasse 2

MAP : 2002-033
 DATUM : 23-7-2002

Gemeentewerken
 ROTTERDAM
 Ingenieursbureau
 Geotechniek



APPENDIX: CALCULATION RESULTS EMO

The results of the sensitivity analysis with uncorrelated parameters for the limit state yielding of the combi-wall are given below.

FORM event probability	0.00014			
General reliability index	3.62			
Hasofer reliability index	3.62			
Number of evaluations	141			
Number of iterations	5			
The standard point origin is in the failure space	FALSE			
Parameter	Standard space design point	Physical space design point	Importance factors U-space	Importance factors Y-space
SandModerate1A2-phi	-0.14	34.52	0.00	0.00
SandDense2A3-phi	-0.18	36.84	0.00	0.00
ClayWSandyModerate2C-phi	-0.08	24.81	0.00	0.00
Sand4A-phi	-0.23	34.21	0.00	0.00
SandClayLayers4A1-phi	-1.02	26.76	0.08	0.08
SandDense5A3-phi	-3.27	25.24	0.81	0.81
SandModerate1A2-E50ref	0.08	48193	0.00	0.00
SandDense2A3-E50ref	-0.26	43455	0.01	0.01
ClayWSandyModerate2C-E50ref	-0.03	3068	0.00	0.00
Sand4A-E50ref	-0.11	43517	0.00	0.00
SandClayLayers4A1-E50ref	-0.05	40412	0.00	0.00
SandDense5A3-E50ref	-0.08	45889	0.00	0.00
SandModerate1A2-gammaUnsat	0.27	18.24	0.01	0.01
SandDense2A3-gammaUnsat	0.15	19.14	0.00	0.00
ClayWSandyModerate2C-gammaUnsat	0.02	17.02	0.00	0.00
Sand4A-gammaUnsat	0.06	19.06	0.00	0.00
SandClayLayers4A1-gammaUnsat	0.00	18.00	0.00	0.00
SandDense5A3-gammaUnsat	-0.83	18.21	0.05	0.05
CombiWall-t_tube	-0.11	0.02	0.00	0.00

CombiWall-d_tube	0.01	1.42	0.00	0.00
fy_tube	-0.63	480653	0.03	0.03
Final absolute error	1.220			
Final relative error	0.337			
Final residual error	4.66E-17			
Final constraint error	2240.22			

K

APPENDIX: RESULTS FOR NON-CALIBRATED QUAY WALL

In this appendix, the results are given for the non-calibrated design of the EMO quay wall. The applied soil parameters for both limit states are given in Table K.1 and Table K.2.

Table K.1 Mean soil strength parameters

Level [m w.r.t. NAP]	Description	$\gamma_{unsaturated}$ [kN/m ³]	$\gamma_{saturated}$ [kN/m ³]	ϕ' [°]	c' [kN/m ²]
5.0	Sand, moderate, top	18.0	20.0	38.9	0
-3.0	Sand, dense	19.0	21.0	41.9	0
-7.8	Clay, w. sandy, moderate	17.0	18.0	29.9	11.2
-9.1	Sand, moderate, 2	18.0	20.0	38.9	0
-12.0	Sand, clay layers	18.0	19.0	32.3	0
-19.0	Sand, Pleistocene	19.0	21.0	41.9	0

Table K.2 Mean Hardening soil parameters

Description	Re [%]	E_{50}^{ref} [MN/m ²]	E_{oed}^{ref} [MN/m ²]	E_{ur}^{ref} [MN/m ²]	m [-]	ψ [°]	R_{inter} [-]
Sand, moderate, top	79	47	47	189	0.5	5.0	0.8
Sand, dense	78	47	47	186	0.5	7.5	0.8
Clay, w. sandy, moderate	-	3.1	1,6	11,1	0.9	0	0.8
Sand, moderate, 2	74	45	45	180	0.5	5	0.8
Sand, clay layers	68	41	41	163	0.5	0	0.8
Sand, Pleistocene	78	47	47	187	0.5	7.5	0.8

Table K.3 Results for the limit state soil mechanical failure

FORM event probability	2.36E-05			
General reliability index	4.069238704			
Hasofer reliability index	4.069238704			
Number of evaluations	22			
Number of iterations	2			
The standard point origin is in the failure space	FALSE			
Parameter	Standard space design point	Physical space design point	Importance factors U-space	Importance factors Y-space
SandModeratetop-phi	-0.24	37.95	0.00	0.00
SandDense-phi	-0.20	40.95	0.00	0.00
ClayWSandyModerate-phi	0.00	29.90	0.00	0.00
Sand, moderate, 2 -phi	-0.19	38.16	0.00	0.00
SandClayLayers-phi	-0.53	30.59	0.02	0.01
Sand, Pleistocene - phi	-3.95	25.32	0.94	0.63
Sand, Pleistocene - gammaUnsat	-0.74	16.52	0.03	0.28
Sand, Pleistocene - E50ref	-0.03	31521	0.00	0.07
Final absolute error	0.238			
Final relative error	0.058			
Final residual error	1.52E-18			
Final constraint error	0.000893351			

Table K.4 Results for the limit state yielding of the combi-wall

FORM event probability	2.86E-05			
General reliability index	4.023866628			
Hasofer reliability index	4.023866628			
Number of evaluations	82			
Number of iterations	5			
The standard point origin is in the failure space	FALSE			
Parameter	Standard space design point	Physical space design point	Importance factors U-space	Importance factors Y-space
SandModeratetop-phi	-0.24	37.95	0.00	0.00
SandDense-phi	0.01	41.81	0.00	0.00
ClayWSandyModerate-phi	-0.04	29.78	0.00	0.00
Sand, moderate, 2-phi	-0.24	37.94	0.00	0.00
SandClayLayers-phi	-0.87	29.49	0.05	0.03
Sand, Pleistocene -phi	-3.76	26.12	0.87	0.57
SandClayLayers-E50ref	-0.11	37220	0.00	0.00
Sand, Pleistocene -E50ref	-0.64	29423	0.03	0.10
SandModerate-gammaUnsat	0.10	17.97	0.00	0.00
SandClayLayers-gammaUnsat	0.01	17.58	0.00	0.01
Sand, Pleistocene - gammaUnsat	-0.64	16.51	0.02	0.27
CombiWall-t_tube	-0.12	0.02	0.00	0.00
CombiWall-d_tube	-0.07	1.42	0.00	0.00
max_stress_plate_plus_sign-fy_tube	-0.57	451272	0.02	0.01
Final absolute error	0.444729821			
Final relative error	0.110523003			
Final residual error	7.76E-18			
Final constraint error	3134.474839			

